Assessing the provenance and contribution of local vs regional drainage systems for the Upper Triassic fluvial deposits, High Atlas, Morocco

A dissertation submitted to the University of Manchester for the degree of Master of Science by Research in the Faculty of Science and Engineering.

2018

James M. Lovell-Kennedy
School of Earth and Environmental Sciences

Chapter 1 Table of Contents

Figures

Tables

Abstract

The inverted Mesozoic rift basins of the High Atlas Mountains, Morocco, provide excellent exposure to study the sedimentology of syn-rift continental facies and the development of regional and local drainage networks during continental break up. A complex suite of Triassic facies was deposited in a number of rifted basins that outcrop on either side of the Massif Ancien, a drainage divide between the Atlantic and Tethyan domains within the Central High Atlas during the Triassic.

The study combines outcrop data with data provided from oil exploration wells drilled in the Tendrara Field, High Plateaux Basin, to study the temporal and spatial variations in basin fill. A stratigraphic correlation has been proposed between the Central High Atlas and the Middle High Atlas based on subtle variations in lithofacies and stratigraphic architecture within the fluvial syn-rift succession in the absence of a robust biostratigraphic or chronostratigraphic framework.

To supplement this sedimentological correlation, and to test the hypothesis that the Middle and High Atlas Rifts were linked during the Triassic, a provenance study has been conducted utilising petrographic and heavy mineral analysis on samples from the Oukaimeden Basin, Kerrouchen Basin and the Tendrara Field. Samples were selected from reservoir quality fluvial facies in order to identify the provenance and distribution of reservoir intervals and to identify the scale of drainage networks during the Triassic.

The provenance data suggests the rift basins of the Atlas Mountains were in communication during the Triassic, with sediment sourced from the Anti-Atlas transported towards the proto-Tethyan Ocean. The observation of a temporal variation in detrital heavy mineral assemblage, from a recycled to mafic heavy mineral assemblage suggests that an unroofing event occurred, with initial erosion from Palaeozoic sedimentary cover before erosion into underlying mafic units. However, the absence of unique heavy minerals within the detrital assemblages, and a sparse heavy mineral data set for the Anti-Atlas, makes accurate identification of the source regions or regionally significant drainage networks impossible at the current time.

This study demonstrates the potential of provenance analysis in identifying the likely distribution of reservoir sands and in providing well to well correlation and insight into the lateral and vertical variation in reservoir quality within sparsely fossiliferous sandstone reservoirs alongside regional paleogeographic reconstruction. In order to fully utilise this within the Triassic of Morocco, further detrital heavy mineral analysis and a detrital geochronological study are required.

Declaration

No portion of the work referred to in the dissertation has been submitted in support of an application for another degree or qualification of this or any other university or other institute of learning.

Copyright Statement

i. The author of this dissertation (including any appendices and/or schedules to this dissertation) owns certain copyright or related rights in it (the “Copyright”) and s/he has given The University of Manchester certain rights to use such Copyright, including for administrative purposes.

ii. Copies of this dissertation, either in full or in extracts and whether in hard or electronic copy, may be made only in accordance with the Copyright, Designs and Patents Act 1988 (as amended) and regulations issued under it or, where appropriate, in accordance with licensing agreements which the University has from time to time. This page must form part of any such copies made.

iii. The ownership of certain Copyright, patents, designs, trademarks and other intellectual property (the “Intellectual Property”) and any reproductions of copyright works in the dissertation, for example graphs and tables (“Reproductions”), which may be described in this dissertation, may not be owned by the author and may be owned by third parties. Such Intellectual Property and Reproductions cannot and must not be made available for use without the prior written permission of the owner(s) of the relevant Intellectual Property and/or Reproductions.

iv. Further information on the conditions under which disclosure, publication and commercialisation of this dissertation, the Copyright and any Intellectual Property and/or Reproductions described in it may take place is available in the University IP Policy, in any relevant Dissertation restriction declarations deposited in the University Library, The University Library’s regulations and in The University’s policy on Presentation of Dissertations.

Chapter 1 Geological Setting

1.1. Introduction

The High and Middle Atlas expose an inverted Mesozoic rift succession which allows the study of pre, syn and post-rift sedimentary processes during continental break up at a triple junction and the subsequent onset of sea floor spreading and passive margin development (Le Roy & Piqué 2001; Laville *et al.* 2004). During the break up of Pangea, Morocco was uniquely situated at the hinge point between the Tethyan Domain to the north and the Atlantic Domain to the west (Ellouz *et al.* 2003) making Morocco an ideal place to study the paleogeography of Central Pangea. This study will aim to build on previous work completed in the Central High Atlas by analysing facies distribution and depositional style within the Middle Atlas Kerrouchen Basin during the syn to post-rift Triassic succession. The field data was then combined with a heavy mineral study to analyse the source to sink pathways during the Triassic across the Tethyan domain of Morocco.

Within the Kerrouchen Basin, fieldwork has been undertaken to identify the various depositional systems which were active during the Triassic. The identification of axial fluvial systems and transverse alluvial-fluvial systems allows discrimination between local (transverse depositional system) and regional (axial depositional system) provenance signals recorded within the heavy mineral assemblages. To identify the regional signal samples collected from the Oukaimeden F5 formation (Fabuel-Perez *et al.* 2009) have also been incorporated into this study, as this formation has been interpreted to represent the Triassic axial fluvial system within the Oukaimeden-Ourika Valley (Fabuel-Perez *et al.* 2009). The paleoflows recorded within the Oukaimeden Basin indicate a drainage network sourced from the south, flowing northeast towards the Middle Atlas (Fabuel-Perez *et al.* 2009; Domènech *et al.* 2018). It is possible however; that the Central High Atlas was linked to the High Plateaux region, near the present-day Moroccan-Algeria border, and the Middle Atlas had a separate drainage network. The present study aims to test the predicted fluvial system linkage between the Central High Atlas and Middle High Atlas rifts of Morocco. The overall depositional setting is believed to be analogous to the coeval Budleighensis River System of NW Europe that has an axial system routing into the North Sea. The detrital heavy mineral assemblage of the Triassic fluvial deposits in the North Sea has been proven as an effective way to determine provenance alongside chemostratigraphy(Morton & Hallsworth 1994; Tyrrell *et al.* 2012; Mckie 2014; Flint *et al.* 2015; Amorosi & Sammartino 2018), and this study aims to utilise a similar methodology to improve our understanding of Triassic provenance and depositional systems in Morocco.

Subsurface samples and thin sections from the Tendrara region were provided by Sound Energy Plc. As this data is collected from the subsurface, it is difficult to identify paleoflow for the depositional system sampled, however the use of heavy minerals can assist in discriminating axial and transverse systems by identifying local versus regional signals (Kilhams *et al.* 2014). Within the High Plateaux Basin, a number of previous studies have been conducted, with the majority of paleogeographic models predicting regional drainage towards the south within the Eastern Meseta region, towards the Atlantic Ocean (Kape 2017). However, recent work from the Central High Atlas has identified a

drainage divide in the Central High Atlas, which would have split central Pangea into an Atlantic and Tethyan realm, with the High Plateaux firmly in the Tethyan domain (Laville *et al.* 2004; Fabuel-Perez *et al.* 2009; Mader *et al.* 2017; Domènech *et al.* 2018).

This study will aim to identify the sediment dispersal pathways during the Triassic across Morocco and make paleogeographic reconstructions to predict where major fluvial systems developed during the Triassic. The fluvial-aeolian Triassic sands, known as the TAGI-sandstone, are a major reservoir interval across North Africa (Rossi *et al.* 2002; Mader *et al.* 2017) and understanding the distribution of the TAGI sandstone across Morocco is vital for accurate play fairway analysis and understanding of the petroleum systems across Morocco. The geological evolution of the Mesozoic Atlasic rift and North African passive margin consists of three distinct phases; pre-rift, syn-rift and post rift (Pique *et al.* 1998). During the late Palaeozoic and early Mesozoic, Morocco was situated in Central Pangea *(Figure 1.1)* (Golonka & Ford 2000; Ford & Golonka 2003).

Post orogenic collapse following the end of the Variscan Orogeny and the assembly of the Pangean supercontinent (Michard *et al.* 2008), leading to the formation of small, NE-SW intra-montane basins in the Permian which were filled by conglomerates *(Figure 1-2)* (Baudon *et al.* 2012). An extended sedimentary hiatus then occurred, before the onset of active rifting in the Carnian, which resulted in the opening of the Central Atlantic to the west and the formation of the Alpine-Tethys to the north *(Figure 1-1).* The rifting led to the formation of several major rift basins, primarily the Argana – Essaouira Basin in the south-west, the Oukaimeden Basin in the Central High Atlas, the Kerrouchen Basin within the Middle Atlas and the High Plateaux Basin (e.g. Oujidi *et al.* 2000) *(Figure 1-3).* These basins where filled by extensive continental red beds (Guiraud 1998; Oujidi *et al.* 2000; Laville *et al.* 2004), with the end of the Triassic marked across Morocco by the eruption of the CAMP basalts between 210 and 200 Ma *(Figure 1-2)* (Fiechtner *et al.* 1992; Lachkar *et al.* 2000)

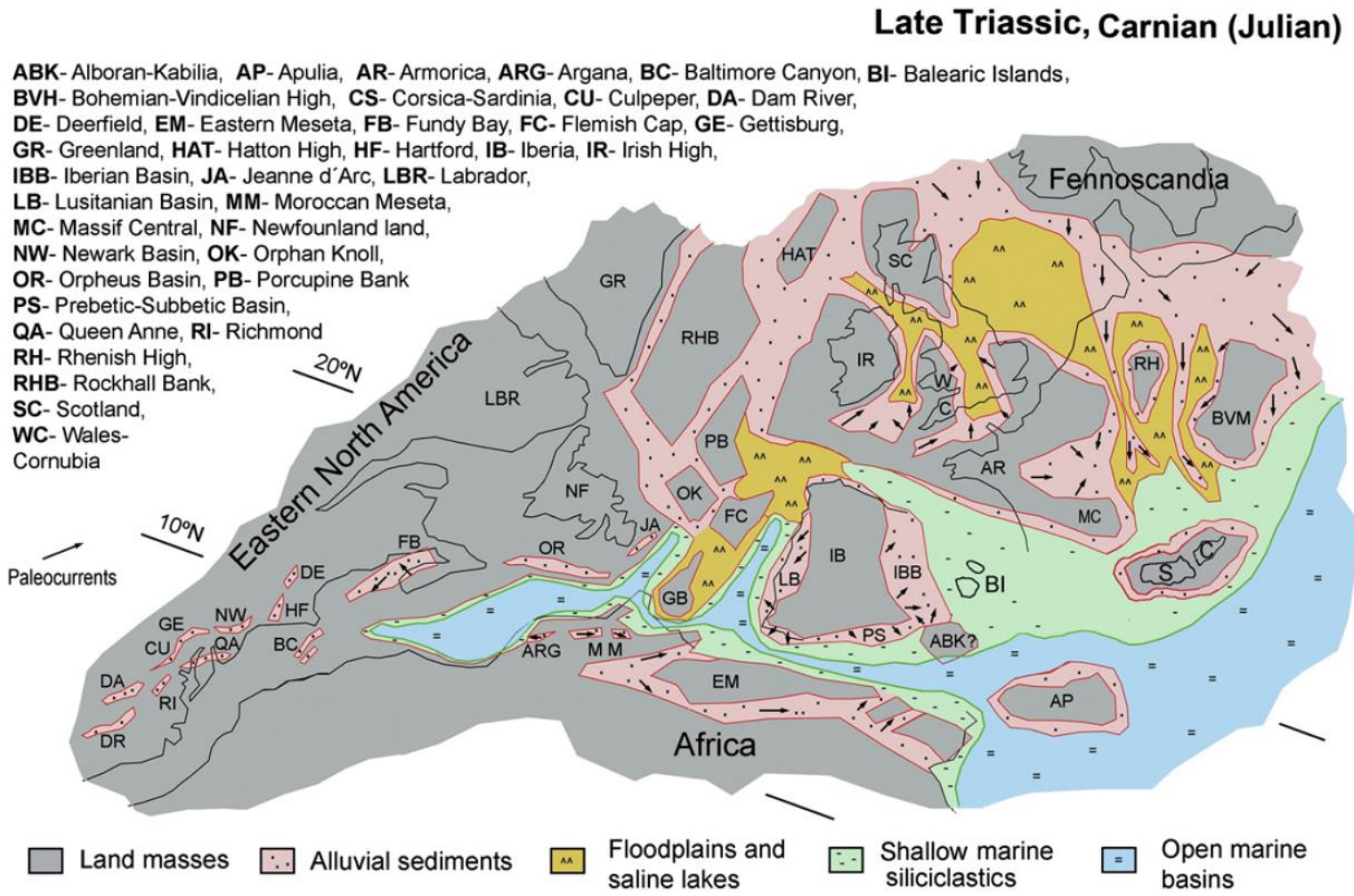

Figure 1-1: Carnian paleogeography of Central Eastern Pangea, showing the distribution of continental, shallow marine and open marine conditions (Arche & López-Gómez 2014, p. 30) ..

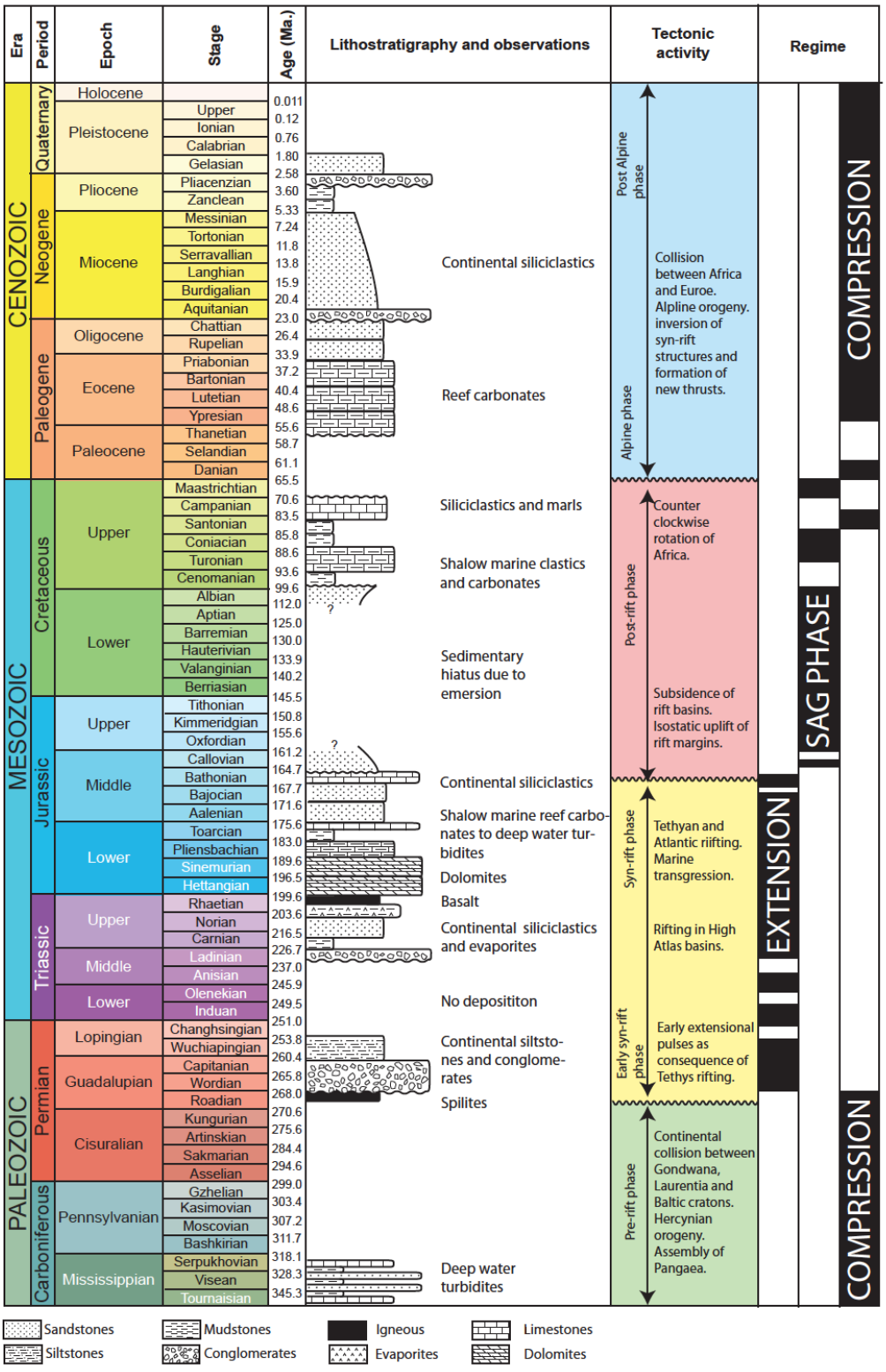

Figure 1-2: Tectono-stratigraphic chart of the High Atlas (Fabuel-Perez 2008, p. 65). The Triassic Period was characterised by extensional tectonics and with deposition of continental siliciclastic and extensive evaporites beginning in the Upper Triassic capped by the CAMP basalts at the Triassic-Jurassic Boundary.

1.2. Aims and Objectives

Previous work on the fluvial systems recorded within the Triassic of Morocco has mainly been focused in the Oukaimeden Basin (Benaouiss *et al.* 1996; Fabuel-Perez 2008; Fabuel-Perez *et al.* 2009) and the Argana Valley (Brown 1980; Hofmann *et al.* 2000; Mader & Redfern 2011; Baudon *et al.* 2012; Mader *et al.* 2017) within the High Atlas. In contrast, the fluvial deposits of the Kerrouchen Basin, Middle Atlas, have not been extensively studied, with the main focus being on the development of biostratigraphic models (Lorenz 1976; Lachkar *et al.* 2000; Ouarhache *et al.* 2000). The majority of the work in the Eastern Meseta has been done in an to attempt to reconstruct the paleogeography of Morocco during the Triassic and understand the Tethyan Marine transgression (Ouijidi *et al.* 2000; Oujidi *et al.* 2000; Courel *et al.* 2003). More recently, thermochronology studies have generated uplift data and identified the Massif Ancien as acting as a drainage divide between the Oukaimeden and Argana Basins within the High Atlas (Domènech *et al.* 2015, 2016; Gouiza *et al.* 2017; Charton *et al.* 2018), further constraining paleogeographic models. However, there have been only limited attempts to utilise the provenance of the fluvial sands as a way of constructing paleogeographic models between the 'sources' (e.g. Massif Ancien) and 'sinks' (e.g. Oukaimeden Basin), which have mainly focused on the High Atlas region (Domènech *et al.* 2018).

This study aims to build on the previous work undertaken in the Oukaimeden Basin by studying the stratigraphy of the Kerrouchen Basin *(Figure 1-3)* to identify facies variations caused by deposition by local or regional drainage networks. The extent of drainage systems will be assessed by petrographic and heavy mineral analysis in order to assess the provenance of the Triassic fluvial sands and create source to sink maps, linking the uplifted regions to the proto-Alpine Tethys. The main objectives of this Msc by Research are to:

- Utilise provenance data to assess whether a regional fluvial system connected the Oukaimeden, Kerrouchen and High Plateaux Basins during the Upper Triassic and to reconstruct the regional paleogeography during the Upper Triassic

- Assess whether regional, axial fluvial and local, transverse, fluvial systems be distinguished within the Triassic rift basins of Morocco based on both facies and provenance analysis. If both regional and local drainage networks are present within a basin, it is predicted that they will preserve distinct provenance signals from one another.

- Identify the extent that sediment eroded by local and regional drainage networks contributes to the economically significant TAGI reservoir and highlight uses of provenance data within both exploration and development of hydrocarbon reservoirs.

The provenance methodology within this project has been applied to similar regions alongside complementary techniques (e.g. chemostratigraphy) as a way of collecting data for both provenance

analysis and paleogeographic reconstructions as well as exploration and development of petroleum reserves, especially in fields where traditional datasets (e.g. biostratigraphy), are unsuitable.

1.3. Field and core analysis

Three of the major Triassic Rift basins within the Tethyan domain of Morocco, Oukaimeden, Kerrouchen and the High Plateaux (Ouijidi *et al.* 2000; Ellouz *et al.* 2003), were selected for stratigraphic analysis *(Figure 1-3).* Building on previous work done within the Oukaimeden Basin, outcrop analysis was undertaken in the Kerrouchen Basin, alongside analysis of core provided by Sound Energy from the Tendrara Field within the High Plateaux Basin. The Oukaimeden Basin is situated in the High Atlas, to the east of a drainage divide within the Tethyan domain (Mader 2005, p. 256). The Kerrouchen Basin is situated approximately 300km to the NE of the drainage divide in the Middle Atlas, located between the Central and Eastern Meseta tectonic domains (Michard *et al.* 2008). The High Plateaux Basin and the Tendrara Field are located nearly 600km to the ENE of the drainage divide within the Eastern Meseta tectonic domain *(Figure 1-3)* (Ouijidi *et al.* 2000; Michard *et al.* 2008).

The analysis of these three rift basins located within the Tethyan domain will allow for the paleogeographic reconstruction of central Morocco during the late Triassic, and the distribution of economically important fluvial sands across Morocco. The sand-rich fluvial intervals were sampled for petrographic analysis in order to constrain the provenance and aid the reconstruction of the drainage networks within Morocco during the Late Triassic. The analysis of the facies and the distribution of those facies within the Oukaimeden and Kerrouchen Basin could be utilised to model reservoir distribution and quality within the Tendrara Field.

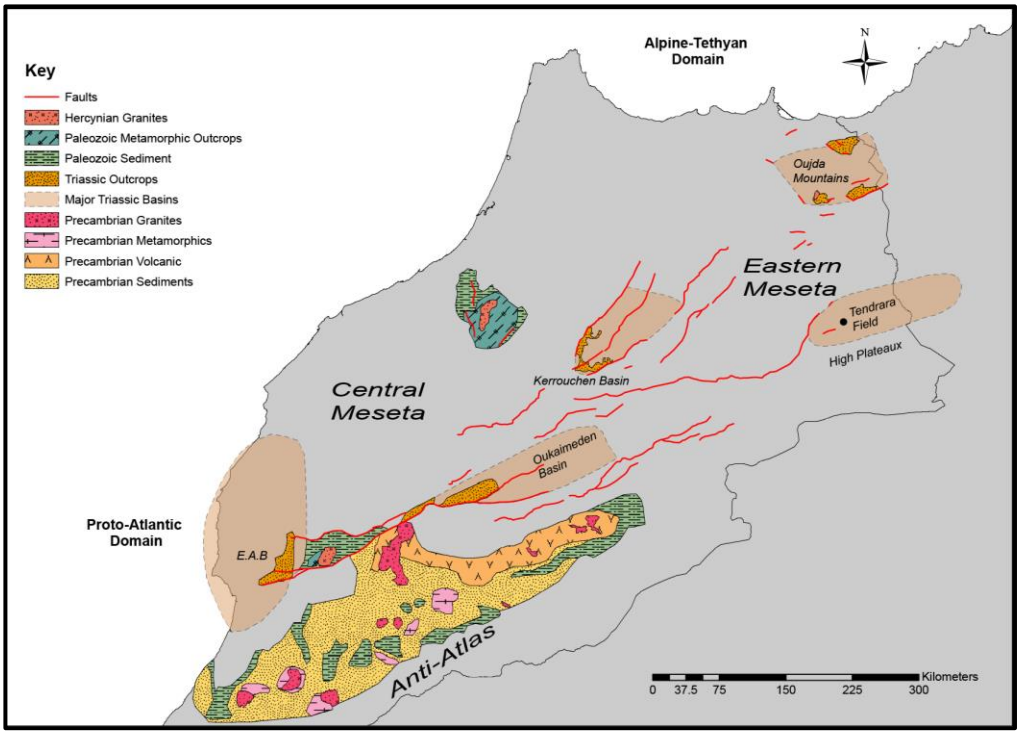

Figure 1-3: Map of the Triassic rift basins of Morocco with the remnants of the Variscan Chain. The Oukaimden, Kerrouchen and the Tendrara region of the High Plateaux were studied as part of this thesis (modified from Michard et al. 2008).

1.3.1. Oukaimeden Basin Literature Review

The Oukaimeden-Ourika basin in the Central High Atlas *(Figure 1-3)* is a 50km by 10km ENE-WSW valley which preserves a Permo-Triassic continental syn-rift succession within an inverted rift basin (Benaouiss *et al.* 1996; Domènech *et al.* 2015). The mid-Triassic rifting led to the formation of a series of NE-ENE trending horsts and grabens controlled by reactivated Hercynian or older faults (Baudon *et al.* 2009; Domènech *et al.* 2015). The Oukaimeden-Ourika Valley also contains a secondary fault population which trends NNE-SSW, sub-parallel to the major structural trend within the Atlasic Rift (Le Roy & Piqué 2001; Laville *et al.* 2004), which were active during sedimentation in the Triassic (Baudon *et al.* 2009).

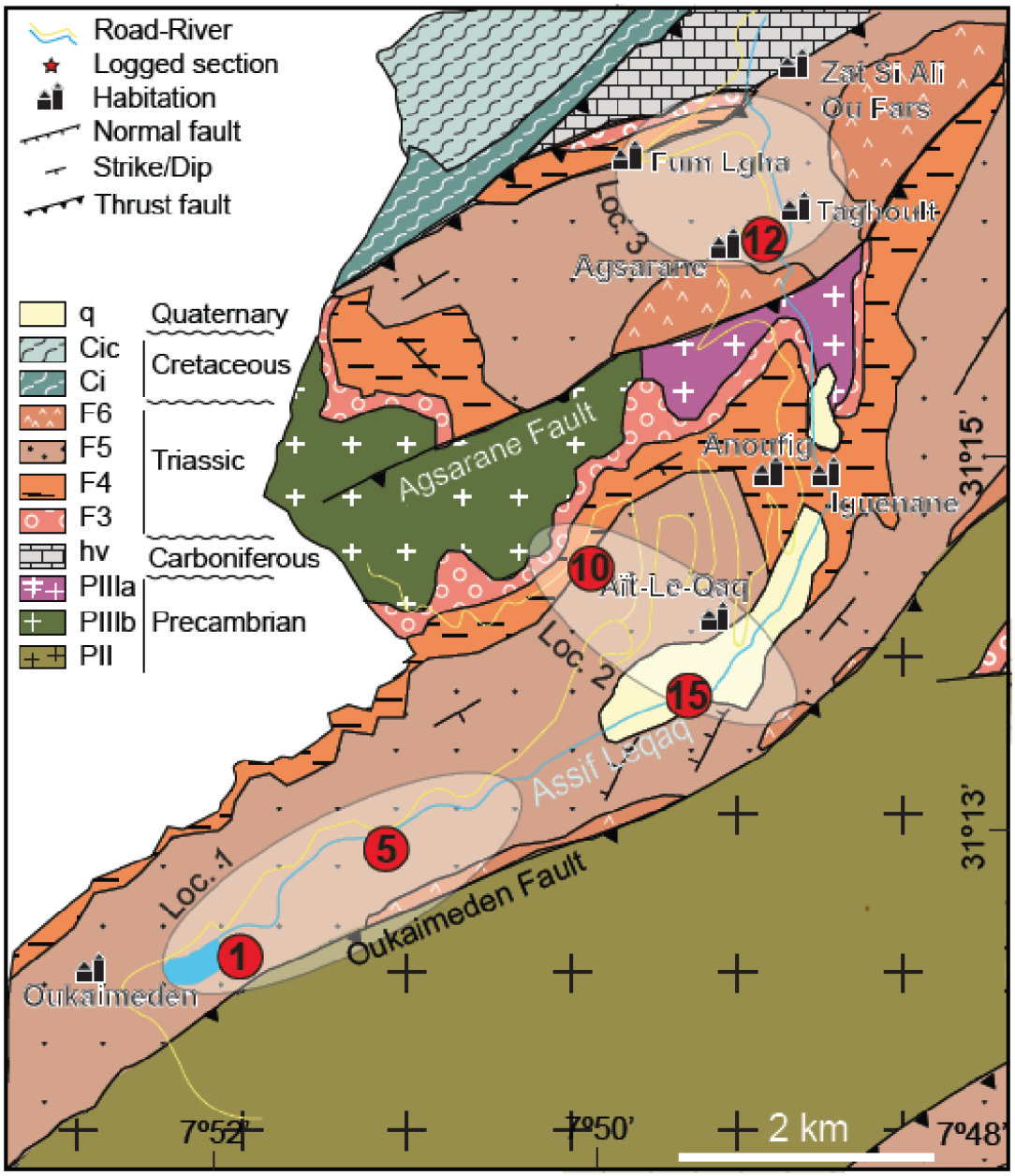

Figure 1-4: Map of the Oukaimden Basin with the key localities of study within the basin (Fabuel-Perez et.al. 2009)

The stratigraphy of the Oukaimeden Valley and the Central High Atlas is well constrained and can be summarised as a syn-rift continental succession similar to those observed across Morocco *(Figure 1-2)* (Beauchamp 1988; Oujidi *et al.* 2000). The basal Permian formations, the Anrar Conglomerate (F1) and Cham-El-Houa Siltstones (F2), are not present within the Oukaimeden Basin (Baudon *et al.* 2009), with the basal Triassic conglomerate directly overlying the Palaeozoic basement (Fabuel-Perez *et al.* 2009). The 45m thick basal conglomerate (F3) consist of massive conglomerates interbedded with sandstones and siltstones, which are interpreted as Alluvial-Fluvial fans (Baudon *et al.* 2009). This is overlain by the Ramuntcho Siltstone (F4), a 175m thick unit of siltstones and trough cross-bedded medium grained sandstones representing braided streams and floodplain deposits

(Baudon *et al.* 2009; Fabuel-Perez *et al.* 2009). The Ramuntcho Siltstones is sharply overlain by the Oukaimeden Sandstone (F5), up to 300m of fluvial-aeolian to tidally influenced deposits, which are unconformably overlain by the evaporitic mudstone of the Upper Siltstone (F6) (Beauchamp 1988; Benaouiss *et al.* 1996).

The Oukaimeden Sandstone (F5 Formation) can be subdivided into 3 members (Figure 1-5) and has been found to consist of five principle facies associations (Figure 1-6) (Fabuel-Perez *et al.* 2009). The Lower-F5 consists of isolated sandy channels with accretionary bars within extensive overbank mudstones interpreted to be deposited as part of an ephemeral braided fluvial system (Fabuel-Perez *et al.* 2009). The Middle F5 is marked by a regional erosive surface *(Figure 1-6) (*(Fabuel-Perez *et al.* 2009). This member is marked by the occurrence of thick, sand-rich multi-storey channel complexes representing a perennial fluvial system (Fabuel-Perez *et al.* 2009). The Upper F5 formation is a aeolian-fluvial mixed system consisting of FA-1, FA-2 and FA- and is characterised by the first occurrence of aeolian deposits within the Oukaimeden valley (Fabuel-Perez *et al.* 2009) with occurrences of tidal deposits in the north-eastern extremes of the basin (Benaouiss *et al.* 1996; Fabuel-Perez *et al.* 2009). The occurrence of these tidal deposits represents the first evidence of the Tethyan occurrence into the Central High Atlas Rift (Benaouiss et al. 1996).

The Lower-F5 is believed to have formed during the initiation of rifting during an arid climatic interval, resulting in the formation of an ephemeral axial fluvial system (Fabuel-Perez *et al.* 2009). The Middle-F5 member represents a transition to a more humid climate, with increased runoff leading to fluvial rejuvenation and incision into the underlying lower-F5 (Fabuel-Perez *et al.* 2009). The transition to fluvial-aeolian deposits recorded in the Upper-F5 member indicates a shift back towards the arid conditions of the Lower-F5 member prior to the onset of coastal plain to shallow marine conditions of the Upper Siltstone formation (Fabuel-Perez *et al.* 2009).

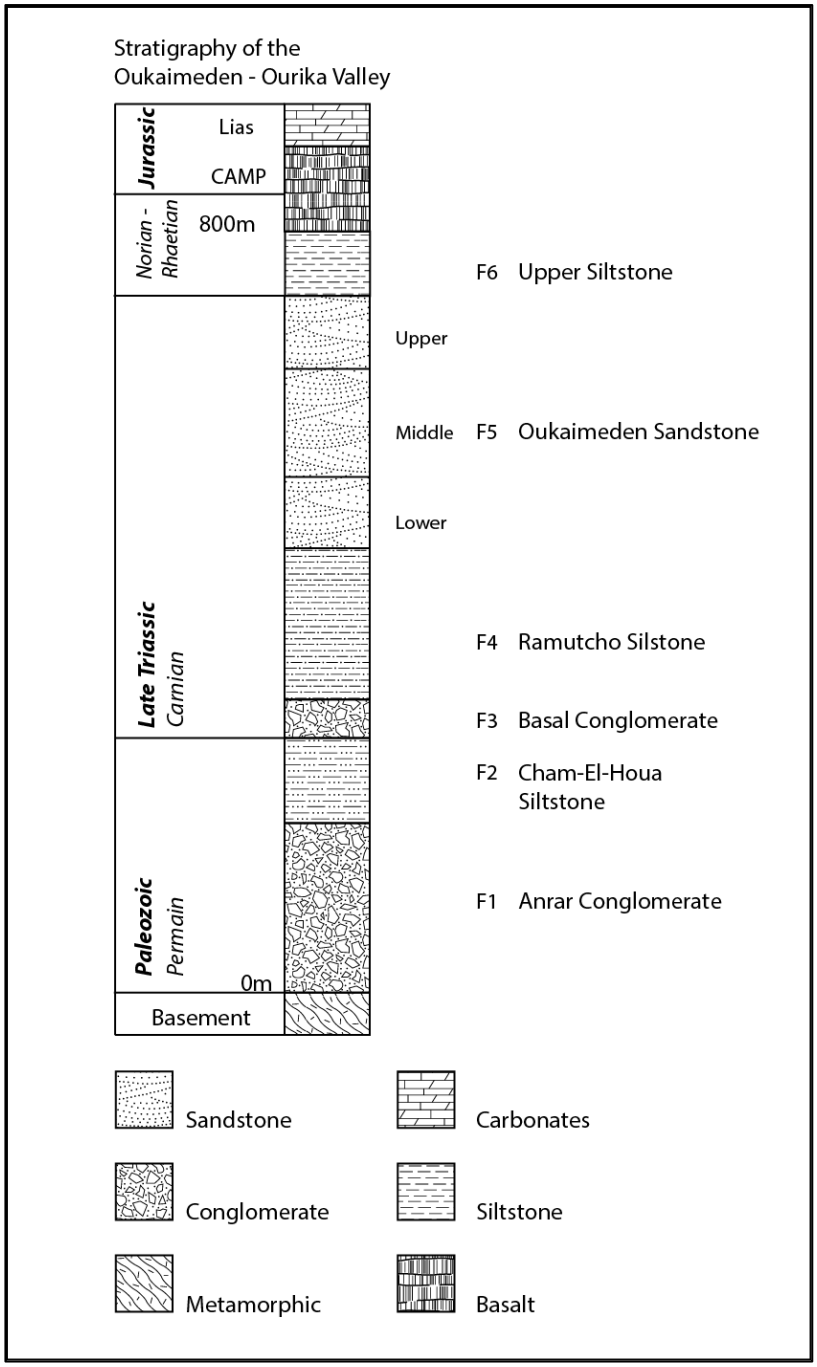

Figure 1-5: Triassic stratigraphy of the Oukaimeden-Ourika Valley. Created from data published in (Baudon et al. 2009; Fabuel-Perez et al. 2009) and references therin.

The Oukaimeden Sandstone represents an axial fluvial system which was tectonically controlled and flowed towards the NE as evidenced by the orientation of paleoflows parallel to the major structural trends (Baudon *et al.* 2009) *(Figure 1-6)*. The fluvial system was sourced in part by transverse alluvial fans flowing into the basin axis perpendicular to the major faults, from which they were sourced *(Figure 1-6)* (Baudon *et al.* 2009).

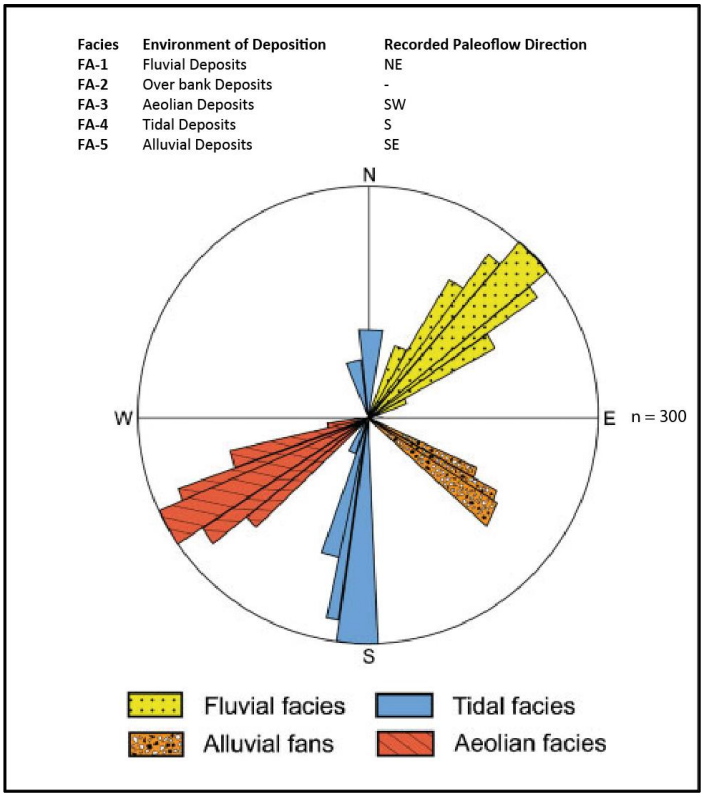

Figure 1-6: Facies Associations observed within the Oukaimeden Basin with interpreted environment of deposition and paleoflow direction variation with facies. The paleoflow directions recorded in the fluvial facies run between NNE-ENE, parallel to sub-parallel to the major structural trends (Baudon et al. 2009; Fabuel-Perez et al. 2009). The paleoflow data suggests the fluvial system was directed towards the Middle Atlas Rift and there was a tectonic control on the fluvial system.

1.3.2. Kerrouchen Basin

Introduction

Three days fieldwork was undertaken in the Kerrouchen Basin, situated in the southern Middle Atlas mountain belt between the Coastal and Eastern Meseta *(Figure 1-3)* (Hoepffner et al. 2005; Michard et al. 2008). The Kerrouchen Basin preserves a Triassic fluvial red bed sequence (Lorenz 1976, 1988). This field study builds on the wealth of work done in the Triassic of the Central High Atlas (e.g. Benaouiss *et al.* 1996; Baudon *et al.* 2009; Fabuel-Perez *et al.* 2009; Mader & Redfern 2011; Mader *et al.* 2017) in a basin which could be an important analogue for sub-salt Triassic plays in the Eastern Meseta.

Previous Workers

The previous literature on the Triassic succession of the Kerrouchen Basin is sparse, however it is known to be a inverted asymmetric half graben filled by 600m of Triassic syn-rift continental sediments overlain by the Jurassic carbonates towards the north of the basin *(Figure 1-7)* (Lorenz 1976). The basin was inverted during the Cenozoic Atlasic Orogeny, preserving the original geometry (Laville *et al.* 2004). The basin is bounded by major faults trending NNE-ENE with the Southern Middle Atlas Fault (SMAF) accommodating most of the displacement along the eastern boundary of the basin (Ouarhache *et al.* 2012). The major bounding faults are likely to have been active during the Variscan Orogeny and subsequently reactivated during the subsequent rifting of Pangea and Atlasic inversion as observed across the Marrakech and Central High Atlas (Le Roy & Piqué 2001; Baudon *et al.* 2009; Soulaimani *et al.* 2014; Domènech *et al.* 2015). The Kerrouchen Basin is cut by numerous smaller faults which are sub-parallel to the major structural trend which could have formed a series of intra-basinal highs in the Triassic with important implications for sediment sourcing and routing within the basin (Baudon *et al.* 2009).

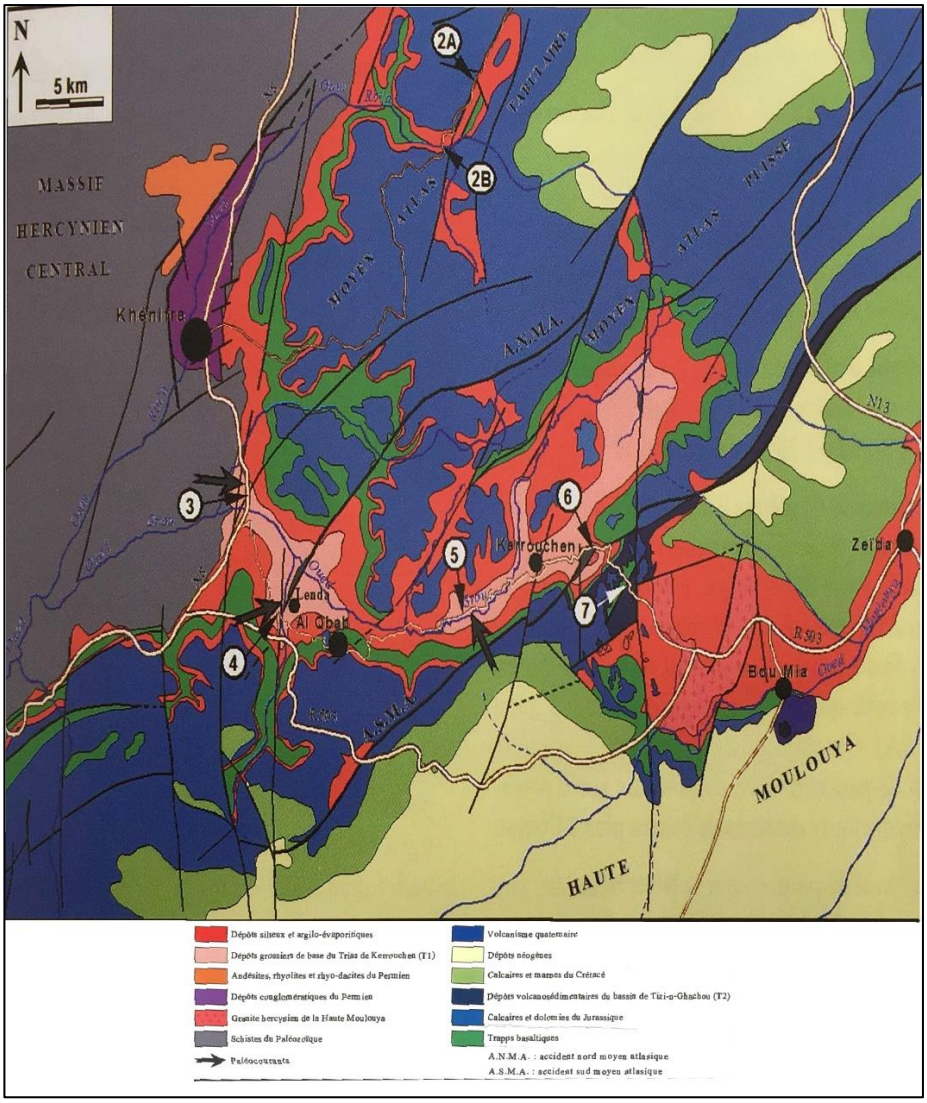

Figure 1-7: Map and cross-sections of the Kerrouchen Basin, indicating how the basin geometry has been inverted, but the original geometry has been mostly preserved. Key sampling locations within this study were localities 3,4,5 and 6. (Charriere *et al.* 2011, p. 69)

The Triassic stratigraphy of the Kerrouchen Basin contains a Carnian-Norian coarse continental syn-rift succession overlain by a Norian lagoonal mudstone *(Figure 1-8),* consisting of basal conglomerate of variable thickness (K1 Formation) overlain by 80m of fluvial sands (K3 Formation) and 250m of alluvial conglomerates and fluvial arkoses (K4 formation). The sequence is capped by 50 to 275m of mudstones which have been described as evaporitic (K5 Formation) (Lorenz 1976, 1988; Ouarhache *et al.* 2012). There are thick tholeiitic basalts present across the basin which erupted in a series of lava flows between Norian and the Sinemurian, 210±2.1 to 201±1.0 Ma, representing the CAMP volcanic event (Fiechtner *et al.* 1992).

Field Observations

During the fieldwork conducted within the Kerrouchen Basin, 9 principal lithofacies were observed and described here for the first time, which formed 5 distinct facies associations *(Table 1-A).* Facies association 1 (FA-1) comprises conglomeratic (Gms-b) overlain by massive mudstones (Fm). The conglomerates of FA-1 are found near the basin margin and intra-basinal paleohighs where they onlap Palaeozoic phyllites *(Figure 1-9)* and were observed at locality KH-70 *(Figure 1-7)*. The conglomerates thicken downslope before rapidly grading into laterally discontinuous mudstones.

Facies association 2 (FA-2), is the most sand rich within the Kerrouchen Basin and occurs predominantly to the west of the basin, along transect D between localities KH-10 and KH-20,30 *(Figure 1-7).* This facies association has 3 members form east to west, FA-2a, FA-2b, FA-2c, which all share similar characteristics. FA-2a consists of conglomerates and coarse sand channels, Gms-m, overlain by sheet-like medium sands, Sh, and siltstones, Fm. This repetition of lithofacies forms sequences of up to 3m thickness, with a total thickness of up to 20m.

FA-2b consists of up to 40m of small stacked sandstone channels of lithofacies Sl, with laterally equivalent deposits sheet like sandstones and interbedded mudstones, lithofacies Sh and Fm respectively. Within Fa-2b, lithofacies Sh is locally calcareous forming calc-arenites. FA-2c consists of 20m of isolated sand rich channels of lithofacies Sp within laterally extensive bodies of lithofacies Fm. In total, FA-2 was observed to be 80m thick and located in more axial basin positions than FA-1.

Facies association 3 (FA-3), contains a combination of lithology's observed in FA-1 and FA-2. It is primarily recorded further in the east of the Kerrouchen Basin between localities KH-40,50 and 60. At KH-60, stacked conglomeratic channels of lithofacies Gms-c cut into well-developed paleosols. These channels are laterally equivalent to sheet-like medium sands with small isolated channels overlain by silt-rich mudstones, lithofacies Sh and Fl. Moving up through the stratigraphy to the west towards KH-50 and KH-40, the conglomeratic channels become rarer and the sand-mud intervals become less distinct, with lithofacies Sh having increased silt content, until at the top of the succession only lithofacies Fl remains *(Figure 1-11)*

The Triassic sequence within the Kerrouchen Basin is capped by massive silty mudstones of lithofacies Fsc. This facies association directly overlies FA-1 at the basin margin and FA-2 and FA-3 in more basinward settings.

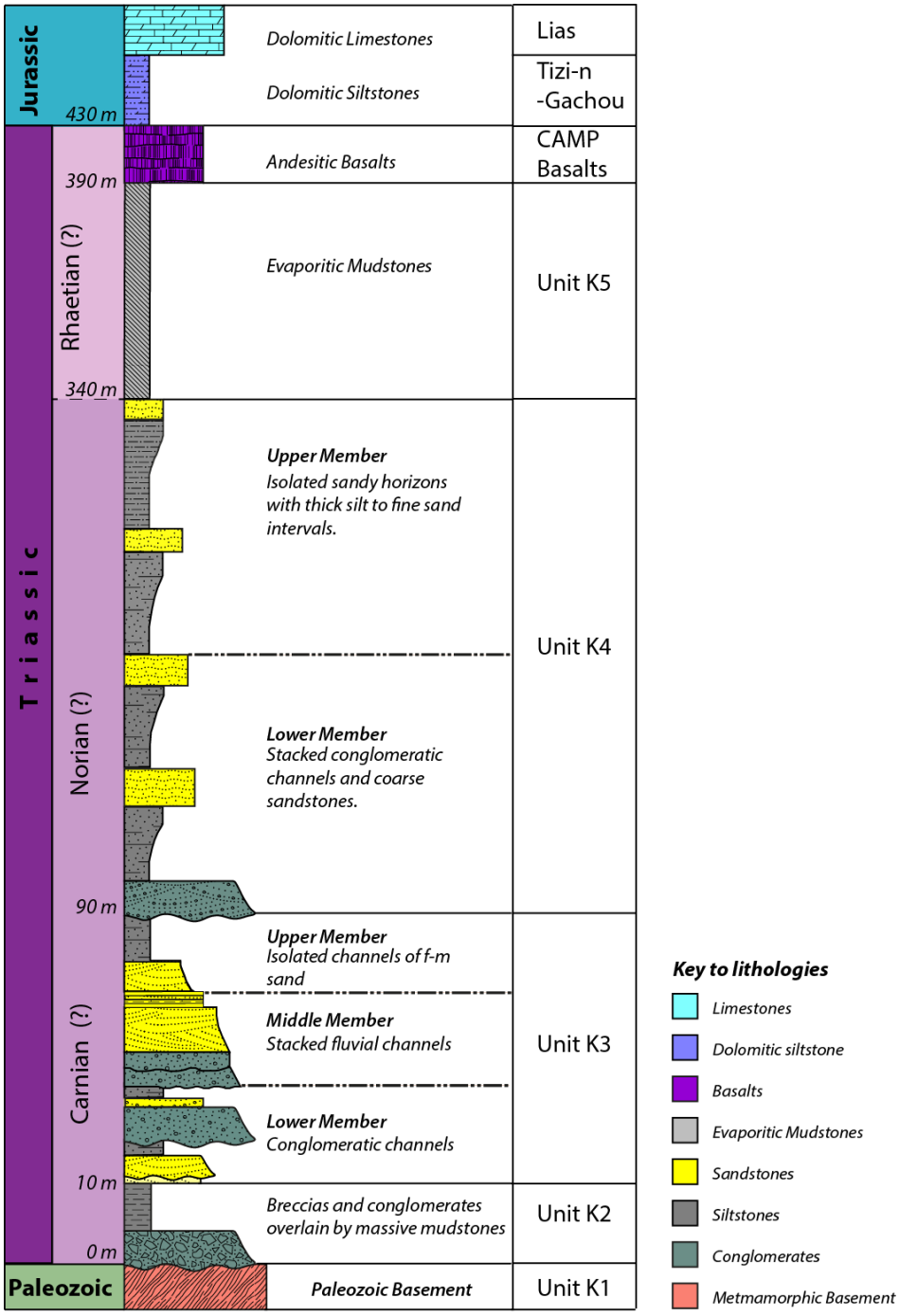

Figure 1-8: Composite log of the Kerrouchen Basin based on merging field observations with the stratigraphy of previous workers (Lorenz 1976; Ouarhache et al. 2012).

Code	Lithofacies	Description	Interpretation	Thickness
Gravel Rich Lithofacies				
Gms - b		Poorly sorted, angular clasts within a silt matrix. Sharp contacts. Thick to massive beds with some indistinct imbrication and large scale cross bedding with forsets dipping up to 30°.	*Debris flow deposits formed as part of alluvial fans.*	0.5m - 5m
Gms - c	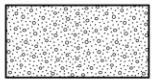	Poorly sorted rounded to sub-rounded clasts within a coarse sand matrix. Occur in cross-cutting channel bodies which display a fining up trend.	*Debris flow deposits forming new alluvial flows (channels).*	1m - 2m
Gms - m	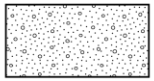	Poorly sorted well rounded, mudclasts in a medium sand matrix. Thin to medium bedded with erosive bases and sharp tops. The beds contain no structures.	*Braided stream deposits.*	0.1m - 0.3m
Sand Rich Lithofacies				
Sh	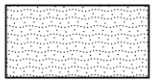	Moderately sorted, rounded , medium to coarse sand grains in a silt matrix. Tabular, thinly bedded with sharp tops and undulating bases. The beds contain ripple laminations and low angle cross bedding.	*Planar bed flow features under lower and upper flow regimes, formed during flash floods in crevasse splays.*	0.1m - 0.3m.
Sp	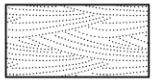	Well sorted, fine to medium, planar (15 °- 35°) cross-bedded sandstones in isolated channel bodies, with a general fining up trend.	*Migration of dunes under lower flow regime conditions in a meandering channel system.*	0.3m - 1.5m
Sl	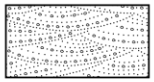	Poorly sorted, medium to coarse sand in thin to thickly bedded sandstones with lags of very coarse sand displaying both trough and low angle planaar (15 °) cross bedding.	*Lower flow regime scour fills, dunes and antidunes, deposited during waning flow conditions.*	0.1m - 1.0m
Mud-rich Lithofacies				
Fl	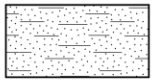	Massive, laterally extensive beds of silt and fine sand containg rare, thin paleosols. Beds display an increased sand content near the top of the beds.	*Overbank or waning flood deposits with long periods of exposure leading to paleosol formation.*	0.5m - 10m
Fm		Thick structureless, siltstone deposits with rare, fine sand lags.	*Overbank deposits.*	0.3m - 10m
Fsc	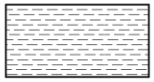	Massive, structureless mudstones	*Delta-plain to marginal marine mudstones.*	2m - 10m

Table 1-A: Lithofacies observed within the Kerrouchen Basin. Lithofacies nomenclature adapted from Miall 1985 (Miall 1985)

Discussion

The observations of the lithofacies within FA-1 match the descriptions of Unit K2, the basal unit of the Triassic of the Kerrouchen Basin *(Figure 1-8).* This formation was first described by Lorenz and is interpreted to represent alluvial fans feeding into the basin, sourced from basinal paleohighs (Lorenz 1976).

The FA-2 lithofacies association matches descriptions by Lorenz and Ouarhache of the K3 formation which has been interpreted to represent an axial fluvial system (Lorenz 1976; Ouarhache *et al.* 2012). However, the observation of 3 distinct sub-facies within the fluvial sands of the K3 Formation had not previously been identified and could indicate subtle shifts in the fluvial style. The conglomeratic channels overlain by sheet like sands and mudstones (FA-2a) suggests high-energy ephemeral fluvial system. The stacked sandstones channels of FA-2b suggest a transition to more perennial conditions with the local carbonates forming due to evaporation of calcite rich water on the floodplain *(Figure 1-10)*. The transition back to isolated sandy channels of lithofacies Sp within muddy overbank deposits of lithofacies Fm, is interpreted to represent a lower-energy, meandering perennial to ephemeral fluvial system. Whilst this model explains the observations made, detailed fieldwork is required to assess whether these variations can be recognised across the basin.

Figure 1-9: Basin Margin Unconformities. Photo A and B show the Triassic eroding into Paleozoic basement in the western part of the basin. Photo C and D show the Triassic onlapping onto Hercynian Basement at the eastern basin margin.

FA-3 matches descriptions made by previous workers of the K4 formation *(Figure 1-8)* and was interpreted as an alluvial or fluvial system which displays decreasing energy due to proximity to a large body of water, potentially the fluvial system responding to the Tethyan incursion along the

Middle Atlas rift (Lorenz 1976; Ouarhache *et al.* 2012). However, this facies variation can also be explained as an alluvial-fluvial fan, as there is a fining trend towards the basin centre observed within FA-3 of the K4 formation.

FA-4 is the equivalent of the K5 formation which has been interpreted to have been deposited to be a coastal plain to lagoonal mudstone which was deposited regionally during the upper Triassic (Lachkar *et al.* 2000; Ouarhache *et al.* 2000; Fabuel-Perez *et al.* 2009) and thought to be related to the onset of the Tethyan transgression along the Middle Atlas Rift and forms Unit K5 in the Kerrouchen Basin *(Figure 1-8)* (Ouarhache *et al.* 2012). Previous workers have described the K5 Formation as evaporitic, however no evidence of this was observed in the field.

Figure 1-10: FA-2b exposed near the basin axis. FA-2b is comprised of amalgamated fluvial sands, with minimal overbank fines. The facies association reaches up to 30m thick in this locality, indicating a perennial fluvial system was responsible for the deposition of these sands.

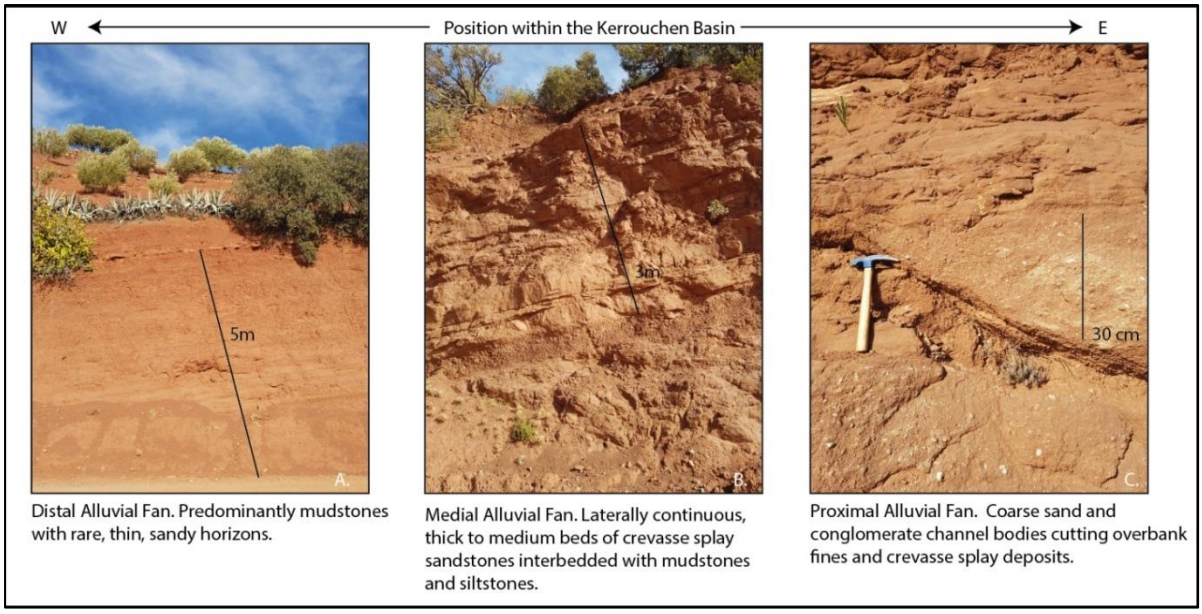

Figure 1-11: A) Photo of lithofacies Gms-c. B) Photo of lithofacies Sl and Fm. Note the sandier intervals (Sl) stack, however this decreases as you move through the formation as seen in photo C). C) Thin, isolated beds of lithofacies Sl with thick mudstones of lithofacies Fm, near the top of the K4 formation.

Within the Kerrouchen Basin, it is clear that three principle depositional systems existed at varying times throughout the basins history; transverse (K2 formation), axial (K3 formation) and transverse-axial (K4 formation). The paleoflows recorded in these depositional systems supports the idea of transverse alluvial fans and axial fluvial systems running parallel to the basin trend *(Figure 1-12).* Within the K2 and K4 formation, paleoflows within the conglomeratic facies indicate flows from paleohighs in all directions towards the basin floor. However, within the sand rich intervals of the K3 and K4 formations paleoflows are consistently towards the NNE-ENE, indicating flow from the SSW-WSW. The paleoflow data supports the recognition of the three depositional systems and allows reconstruction of the basin paleogeography, with transverse alluvial fans flowing from paleohighs towards the basin where axial fluvial systems have developed. The presence of the sand rich K2 formation in the west of the basin has been interpreted to suggest the axial fluvial system could perhaps have been pinned in the west of the basin.

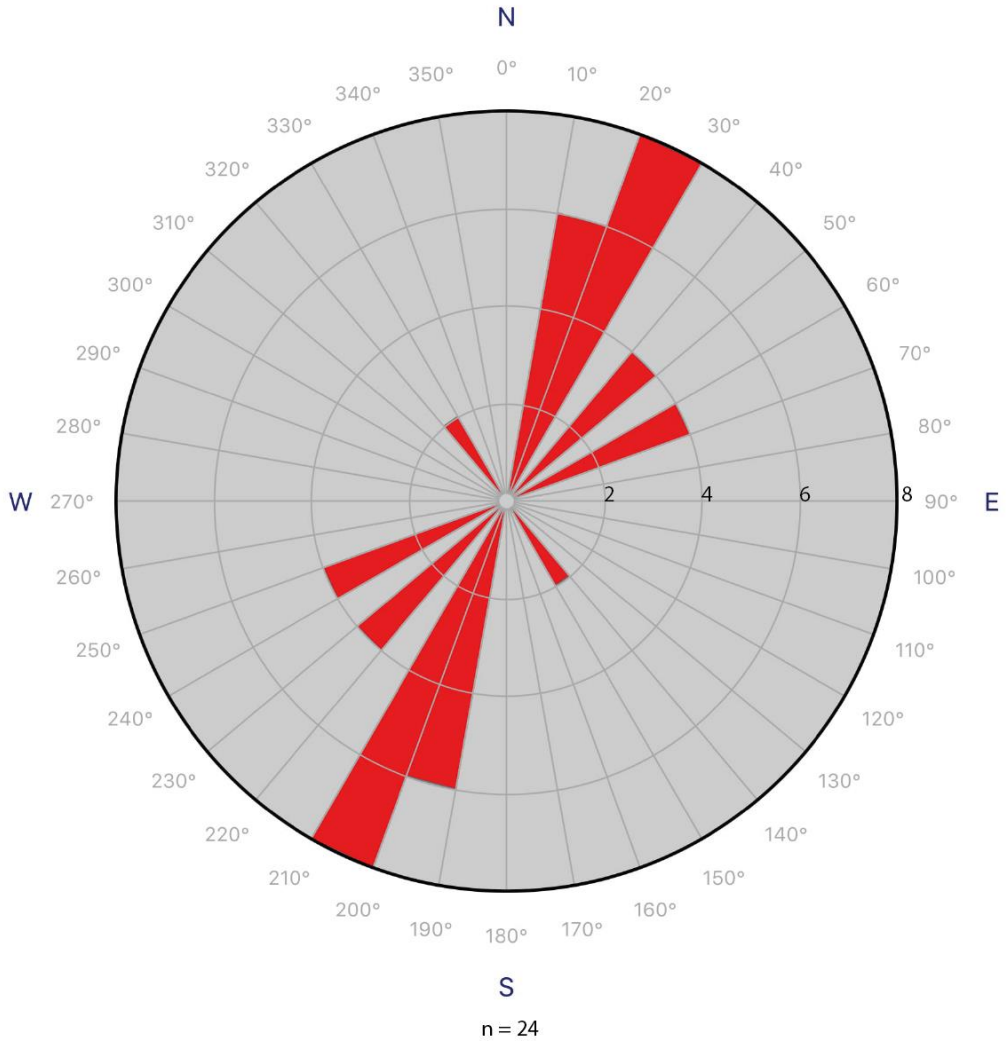

Figure 1-12: Paleoflow data from the Triassic of the Kerrouchen Basin. The primary paleoflow direction of NNE is recorded within K3 and K4 formations and runs parallel to sub-parallel to the major basin structures. The SE orientated paleoflows were recorded in a K2 formation conglomerate resting unconformably on a basement paleohigh, flowing towards the major basin depocentre, shown in the image on the right

1.3.3. Tendrara Field

The Tendrara Fieldis situated in the Eastern Meseta tectonic domain *(Figure 1-3)* (Michard *et al.* 2008) and is part of the larger High Plateaux Basin, a Triassic rift basin with a predominantly evaporitic basin fill (Ouijidi *et al.* 2000). The Tendrara Fieldis a trans-tensional rift basin controlled by deep rooted basement faults orientated NE-SW (Hafid & Benaouiss 2010; Kape 2017) which have been reactivated in multiple orogenic cycles (Hafid & Benaouiss 2010), similar to the faults controlling Triassic basins within the Central High Atlas (Domènech *et al.* 2016).

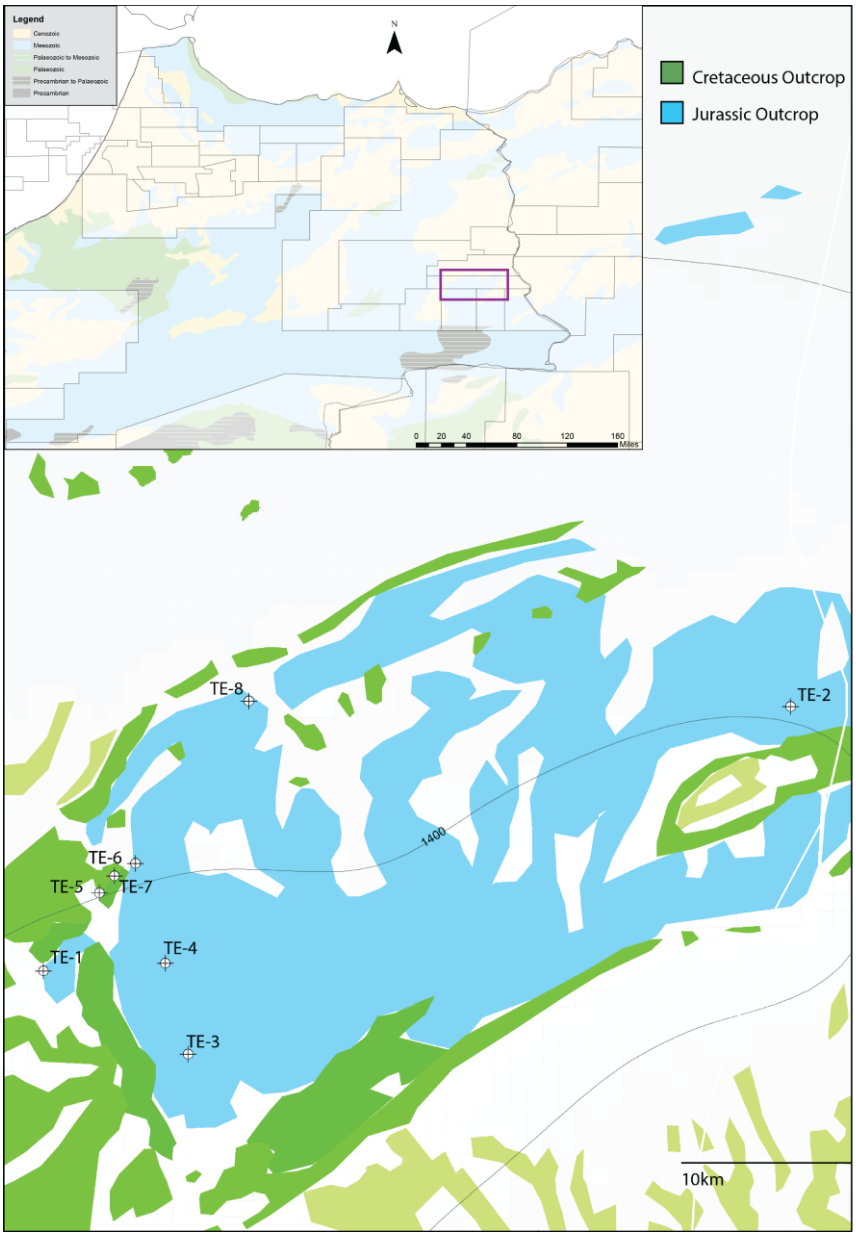

Figure 1-13: Location of the Tendrara Wells within the High Plateau Basin and the position of the basin within Morocco. In this study, all wells were analysed petrographically, with the TE-6 and TE-8 wells logged and samples selected from Heavy Mineral Analysis. Image provided by Sound Energy

As seen elsewhere in Morocco, rifting began in the Middle Triassic (Laville *et al.* 2004; Hafid & Benaouiss 2010) with syn-rift deposition of a continental siliciclastic sequence overlain by evaporites related to the Tethyan transgression throughout the Late Triassic *(Figure 1-5)* (Ouijidi 2000; Fabuel-Perez *et al.* 2009). Within the Tendrara Basin, the TAGI reservoir interval, a major oil and gas reservoir across North Africa (e.g. Rossi *et al.* 2002), has been drilled (Hafid & Benaouiss 2010). The regional occurrence and correlation of the TAGI-I and TAGI-II sequences from the Tendrara Fieldwith the TAGI in Algeria has been interpreted by previous workers to suggest an extrinsic control on deposition, likely related to regional tectonic (e.g. hinterland reorganisation) or climatic (e.g. variation in precipitation) changes (Kape 2017). However, there is little chronological data to support this correlation and correlating sand bodies between wells from within the TAGI-I and TAGI-II has not been achieved accurately (Kape 2017) with attempts based on spatial and temporal facies variations (e.g. Benvenuti 2017). Within both the TAGI-I and II a fining up pattern can be observed (Kape 2017), and 8 lithofacies associations have been identified from across the cored intervals within the Tendrara wells and are displayed in an 'idealised sequence' below *(Figure 1-14)* (Hafid & Benaouiss 2010).

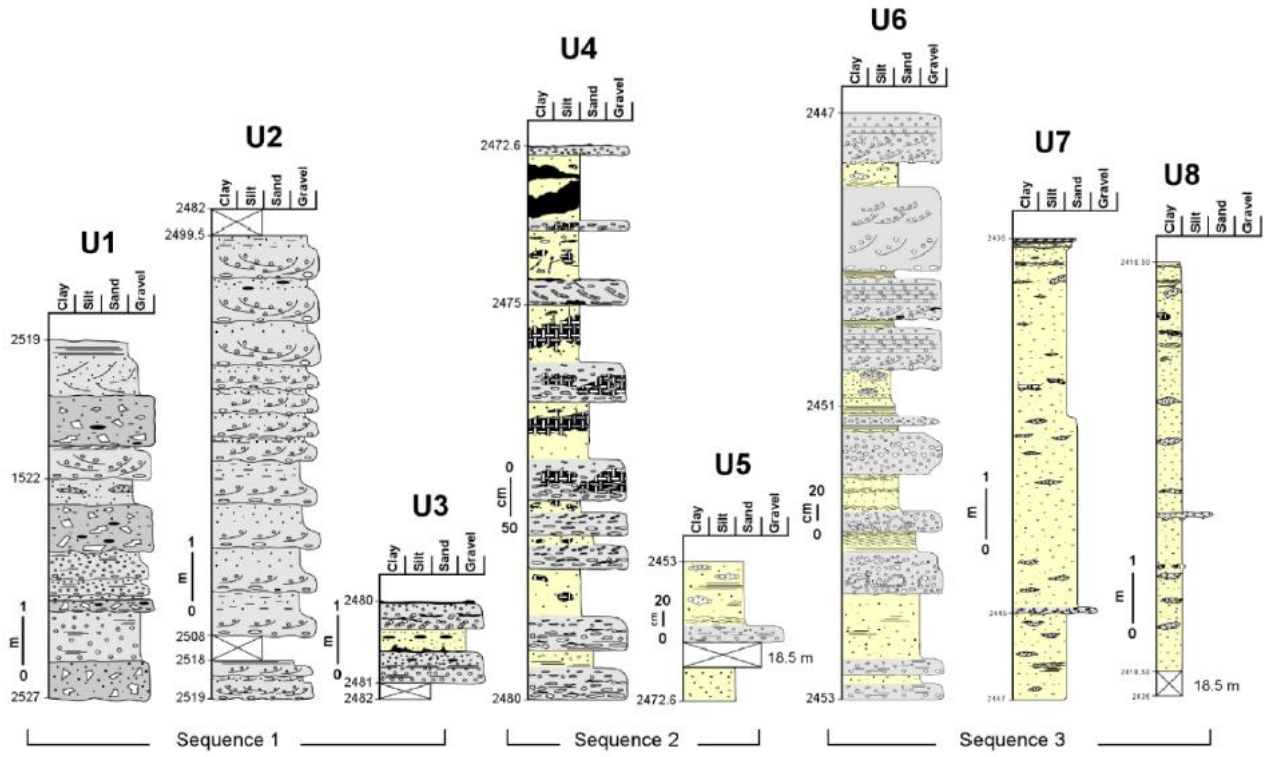

Figure 1-14: Idealised logs of the depositional sequences (U1 to U-8) identified from the Triassic Formation in the Tendrara Cores from by Hafid & Benaouiss 2010

TE-6 and TE-8 Core Analysis

Sound Energy provided access to the TE-6 and TE-8 core at the ALS core facility, Normandy, Surrey in order to compare the lithofacies identified by previous workers to the facies observed during fieldwork within the Kerrouchen Basin. Further analysis was conducted on the TE-6 and TE-8 cores collected by Sound Energy, with samples and thin sections provided for petrographic and heavy mineral analysis (Appendix 1, Appendix 2). All lithofacies (U1-U8) *(Figure 1-14)* were recognisable within these cores, however not in the sequential model proposed by previous workers (Hafid & Benaouiss 2010) and are described below.

Lithofacies U1 consisted of conglomerates with gravel sized clasts in a silt-rich matrix and was overlain by lithofacies U2, matrix supported gravelly conglomerates which graded into coarse sands within metre scale beds with erosive bases. The U3 lithofacies consisted of alternating beds of clay rich matrix supported gravelly conglomerates with sharp contacts with sandstones with rare gravelly lags (*Figure 1-14).* These three lithofacies have been identified as belonging to sequence 1 of the Triassic within the Tendrara field, which contains the lowermost TAGI-I interval (Hafid & Benaouiss 2010).

Sequence two begins with lithofacies U4, which consists of 8m of conglomerate – sandstone - siltstone packages, starting with a basal conglomerate containing reworked paleosols sharply overlain by clay rich sands which grade into sand rich siltstones. In general, lithofacies U4 fines upwards, with each package being finer than the preceding one. The U5 lithofacies is similar, however the sand intervals have been observed to have low angle to parallel planar lamination in parts (Hafid & Benaouiss 2010). The U4 and U5 lithofacies have been grouped together as sequence 2 and contains the upper TAGI-I interval (Hafid & Benaouiss 2010)

Sequence 3 of the Triassic of the Tendrara field is comprised of three lithofacies, U6, U7 and U8. Lithofacies U6 contains thick conglomeratic intervals with matrix supported gravelly clasts overlain by parallel laminated sands, with convolute lamination reported in some cores (Hafid & Benaouiss 2010). The sand intervals fine to silt near the top of U6. Lithofacies U7 is fine sand and silts with thin, rare conglomeratic beds. Lithofacies U8 is a mudstone with pedogenic carbonates *(Figure 1-14).*

Discussion

The lithofacies associations described in the Tendrara cores have been interpreted as either axial fluvial deposits (Hafid & Benaouiss 2010) or alluvial-fluvial fan deposits (Benvenuti 2016, 2017; Kape 2017). Based on a comparison between the lithofacies associations observed in the TE-6 and TE-8 core and the lithofacies within the Kerrouchen Basin, the cores most closely resemble the K4 formation *(Figure 1-15,Figure 1-16)* which is interpreted as an ephemeral alluvial-fluvial fan system. Within continental basins, this type of unconfined, distributary system is the predominant fluvial style

(Weissmann *et al.* 2010) and is common in basins suggested as an analogue for the Tendrara field such as within the Basin and Range Province, USA (Kape 2017) or the Kobo Basin, Ethiopia (Benvenuti 2016). Whilst these systems can be high quality reservoir intervals, for example within the TAGI of Algeria (Galeazzi *et al.* 2010), the presence of pedogenic carbonates in the TE-6 core could reduce porosity and reservoir quality *(Figure 1-15).*

Paleoflow indicators have not been identified from the cores, however regional isopach data has found the TAGI thickens to the SW (Kape 2017). This has been interpreted as the regional drainage direction, with drainage from the N/NE flowing S/SW towards the Atlantic domain (Kape 2017). However, when the paleoflow data from the CHA *(Figure 1-6)* and the Kerrouchen Basin *(Figure 1-12)* alongside the drainage divide across the Marrakech High Atlas (Fabuel-Perez *et al.* 2009; Domènech *et al.* 2015; Mader *et al.* 2017) and the presence of regional south to north sediment transport during the Triassic (Domènech *et al.* 2018) are considered, this paleogeographic model appears to be incorrect.

If the Central and Middle High Atlas were not in communication during the Triassic, there is then a possibility that the High Plateaux and Tendrara Fieldwere part of a regional drainage system within the Eastern Meseta which drained north to south (Hafid & Benaouiss 2010; Kape 2017). This drainage system would have drained the remnant internal Variscan belt and volcanic arc of the Eastern Meseta (Michard *et al.* 2008). However, this drainage network is unlikely to have reached the Atlantic due to the uplift zones between the High Plateaux and the Atlantic (Domènech *et al.* 2015, 2018), implying the presence of sink to the south of the High Plateaux. Identifying whether these basins have a shared sediment provenance will allow for the identification of a likely source terrain and regional drainage and sediment dispersal reconstructions.

It has been suggested that the TE-8 80 sample correlates with the F4 formation and the TE-8 73, 65 and TE-6 77 sample correlate with the F5 formation of the CHA *(Figure 1-5)* (Benvenuti 2017). Based on the facies analysis of the core and field observations in the Kerrouchen and Oukaimeden Basins, as well as previous workers in the Central High Atlas (Fabuel-Perez *et al.* 2009; Mader & Redfern 2011) a more accurate correlation would be with the K4 formation of the Kerrouchen Basin *(Figure 1-8, Figure 1-15,Figure 1-16).* To utilise the Kerrouchen Basin as an analogue for the Tendrara Field more work is required within the Kerrouchen Basin to better understand the distribution and controls on the distribution of sand rich facies in order to develop a reservoir model for the Tendrara Field.

To test these hypotheses 27 thin sections from the TAGI reservoir intervals and four samples from the TAGI (TE-6 77, TE-8 65, 73, 80) have been selected for heavy mineral analysis. The TE-6 77 sample is from lithofacies U4 (Hafid & Benaouiss 2010) and represents a broad fluvial channel (Benvenuti 2016) within the upper TAGI-I interval. The TE-8 65, TE-8 73 and TE-8 80 samples are from lithofacies U3 of the lower TAGI-I (Hafid & Benaouiss 2010) and are interpreted to be a crevasse channel (Benvenuti 2017). The variations seen within the TAGI facies which have been recognised

from Algeria and within the Tendrara Field(Kape 2017) should be identifiable within the heavy mineral assemblage. A tectonic event should change the available source material for weathering and be preserved as a change in provenance, whereas a climatic event should result in a variation in apatite preservation with no other change in provenance (e.g. Morton & Hallsworth 1994).

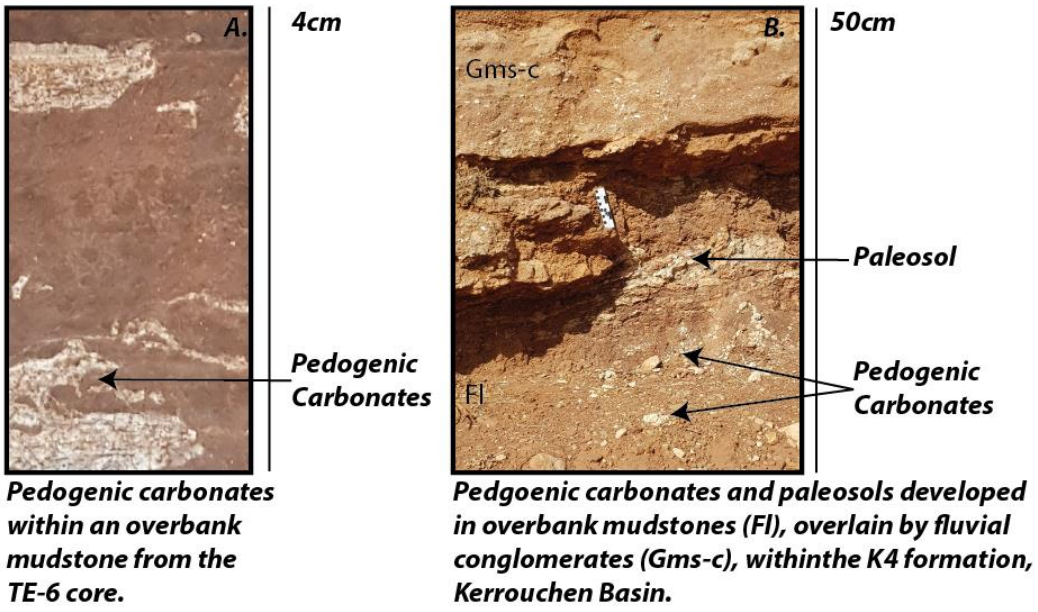

Figure 1-15: Pedogenic carbonates and paleosols within the TE-6 core and the K4 formation, Kerrouchen Basin. The presence of these features is interpreted to represent evaporation of standing water on the flood-plain and could impact the reservoir quality within the Tendrara Field.

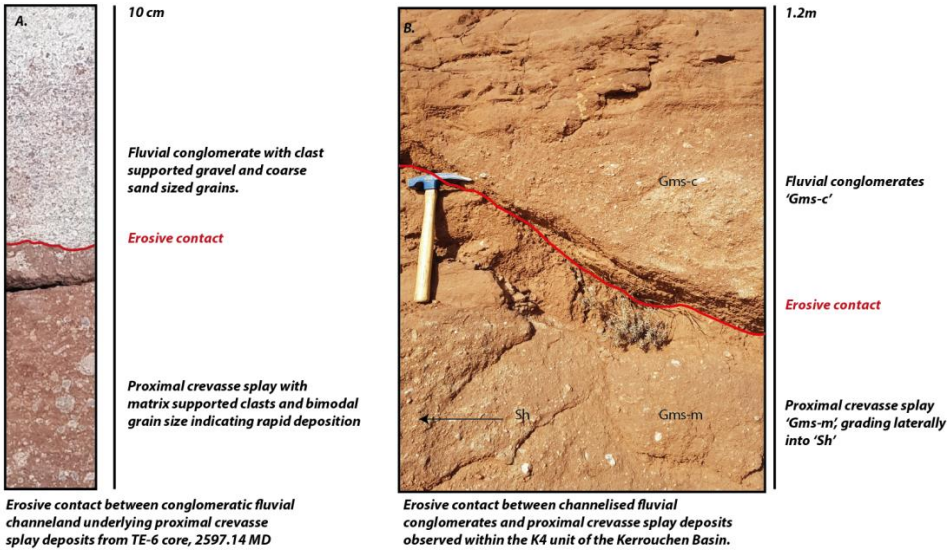

Figure 1-16: Showing a comparison between the TE-6 core (A) and the lithofacies seen in the Kerrouchen Basin (B). The facies observed in the Tendrara Core are more similar to those observed in the Kerrouchen Basin than those observed in the Central High Atlas

1.4. Regional Correlation

In order for the results of the provenance analysis across the three basins to be relevant, the samples analysed must have been deposited approximately synchronously across Morocco. Within the Triassic of Morocco, there is an absence of good high-resolution biostratigraphy due to the low abundance and diversity of fossils. This makes it difficult to correlate formations from the Central High Atlas (CHA) to the Middle High Atlas (MHA) based on the available biostratigraphic data. In an attempt to build a correlation across Morocco, periods of similar tectonic and depositional style have been recognised from across the Central High Atlas and the Middle High Atlas Triassic basins.

Within the Triassic series of Morocco there has long been the recognition of three tectono-stratigraphic sequences (Lorenz 1988; Ouarhache *et al.* 2012), an early syn-rift sequence characterised by conglomerates and coarse sedimentation (S1) overlain by a middle syn-rift sequence characterised by the deposition of fluvial sandstones in meander belts parallel to the axis of the rift basins (S2). The final component of the Triassic series of Morocco (S3) characterised by the deposition of regional evaporitic mudstones related to the onset of the marine-transgressions from the Alpine-Tethys along the Atlas rift (Oujidi *et al.* 2000; Courel *et al.* 2003).

The recognition of these three syn-rift packages has been utilised in order to build a proposed regional correlation *(Figure 1-17)*. The early syn-rift sequence, S1, is represented in the Oukaimeden Basin by the F3 formation (Fabuel-Perez *et al.* 2009) and within the Kerrouchen Basin by the conglomerates and siltstones of the K2 formation. The first occurrence of fluvial sandstones defines the base of the S2 sequence and occurs in the K3 and lower-K4 formation of Kerrouchen and throughout the F4 and F5 formations of the Oukaimeden Basin (Fabuel-Perez *et al.* 2009) *(Figure 1-17).*

The late syn-rift sequence, S3, is recognised by the first occurrence of marine influence within the fluvial deposits. Within the Oukaimeden Basin the upper F5 contains evidence of tidal influence on the fluvial system (Benaouiss *et al.* 1996) and therefore the Upper F5 forms the base of the S3 late syn-rift sequence. Within the Kerrouchen Basin, the U-K4 has been recognised as being influenced by the presence of a large body of water, interpreted as the advancing Tethyan transgressions (Oujidi *et al.* 2000; Ouarhache *et al.* 2012), and forms the base of the S3 in the Middle High Atlas.

In the proposed model, the paleoflows varies and therefore the provenance is predicted to vary between the S1 and S2 syn-rift sequences. The S1 is probably locally sourced from basin margin highs and thins towards the basin centre as observed within the K2 formation of the Kerrouchen Basin (Lorenz 1976) and suggested by paleflows recorded in both Oukaimeden *(Figure 1-6)* and Kerrouchen *(Figure 1-12*). In contrast, the S2 sequence is thinner at the basin margin and thickens towards the basin axis. Within the Kerrouchen Basin the S2 sequence is predicted to thin to the north in the direction of the proto-Tethyan Ocean. The S3 sequence, thought to be deposited by the

advancing Tethyan transgression (Ouarhache *et al.* 2012), is expected to thin towards the Central High Atlas and the Oukaimeden Basin, with thicker evaporites found to the north as seen by the higher proportion of evaporitic Triassic basins within north-east Morocco (Oujidi *et al.* 2000).

The identification of these sequences forms a basis for correlation across Morocco; however, there is no proof that these sedimentary packages were deposited simultaneously. It is possible for example that the S2 sequence was deposited at different times within the Kerrouchen and Oukaimeden Basins. There is fossil evidence that the Triassic sediment across Morocco are no older than the Carnian (Lachkar *et al.* 2000; Ouijidi 2000; Ouarhache *et al.* 2012), and the dating of the extensive CAMP basalts shows they are no younger than 202 Ma (Fiechtner *et al.* 1992). Whilst these dates allow us to correlate the onset and cessation of deposition, they do not provide data of sufficient resolution to allow for correlation of the sequences from the Middle High Atlas to the Central High Atlas. Further field work and biostratigraphic will be needed to refine these correlations, alongside exploring other potential methods for correlating sedimentary bodies, such as chemo-stratigraphy or magneto-stratigraphy.

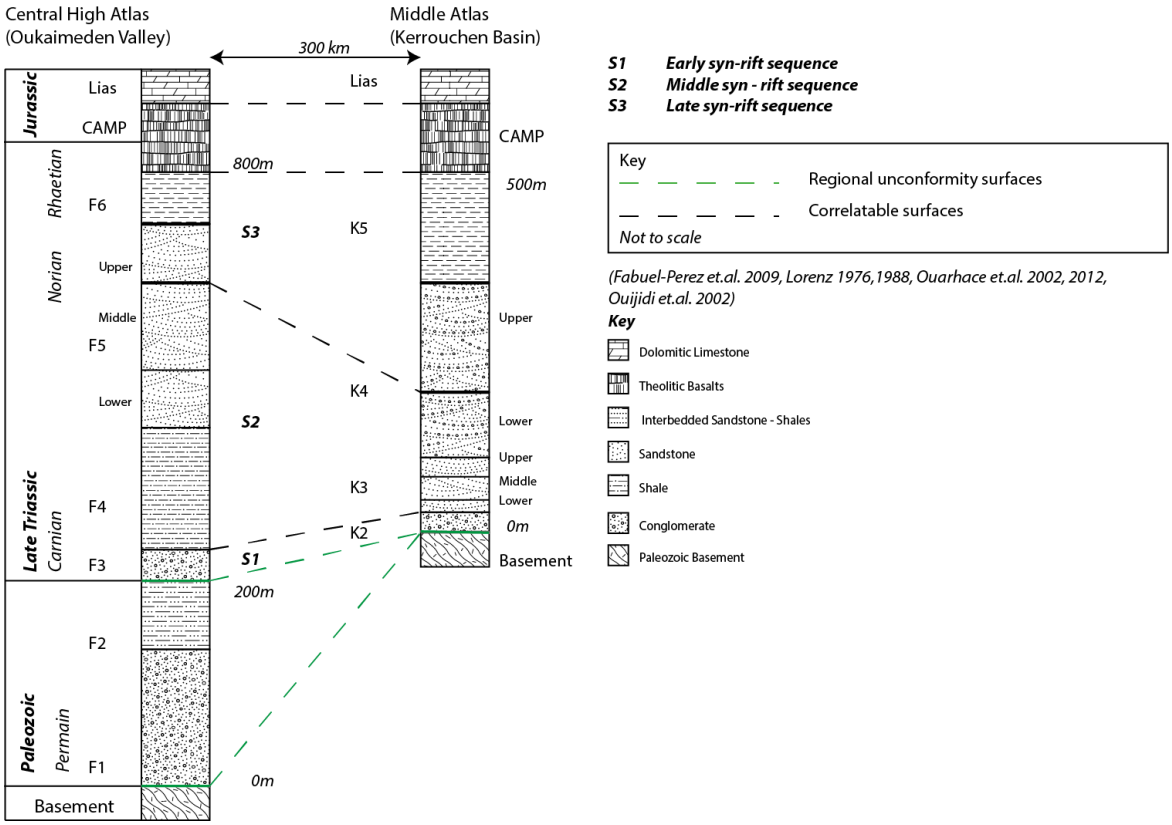

Figure 1-17: Proposed regional correlation between the Central High Atlas and Middle High Atlas (Fabuel-Perez et.al. 2009, Lorenz, 1976,1988, Ouarhache et.al. 2002, 2012, Oujidi et.al. 2002)

1.5. The Kerrouchen Basin as an analogue for the Tendrara Field

The stratigraphy of the Tendrara field has been correlated to the Triassic of the Oukaimeden Basin *(Figure 1-5)* however facies analysis of the TE-6 and TE-8 core shows that the facies and depositional style present in the Tendrara field are more similar to those present within the Kerrouchen Basin during the Triassic *(Figure 1-16)* (Benvenuti 2016, 2017). This suggests that the distribution of facies within the Kerrouchen Basin could provide an analogue for the distribution of facies within the Tendrara Field and thereby act as an analogue for the Tendrara Field.

By utilising the Kerrouchen Basin as an analogue for the Tendrara field, paleogeographic reconstructions of the Kerrouchen Basin could allow for the prediction of facies away from drilled wells to enhance well planning. The highest quality Triassic reservoirs in North Africa are found within fluvial-aeolian sands (Rossi *et al.* 2002; Mader *et al.* 2017), so understanding the distribution and extent of such facies is vital for accurate reservoir modelling.

Within the Kerrouchen Basin, fluvial sands are concentrated towards the basin axis with smaller volumes of fluvial sands near the basin margins, linked to the large-scale alluvial fans sourced from the hanging wall of the eastern boundary fault *(Figure 1-18).* The fluvial system flowed towards the NNE *(Figure 1-12),* roughly parallel to the major structural trend of the Middle Atlas Rift *(Figure 1-18*). This distribution of fluvial facies was also observed within the Oukaimeden Basin (Baudon *et al.* 2009; Fabuel-Perez *et al.* 2009), suggesting the major structural trend of the Triassic rift basins provides a control on the distribution of the fluvial facies within the basins. Within the Triassic fluvial channel belt of the Kerrouchen Basin locally calcareous overbank fines and evaporitic mudstones occur due to the braided nature of the fluvial system, which have also been observed within the TE-6 core from the Tendrara Field. *(Figure 1-18).*

The position of the fluvial system within the Kerrouchen Basin was likely influenced by a series of intra-basinal paleohighs (Lorenz 1976), which would have provided positive topography which influencing the path of the fluvial system. Erosion from these intra-basinal paleohighs may have led to the development of small piedmont fans, some of which transitioned into fluvial facies which acted as local tributaries for the major fluvial channel belt. Within the Kerrouchen Basin, towards the eastern basin margin, major alluvial fans developed as a transverse depositional system sourced from the major basement faults along the east of the basin, as seen at localities KH-70 *(Figure 1-7, Figure 1-18).* Within these alluvial fans, fluvial sand rich facies do occur, however based on field observation they form a small proportion of the total sediment volume of the transverse alluvial-fluvial systems.

The distribution of facies within the Kerrouchen Basin has important implications for modelling the distribution of reservoir intervals within the Tendrara field. The sand-rich intervals within the Kerrouchen Basin are observed within axial settings. The fluvial outcrops and the paleoflows recorded within the rift basins point indicate that the fluvial systems ran roughly parallel to the structural trend of

the rift basin *(Figure 1-12);* a distribution which is comparable to the observed distribution within the Oukaimeden Basin (Baudon *et al.* 2009; Fabuel-Perez *et al.* 2009). This information can be utilised in the Tendrara Field, as when fluvial facies are recognised their distribution can be predicted based on the major structural trend of the basin.

It is important to note however, that the main axial channel belt within the Kerrouchen Basin would not form a homogenous reservoir. The occurrence of overbank facies within the fluvial channel belt reduces the sand content with a general reduction of sand moving perpendicular to the orientation of the axial fluvial belt. In general, the facies observed moving perpendicular to the axis of the fluvial channel belt are fluvial sands, sand rich overbank facies and evaporitic overbank mudstones *(Figure 1-19).* The sand-rich overbank facies are locally calcareous which reduces the porosity and permeability, and therefore the reservoir quality, of the overbank mudstones.

As seen in Figure 1-18 and Figure 1-19, the occurrence of local paleohighs within the Kerrouchen Basin would have generated positive topography which would have influenced the fluvial system. When predicting the distribution of fluvial reservoirs within the Tendrara Field, the recognition of intra-basinal highs will be important to predict the distribution of fluvial facies. Within the Kerrouchen Basin, the intra-basinal fans are fringed by low reservoir quality alluvial fans and overbank deposits.

Near the basin margin, alluvial fans formed leading to the deposition of conglomeratic facies which grade locally into fluvial facies. However, the high-quality reservoir sands are situated within low N; G intervals where there are a high number of baffles to the flow of hydrocarbons. Within the alluvial-fluvial systems flow was ephemeral, resulting in the formation of pedogenic carbonates and paleosols which reduce porosity and permeability, further reducing reservoir quality and homogeneity near the basin margin.

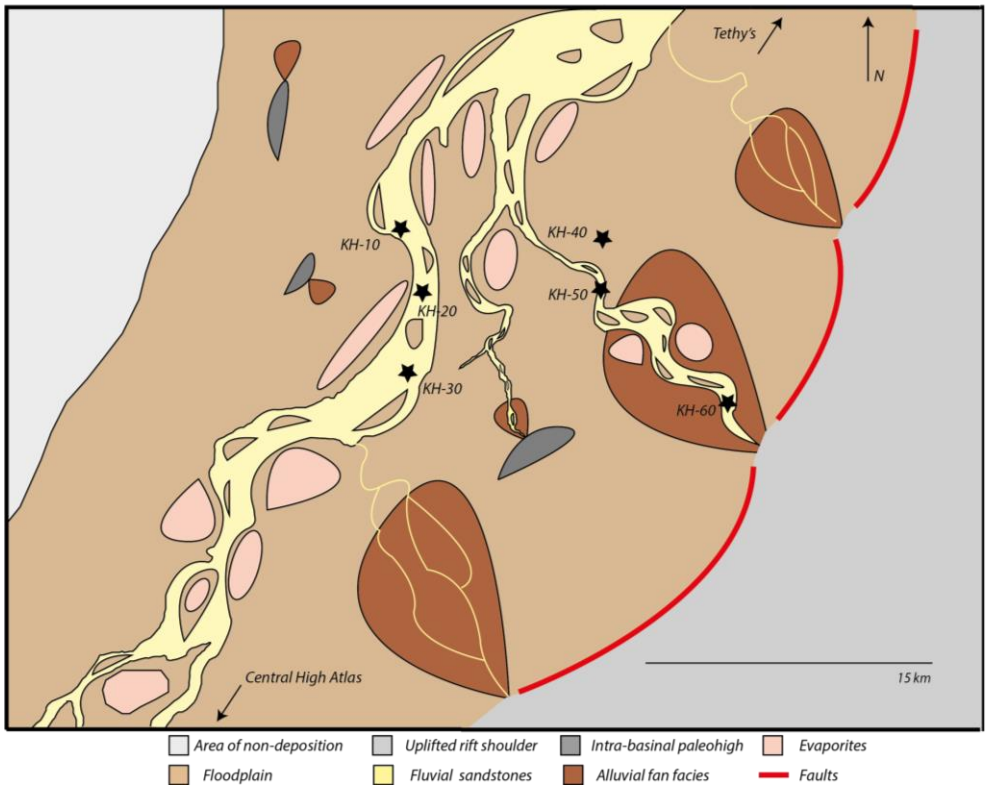

Figure 1-18: A reconstruction of the depositional systems and environments and their spatial distribution within the Triassic Kerrouchen Basin based of field observations.The stars represent the position of key field localities within the paleogeographic reconstruction.The axial fluvial system flows NNE-ENE parallel to the Middle Atlas Rift, with transverse alluvial fans feeding from local intra-basinal paleohighs and the positive topography created by the eastern boundary fault, S.M.A.F.

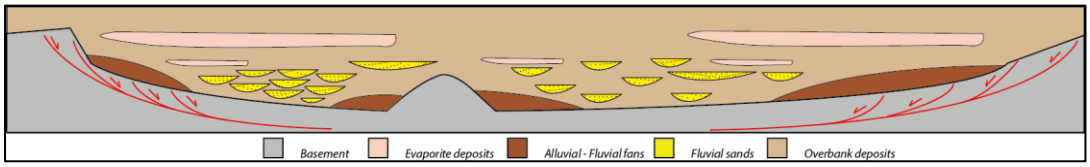

Figure 1-19: Hypothesised distribution of reservoir facies within the a Triassic Rift Basin based upon the paleogeographic reconstruction of the Kerrouchen Basin. The sand rich fluvial facies occur within the main axial fluvial system. Locally, sand rich overbank facies could provide a viable reservoir, however the occurrence of pedogenic carbonates, evaporites and paleosols within these facies could reduce their reservoir quality. In general, the N: G of overbank deposits decreases moving up through the stratigraphy (Figure 1.7), whereas the occurrence and extent of evaporates increases. The basin margins are unlikely to have a high-quality reservoir due to the transport of sand towards the basin centre.

In summary, using the Kerrouchen Basin as an analogue for the Tendrara Field would imply that the higher quality reservoir intervals are located towards the basin centre, with lower reservoir quality conglomeratic and mud-rich facies found towards the basin margins. The fluvial facies within both Oukaimeden and Kerrouchen are distributed sub-parallel to parallel to the major structural trend of the basin (Baudon *et al.* 2009); however local paleohighs could have provided a more subtle, secondary control on the distribution of the fluvial system which should be considered in well planning during the continuing exploration of the Tendrara Field. Whilst previous workers have used Oukaimeden as an analogue for the Tendrara Field, the observations made in the Kerrouchen Basin and the TE-6 and TE-8 core suggest that the Kerrouchen Basin could provide a better analogue for the Tendrara Field. However, before this comparison can be made usefulmapping of the Kerrouchen Basin to constrain the scale of, interaction between and controls on the axial and transverse depositional systems will be required in order to develop accurate reservoir models for the Tendrara field.

Chapter 2 Provenance Study

2.1. Introduction

In order to conduct a provenance study, both petrographic analysis and heavy mineral analysis need to be done in order to accurately constrain the provenance (Garzanti & Andò 2007b; Garzanti et al. 2010; Garzanti 2016). The samples selected to be analysed have been chosen based on their likelihood to record a regional provenance signal, and as such, the majority of samples selected for further analysis are from sand-rich fluvial facies. Within similar facies observed in the Northern European Triassic, regional provenance signals have been recorded which has allowed for regional paleogeographic reconstructions (Tyrrell et al. 2007; Mckie 2014) and for reservoir correlation in the North Sea (Maria A. Mange-Rajetzky 1995; Kilhams *et al.* 2014).

2.2. Heavy Mineral Analysis

When conducting a heavy mineral study, care must be taken to generate representative datasets. All samples are inherently biased due to environmental factors and steps must be taken to minimise these effects on the dataset generated (Garzanti *et al.* 2009). There are three main environmental factors which can induce a bias into the detrital heavy mineral assemblages *(Figure 2-1)* (Morton & Hallsworth 1999):

1. Physical sorting during transport and deposition
2. Mechanical abrasion during transport
3. Dissolution caused by weathering at source, sub-aerial exposure during fluvial transport, burial diagenesis and weathering at outcrop

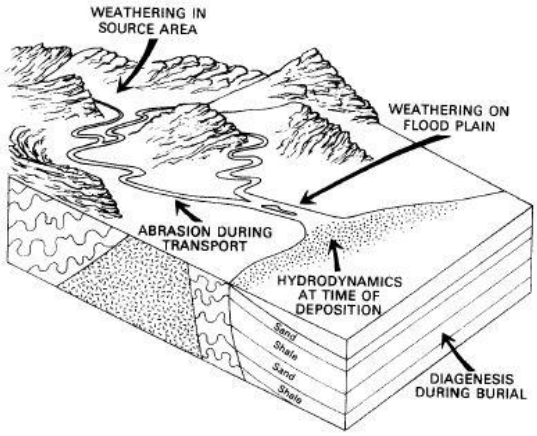

Figure 2-1: Factors which can influence preserved HMA during source to sink transport (Morton & Hallsworth 1994)

Of the three factors outlined above, physical sorting and dissolution have the largest impact on the detrital assemblage. Physical sorting is driven by changes in hydrodynamic conditions which control bulk sediment deposition and therefore the deposition and concentration of heavy minerals within the bulk sediment (Garzanti *et al.* 2008). The effects of mechanical abrasion during transport rarely impacts the preserved heavy mineral assemblage except in exceptional circumstances and can therefore be discounted as a potential bias within detrital heavy mineral studies (Morton & Hallsworth 1999). The third control on detrital heavy mineral assemblages is dissolution, which can occur at any point in the source to sink system *(Figure 2-1)* (Morton 1984; Morton & Hallsworth 1999).

Historically other factors have been proposed as controls on the preserved heavy mineral assemblage, such as burial depth, age and mineral stability. Early workers suggested that with increased burial depth and age of sediment, the preservation of heavy minerals decreased (Pettijohn 1941). Whilst this is usually the case this is caused by increased pore fluid temperature at depth increasing the rate of dissolution reactions (Morton & Hallsworth 1999). In a similar manner, age is not a controlling factor if all other factors are equal (diagenetic environment, burial history etc.), but older sandstones usually have a lower abundance and diversity of heavy minerals due to greater time for dissolution reactions to occur (Morton 1984). There is no universal ranking of heavy mineral stability (Morton 1984), but the preservation and stability of heavy minerals is approximately inverse to Bowen's Reaction Series, with mafic minerals undergoing dissolution earlier than felsic minerals (Hurst & Morton 2014). The factors identified by early workers are in reality related to heavy mineral dissolution and diagenesis during weathering, transport and burial (Morton 1984; Morton & Hallsworth 2007).

Mineral dissolution can cause the preserved heavy minerals assemblage to be an artefact of the environmental conditions, rather than due to a variation in provenance. Dissolution begins during weathering at outcrop and continues during the transport from source to sink (Morton & Hallsworth 1994). The dissolution of minerals during transport can be linked to climate, for example Apatite is unstable in meteoric groundwater and therefore undergoes greater dissolution during humid climatic intervals (Mange & Morton 2007). This phenomenon results in a decrease in the abundance of apatite within detrital assemblages, which, when occurring without any other indicators of provenance variations is indicative of a climatic shift to more humid conditions (Hurst & Morton 2014).

The dissolution of Apatite within meteoric groundwater could be a useful tool for correlation of reservoir sand bodies in the Mid to Late Triassic of Morocco as a sudden decrease in the abundance of Apatite could be related to the Carnian pluvial event (Mader *et al.* 2017). This climatic event was related to an increase in precipitation across central Pangea (Arche & López-Gómez 2014) and therefore could have resulted in a reduction in the abundance of Apatite in detrital assemblages across Morocco.

During the Triassic, Morocco had an arid, continental climate (Parrish 2016) led to the formation of extensive red beds (Ivan Fabuel-Perez *et al.* 2009; Mader & Redfern 2011; Mader *et al.* 2017). In red bed forming environments Ferro-magnesian minerals undergo preferential dissolution (the oxidation of Fe^{3+} gives the beds their distinctive red colouring) resulting in the loss of pyroxenes amphiboles from the detrital heavy mineral assemblage (Morton & Hallsworth 1999). As seen in the extensive work done in the Triassic of the North Sea, ultra-stable minerals (e.g. Tourmaline, Garnet and Zircon) are largely unaffected by the climatic conditions during weathering, transport and deposition, and will form the basis of any heavy mineral studies in the Triassic (Morton 1984; Morton & Hallsworth 1994, 1999; M A Mange-Rajetzky 1995).

Burial dissolution is another factor which can potentially induce a bias into a heavy mineral study by reducing the abundance of minerals (Mange & Morton 2007). Progressive dissolution increases during burial diagenesis, beginning mostly at T > 60°C with olivine, clinopyroxene and Ca-amphibole beginning at T < 60°C (Morton & Hallsworth 2007). The effects of dissolution can be recognised by optical analysis of the heavy minerals (Andò *et al.* 2012), however care needs to be taken as dissolution textures can be inherited (Hubert 1971). The effects of dissolution can be minimised by focusing the analysis on ultra-stable minerals which are unlikely to be affected by dissolution (Morton 1984; Morton & Hallsworth 1994).

The other environmental factor which can induce a major bias into provenance analysis is density driven hydraulic sorting (Garzanti *et al.* 2009). The effects of density on hydraulic sorting of heavy minerals have been extensively studied (Komar *et al.* 1989), and is due to the principle of hydraulic equivalence (Rubey 1933) which states that grains with the same settling velocity are deposited together (Garzanti *et al.* 2008). This results in the deposition of small, dense minerals with low density, large minerals and the concentration of heavy minerals in the 'fine tail' of sediment due to these density differences (Mackie 1923; Garzanti *et al.* 2008).

As a result of hydraulic sorting, each component within detrital sediment (quartz, feldspar etc.) has a lognormal size distribution, with the bulk sediment having a compound normal distribution (Garzanti *et al.* 2008). This is very important for analysing heavy minerals, as they are not evenly distributed throughout detrital sediments, but concentrate into the finer tail (Garzanti *et al.* 2008, 2009). Traditionally, there have been two methods utilised to combat these effects.

The first, popularised by Andrew Morton, is to utilise ratios of minerals with similar hydraulic equivalences as these minerals will be concentrated in the same grain size fraction of detrital sediment *(Table 2-A)* (Morton & Hallsworth 1994). These heavy mineral ratios, HMR, are studied in a narrow grain size fraction, usually 63-125µm and are provenance sensitive (Morton & Hallsworth 1994; Morton *et al.* 2002) as well as reducing the bias of hydraulic sorting (Morton & Hallsworth 1994).

The minerals utilised as HMR are also sensitive to burial dissolution (Garnet) and to changes in climate (Apatite). If the value of the GZi falls, but no other HMR change is noted, it is indicative of deep burial, as garnet is unstable under deep burial (Morton 1984; Morton & Hallsworth 1994; Mange & Morton 2007). As discussed above, apatite is unstable in meteoric groundwater, so a fall in the ATi with no other change in the HMR's is indicative of a climatic change to more humid conditions (Hurst & Morton 2014).

Table 2-A: Heavy mineral ratios (HMR) and the density differentials of the ultrastable heavy mineral ratios (Morton & Hallsworth 1994). For mineral abbreviations see (Whitney & Evans 2010)

Index Abbreviation	Mineral Pair	Index determination	Density Differential %
CZi	Cr-Spl, Zrn	$\frac{100(Cr - Spl\ count)}{\sum(Cr - Spl\ count + Zrn\ count)}$	2
ATi	Apt, Tur	$\frac{100(Apt\ count)}{\sum(Apt\ count + Tur\ count)}$	3
RZi	Rt, Zi	$\frac{100(Rt\ count)}{\sum(Rt\ count + Zrn\ count)}$	9
MZi	Mnz, Zrn	$\frac{100(Mnz\ count)}{\sum(Mnz\ count + Zrn\ count)}$	10
Gzi	Grt, Zrn	$\frac{100(Grt\ count)}{\sum(Grt\ count + Zrn\ count)}$	12

The second method has been popularised by the Laboratory for Provenance Studies (LfPS), and utilises a wider grain size fraction, historically 63-250µm (Garzanti & Andò 2007b), but in more recent times Raman spectroscopy has been utilised to analyse from 5-500µm (Andò *et al.* 2009, 2011). Utilising a narrow grain size fraction increase the effect of grains size on the observed heavy mineral assemblage thereby increasing the bias and reducing the accuracy (Garzanti *et al.* 2009). The use of the wider grain size fraction combats this effect, reducing the bias induced by hydraulic sorting and increasing the accuracy of the results obtained (Garzanti *et al.* 2009; Malusà *et al.* 2016). This can be seen in the density differentials *(Table 2-A)* some HMR have significant density differentials which could result in the minerals involved concentrating in significantly different size fractions.

To reduce the bias significantly, the size window utilised to analyse the detrital heavy mineral assemblage must be greater than the average grain size, preferably greater than 2ϕ sieve windows (Garzanti *et al.* 2009). The wide window approach allows for analysis of a much greater proportion of the heavy mineral assemblage, which allows for more accurate identification of the source regions (Andò *et al.* 2014; Garzanti *et al.* 2016, 2017). By utilising the wider grain size window to generate a more complete picture of the heavy mineral assemblage, a new set of indices where developed which relate the detrital assemblages to the source regions (Garzanti & Andò 2007a) more so than the HMR of Morton (Morton & Hallsworth 1994). A combination of these indices will be used to assess the heavy mineral data generated *(Table 2-B).*

The key indices utilised in the study will be used to identify likely nature of the source regions and indicate whether the samples have shared provenances. The ZTR and T& indices represent stable assemblages which are derived from igneous felsic or reworked sedimentary terranes (Garzanti & Andò 2007b). The Gt, LgM and HgM indices track contributions from low to high grade metamorphic source terranes, whereas Hb, &A, CPX, OPX and OS track contributions from intermediate to ultramafic igneous or meta-igneous source terranes (Garzanti & Andò 2007b). As the analysis will be performed on a QEMSCAN, polymorphs will not be able to be identified. As a result of this, the ZTR and T& indices will be grouped together, as rutile and all its polymorphs, would form in either of these groupings *(Table 2-B)* as these indices both indicate the same source terrane, it can be utilised to identify source terranes and unique provenances.

When analysing the data from the heavy mineral analysis, it is important to remember that the detrital components of a rock only provide an approximation of the lithology's within the source area (Garzanti 2016). The data generated from these samples will allow for the identification of the likely source terranes that the sediment was sourced from, however just because samples were sourced from terranes of the same type, does not necessarily mean they were sourced from the same terrane. The data generated will however be able to identify shifts in provenance or samples with separate provenances as well as highlighting samples which have similar provenances.

Index	Heavy Minerals	Index determination	Index use	Reference
TiO_2:Zi	TiO_2, Zi	$\frac{100(TiO_2\ count)}{\sum(Rt\ count + Zrn\ count)}$	Provenance sensitive HMR	(Morton & Hallsworth 1994)
GZi	Grt, Zrn	$\frac{100(Grt\ count)}{\sum(Grt\ count + Zrn\ count)}$	Provenance and burial sensitive HMR	(Morton & Hallsworth 1994)
ZTR, T&	Zircon, Tourmaline and TiO_2 polymorphs and Ti minerals	Sum of ultrastable and titanium minerals e.g. Zircon, Tourmaline, Rutile, Sphene, Anatase, Apatite.	Indicates the extent to which felsic igneous or reworked sedimentary rocks contributed to the sediment.	(Garzanti & Andò 2007b)
Gt	Garnet	Sum of garnet.	Indicates the extent to which metamorphic rocks contributed to the sediment.	(Garzanti & Andò 2007b)
LgM	e.g.Ep, Cld, Car, Lws	# of low grade metamorphic minerals	Indicates the extent to which low-grade metamorphic rocks contributed to the sediment.	(Garzanti & Andò 2007b)

HgM	e.g. St, Sil, And	# of high grade metamorphic minerals	Indicates the extent to which high-grade metamorphic rocks contributed to the sediment.	(Garzanti & Andò 2007b)
Hb	Hornblende	Sum of hornblende	Indicates the extent to which intermediate to mafic igneous or meta-igneous rocks contributed to the sediment.	(Garzanti & Andò 2007b)
OPX	Orthopyroxene	Sum of Orthopyroxene	Indicates the extent to which intermediate to mafic igneous or meta-igneous rocks contributed to the sediment.	(Garzanti & Andò 2007b)
CPX	Clinopyroxene	Sum of clinopyroxene	Indicates the extent to which intermediate to mafic igneous or meta-igneous rocks contributed to the sediment.	(Garzanti & Andò 2007b)
&A	Other Amphiboles e.g. actinolite, tremolite	Sum of other amphiboles	Indicates the extent to which intermediate to mafic igneous or meta-igneous rocks contributed to the sediment.	(Garzanti & Andò 2007b)
OS	Olivine, Spinel	Olivine + Spinel	Indicates the extent to which intermediate to mafic igneous or meta-igneous rocks contributed to the sediment.	(Garzanti & Andò 2007b)

Table 2-B: Key indices which will be used to analyse the samples

2.3. Sample Selection

In the west of the Kerrouchen Basin, samples were selected from the sand rich intervals of the fluvial dominated K3 formation to analyse both petrographically and for heavy mineral analysis. These samples, from localities 3 and 4 *(Figure 1-7),* have been interpreted to represent an axial fluvial system which was orientated N-NE based on the paleoflows recorded within the formation. Towards the east of the basin, samples from the alluvial-fluvial K4 formation *(Localities 5 and 6, Figure 1-7),* were selected for petrographic analysis, with samples from sand rich horizon's selected for heavy mineral analysis *(Figure 2-2).*

These samples have been selected as a variation in the provenance signal between the K3 and K4 formation could be due to the K3 fluvial deposits being sourced from an extra-basinal source drained by a regional fluvial system whereas the K4 formation was sourced from local basinal sources. This would indicate that there were separate local and regional drainage systems within the Kerrouchen Basin. However, a shared source terrane from these two systems would indicates that the systems are locally sourced and may indicate that the Kerrouchen Basin, and therefore the Middle Atlas Rift, was not connected by a regional fluvial system to the Central High Atlas during the Triassic.

Within the Oukaimeden Valley, 29 samples were analysed petrographically, with four samples from the F5 formation then selected for further heavy mineral analysis *(See Figure 1-4 for the sampling localities)*. The F5 formation represented a major fluvial system during the Triassic (Fabuel-Perez et al. 2009) and therefore if a regional fluvial system existed during the Triassic linking the Central High Atlas to the Middle Atlas and High Plateaux, would most likely be recorded within the F5 formation. Within the F5 formation, 2 samples were selected from the lower F5 and 2 samples from the middle F5. These samples cover an interval of particular interest as the L-F5 to M-F5 transition represent a period of increased precipitation and fluvial rejuvenation (Fabuel-Perez et al. 2009), which could have seen significant changes in the abundance of Apatite within the detrital assemblage due to Apatite's instability in meteoric ground water (Morton & Hallsworth 1994). This climatic event would have been regional in extent (Mader et al. 2017) and could therefore provide a basis for a regional correlation.

From the Tendrara Field, petrographic analysis was undertaken on samples from the TE-1, TE-2, TE-4, TE-5, TE-6, TE-8 wells *(Figure 1-13)* within the TAGI reservoir interval (Benvenuti 2016). The TAGI sandstone interval is of regional occurrence across North Africa (Rossi et al. 2002; Mader et al. 2017) and therefore could record a regional provenance signal within the High Plateaux Basin. Samples from sand rich intervals within the TAGI interval identified within the TE-6 and TE-8 well have been selected for further heavy mineral analysis. These samples include one sample correlated to the F4 formation (Benvenuti 2017) and three which have been correlated to the F5 formation (Benvenuti 2016, 2017). The three samples correlated to the F5 formation should have a shared provenance

signal due to their deposition by a regional fluvial system, whereas the sample correlated to the F4 formation is more likely to record a local, regional signal from within the Tendrara Field. However, based on facies analysis, the TE-6 and TE-8 cores do not share the facies characteristics with the F5 formation of the Oukaimeden Valley and may therefore not have a shared provenance with the samples from the Oukaimeden Valley.

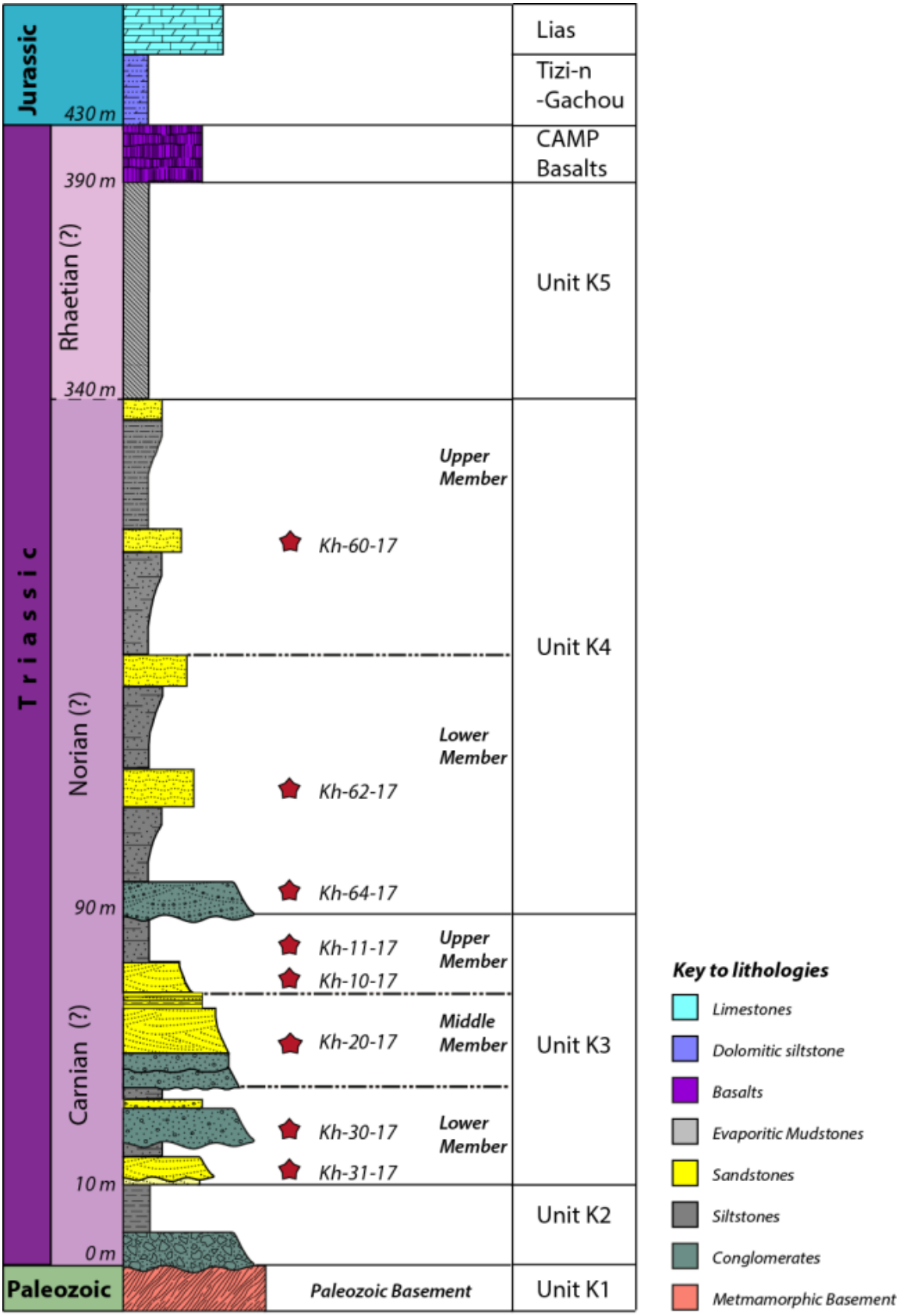

Figure 2-2: Stratigraphic position of the Kerrouchen samples selected for heavy mineral analysis

2.4. Methodology

The petrographic analysis will allow for accurate classification of the sandstones and identification of provenance trends and reservoir quality between the samples. The analysis of samples from the axial K3 and transverse K4 formation within the Kerrouchen Basin could allow for the identification of differences in the petrography and provenance, which could be utilised in the identification and modelling of the TAGI reservoir interval in the Tendrara Field. The petrographic analysis will also allow for the prediction of sand distributions on a basinal and regional scale by classifying of the provenance sand bodies (Dickinson 1985; Garzanti 2016) and the modelling of the source to sink pathways.

2.4.1. Petrographic Analysis

Petrographic analysis was undertaken on 13 samples from the Kerrouchen Basin, 6 from the K4 formation and 7 from the K3 formation, and 27 from the Tendrara Field, wells TE-1, 4, 5, 6 and 8. This data was supplemented by data from 29 samples collected by Fabuel-Perez in the Oukaimeden Valley (Fabuel-Perez 2008, p. 167). In total, 68 samples were analysed using the fleet method (Galehouse 1971), with 300-400 points, measured and identified using PETROG software and an automated software stepping stage at 4x magnification, counted using the Gazzi-Dickson Method (Dickinson 1970). Sedimentary clasts were classified into the following end member groups:

- Quartz including mono and poly-crystalline (Q= Qp + Qm)
- Feldspar, both plagioclase and K-feldspar (F = K-fds + P-fds)
- Lithics, including carbonate clasts (L = Li + Lm + Ls)
- Matrix, including calcitic cement and clay (M = Calcite + Clay)

However, instead of utilising the traditional ternary discrimination diagrams utilised by Dickinson, (Dickinson *et al.* 1983; Dickinson 1985), which display the expected range of sand compositions, the Garzanti method was utilised (Garzanti 2016). This methodology utilises a more precise nomenclature based off the percentage abundance of framework components *(Figure 2-3)* and seeks to utilise the classification of major clast types to better constrain source regions (Garzanti 2016). This classification is based on the principle that detrital components of a sand are not true proxies of the tectonic setting but reflect the lithological components of the source region available for erosion at a given time and the ternary discrimination diagrams generated by the petrographic analysis are best suited for identifying variations in provenance (Garzanti *et al.* 2010; Garzanti 2016).The methodology outlined by Garzanti allows for the identification of five types of provenance *(Table 2-C)* (Garzanti *et al.* 2010; Garzanti 2016).

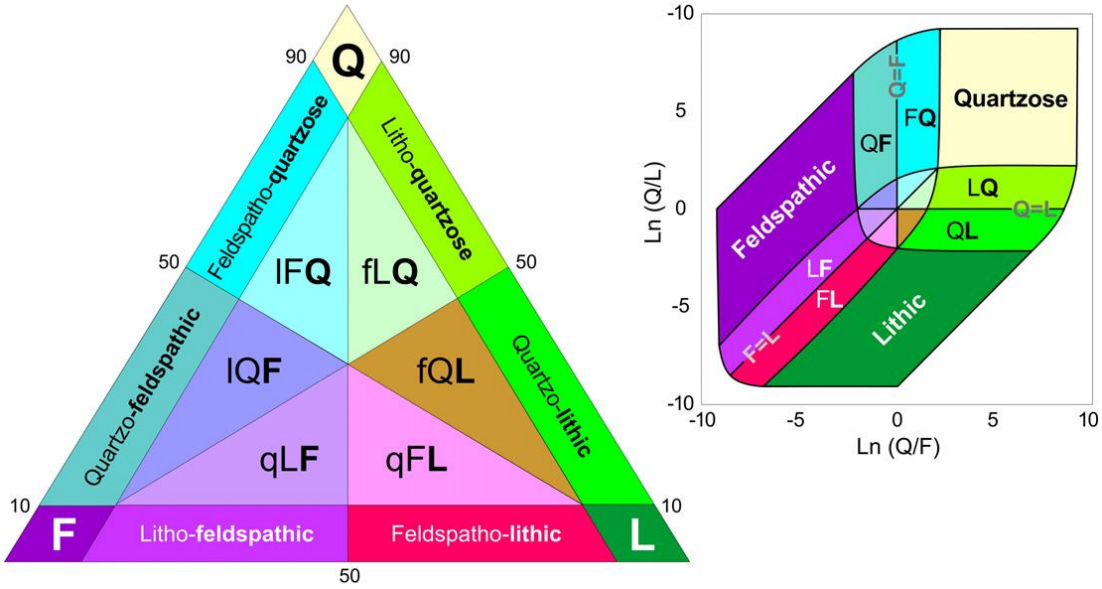

Figure 2-3: Sands are classified based on the abundance of their framework components >10%. The dominant rock fragment (volcaniclastic, plutoniclastic etc.) is added to the classification to aid identification (Garzanti 2016)

Table 2-C: Provenance types and expected lithologies (Garzanti et al. 2010, Garzanti 2016)

Provenance Type	Undissected Lithology	Dissected Lithology
Continental Block Provenance	Lithic clastic sand	Feldspatho-quartzose basementaclastic sand
Magmatic Arc Provenance	Feldspatho-lithic volcaniclastic sand	Quartzo-feldspathic plutonoclastic sand
Ophiolitic Provenance	Lithic ultramafic sand	Lithic volcaniclastic sand
Axial Belt Provenance	Quartzo-lithic metamorphiclastic sand	Litho-feldspatho-quartzose metamorphiclastic sand
Recycled Clastic Provenance	Lithic sedimenticlastic sand	Quartzose sand

2.4.2. Heavy Mineral Analysis

18 samples were selected for heavy mineral analysis. To separate the heavy minerals, 8g of sediment of the 30-250µm grain size fractions were gravitationally separated in separated in Lithium Heteropolytungsate (ρ=2.80gcm^{-3}) and recovered by partial freezing in liquid nitrogen. The heavy mineral's (ρ > 2.80gcm^{-3}) where mounted onto grain mounts in epoxy resin for QEMSCAN analysis in order to identify the minerals in the sample. The SEM\QEMSCAN analysis was performed on a FEI Quanta 650 FEG SEM equipped with a Bruker Quantax EDS system. The Data was collected using QEMSCAN software (**Q**uantitative **E**valuation of **M**inerals by **SCAN**ning electron microscopy). Data was collected at 15kV accelerating voltage using a step size of 10 microns. Data processing was then performed using the iDiscover software of the QEMSCAN system. Once the data has been collected, non-provenance sensitive minerals (e.g. biotite, muscovite, carbonates and gypsum) were removed from the results and percentage abundances were recalculated. Any mineral with an abundance of less than 0.5% were classified as a trace mineral and grouped accordingly.

This utilisation of the wider grain size window will minimise the effect of hydraulic sorting, (Morton & Hallsworth 1994; Garzanti & Andò 2007a; Garzanti et al. 2009), as well as allowing for the collection of provenance sensitive data (HMR, bulk heavy mineral assemblage), climatic indicators (ATi index), burial and stability indices (GZi, ZTR) and the nature of the source regions (MMI) (Hubert 1962; Morton & Hallsworth 1994; Morton *et al.* 2004; Garzanti & Andò 2007a; Andò *et al.* 2014). The data generated from the point counting and heavy mineral analysis is categorical data as it is based on the abundance of discrete components (Vermeesch & Garzanti 2015). By utilising pairwise comparisons, it is possible to quantify how many comparisons between points are possible.

$$P.C. = \frac{n(n-1)}{2}$$

$$n = number\ of\ samples$$

Equation 1

For the point count data:

$$n = 68$$

$$P.C. = \frac{68(67)}{2}$$

$$P.C. = 2278$$

Equation 2

For the heavy mineral analysis

$$n = 18$$

$$P.C. = \frac{18(17)}{2}$$

$$P.C. = 153$$

Equation 3

These results show that a large number of comparisons can be made which lends itself to the use of multidimensional scaling (MDS) (Vermeesch & Garzanti 2015). Multidimensional scaling creates a 2-D map, with similar points plotting together and therefore the level of similarity between samples can be objectively identified. This method removes conformation bias and is a numerical way of analysing provenance data (Vermeesch & Garzanti 2015). In order to undertake MDS, the R package 'provenance' will be utilised, which was designed for the analysis of provenance data (Vermeesch *et al.* 2016).

2.5. Results

2.5.1 Petrographic Results

For petrographic analysis of the Kerrouchen Basin, samples from 7 sand rich horizons within the K3 and 6 from within the K4 formation were selected (see Appendix B for a full Petrographic Database). Within the K3 formation, the samples are fine to medium sands with variable sorting; from poorly sorted sands within the lower to middle K3 formation *(Figure 2-7, Figure 2-6)*, becoming well sorted in the upper K3 *(Figure 2-5).* The observation of a calcitic matrix is thought to be a secondary feature linked to the evaporation of calcitic rich groundwater from on the floodplain (Ouarhache *et al.* 2012).

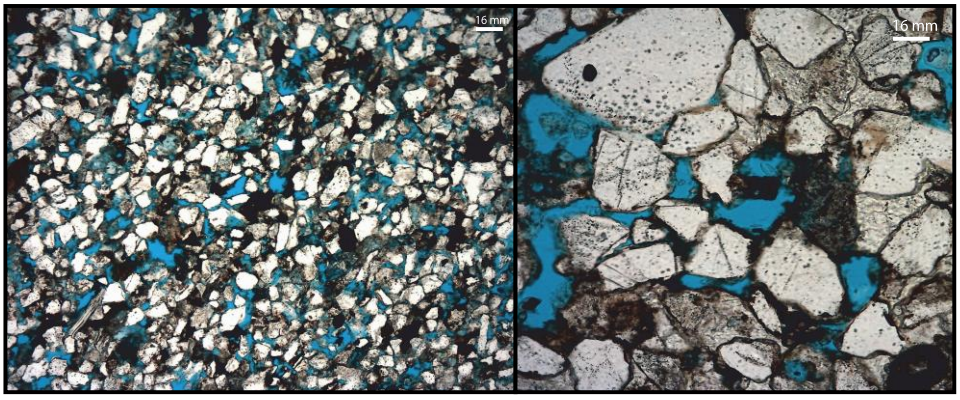

Figure 2-4: Thin section images from sample KH-10-17 of the upper K3 Formation

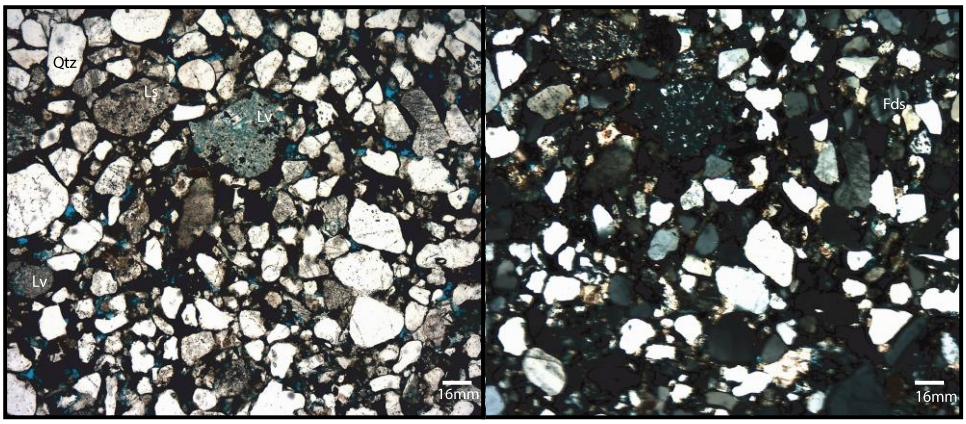

Figure 2-5: Thin Section images of the KH-20-17 sample of the Middle K3 Formation. Lv = Low grade metamorphic or volcaniclast. Ls = Sedimentary clast. Qtz = Quartz

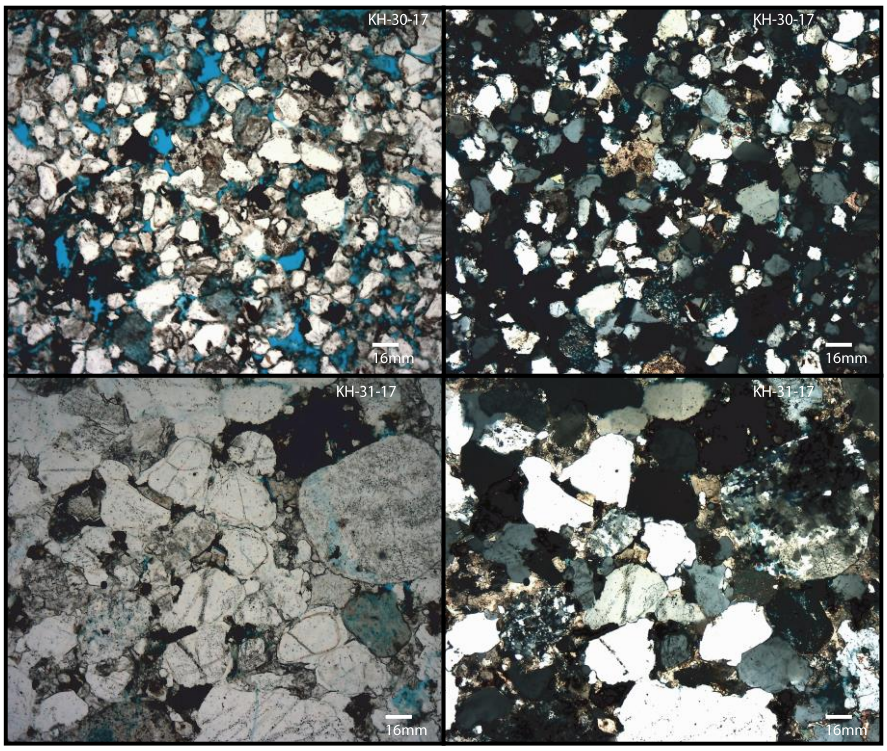

Figure 2-6: Thin section images of the KH-30-17 and KH-31-17 samples form the lower K3 Formation.

The 6 samples of the K4 formation *(Figure 2-7)* show a marked grain size distinction between the upper and lower K4, with the sand rich intervals in the lower-K4 varying from coarse to medium sands with a fining up trend, however there is no significant compositional shift between the K3 and K4 formation.

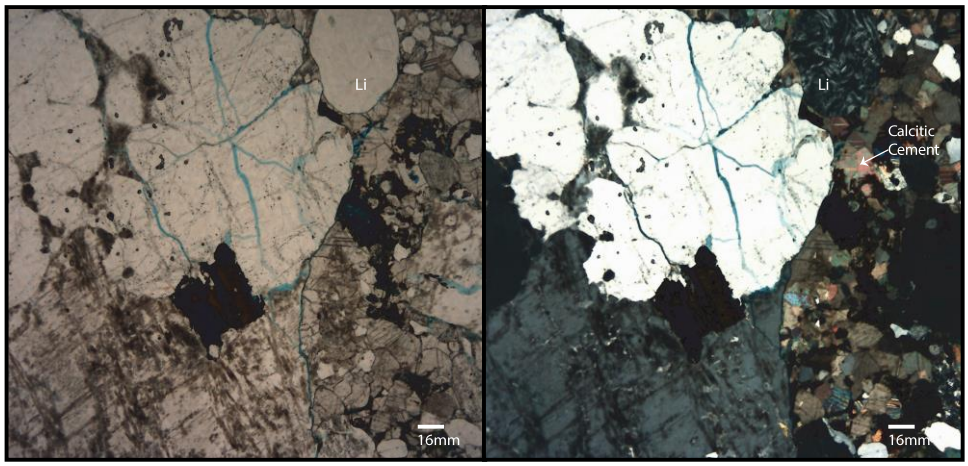

***Figure 2-7: Thin Section images form the KH-60-17 sample of the K4 Formation. Li = igneous clast. The calciitc cement is thought to be the result of evaporation on the floodplain* (Ouarhache *et al.* 2000).**

What can be observed in Figure 2.8 is the homogenous nature of the K3 and K4 formation, with 11 of the 13 samples plotting as quartzo-lithic to feldspatho-quartzo-lithic sandstones. The dominant clasts within both the K3 and K4 formations are low grade metamorphic, volcanoclasts and sedimentary clasts with rare igneous clasts, similar to the local basement. The anomalous sample, KH-20, plots as a feldspatho-lithic-quartzo sedimenticlastic sandstone. This classification of the sandstones indicates a provenance from an undissected axial belt or magmatic arc (Garzanti 2016).

Within the Tendrara field, situated to the east of the Kerrouchen Basin, 27 samples have been analysed from the TAGI reservoir interval from 5 wells, with the results plotted in Figure 2.9 (Hafid & Benaouiss 2010; Benvenuti 2016; Kape 2017). From the TE-1 well the 5 samples consisted of fine to coarse sand. Within TE-1, the predominant lithic clasts are plutoniclasts and chert, leading to the classification of the TE-1 samples as quartzo-lithic-feldspathic to litho-feldspathic plutoniclastic sands

In the TE-4 well, the sands are poorly to very poorly sorted fine to coarse sands, with a calcitic matrix present in all samples. The dominant lithic fragments are granitic within TE-4, leading to the classification of the TE-4 sediment as feldspatho-lithic plutoniclastic sandstones.

The five samples analysed from the TE-5 and TE-6 core consisted of poorly sorted fine to coarse sands with a calcitic matrix present in all samples as seen in TE-4. The most common lithic fragments within the TE-5 and TE-6 samples are chert and plutonic clasts similar to TE-1 leading to the classification of the TE-5 and TE-6 sediment as quartzo-litho-feldspathic to litho-feldspathic plutoniclastic sand.

The nine samples from the TAGI reservoir interval from the TE-8 well are moderately to poorly sorted coarse-grained sands. The clastic composition varies, with igneous clasts dominating the lower samples and metamorphic and volcanoclastic samples at the top of the analysed section. In general, the samples within the TE-8 well classify as quartzo-feldspatho-lithic plutoniclastic sands at the base and feldspatho-quartzo-lithic metamorphiclastic sands at the tops of the TAGI reservoir interval.

The nine samples from the TAGI reservoir interval from the TE-8 well are moderately to poorly sorted coarse-grained sands. The clastic composition varies, with igneous clasts dominating the lower samples and metamorphic and volcanoclastic samples at the top of the analysed section. In general, the samples within the TE-8 well classify as quartzo-feldspatho-lithic plutoniclastic sands at the base and feldspatho-quartzo-lithic metamorphiclastic sands at the tops of the TAGI reservoir interval.

The petrographic analysis of the Tendrara thin sections indicates that the TE-1 to TE-6 samples were likely to be sourced from a moderately dissected magmatic arc, based on their quartzo-lithic-feldspathic to litho-feldspathic plutoniclastic classification (Garzanti 2016). However, the samples from the TE-8 samples suggest a slightly different provenance. As seen in Figure 2-9, samples within the TE-8 well are a mixture of quartzo-feldspatho-lithic plutoniclastic sands and feldspatho-quartzo-lithic

metamorphiclastic sands. The older samples from the TE-8 well are quartzo-feldspatho-lithic plutoniclastic sands, with the younger samples from the TE-8 well are feldspatho-quartzo-lithic metamorphiclastic sands. This suggests the sediment from TE-8 contains a mixture of sources, from a undissected axial belt and a dissected magmatic arc.

The F5 samples collected from the Oukaimeden Valley were analysed as part of Fabuel-Perez PhD thesis (Fabuel-Perez 2008, p. 165) and are plotted in Figure 2.10. FA-1 represents fluvial sands classified as lithic-quartzose sedimenticlastic sands typically interpreted to be sourced from a recycled orogenic provenance (Garzanti 2016). The aeolian deposits of FA-3 have been classified as lithic-quartzose to quartzose sedimenticlastic sands which are interpreted to be sourced from a recycled orogenic provenance (Garzanti 2016). The final facies, FA-4, are the tidal facies from the upper F5 formation and can be classified as the feldspatho-quartzose to quartzose sands, interpreted as a recycled clastic provenance (Garzanti 2016).

There are several possible explanations for the petrographic results, with one interpretation being a similar source region for the TE-8 sands and the K3 and K4 sands, with the Oukaimeden sands having a unique source to both Tendrara and Kerrouchen. It is important to note however, the composition of the sands in the Kerrouchen Basin and the TE-8 core occupy regions on the ternary diagram which can be occupied by sediment sourced from almost any provenance (e.g. Garzanti 2016, p. 9). To accurately discriminate between the provenance of the sands across the three basins, the heavy mineral assemblage will need to be analysed.

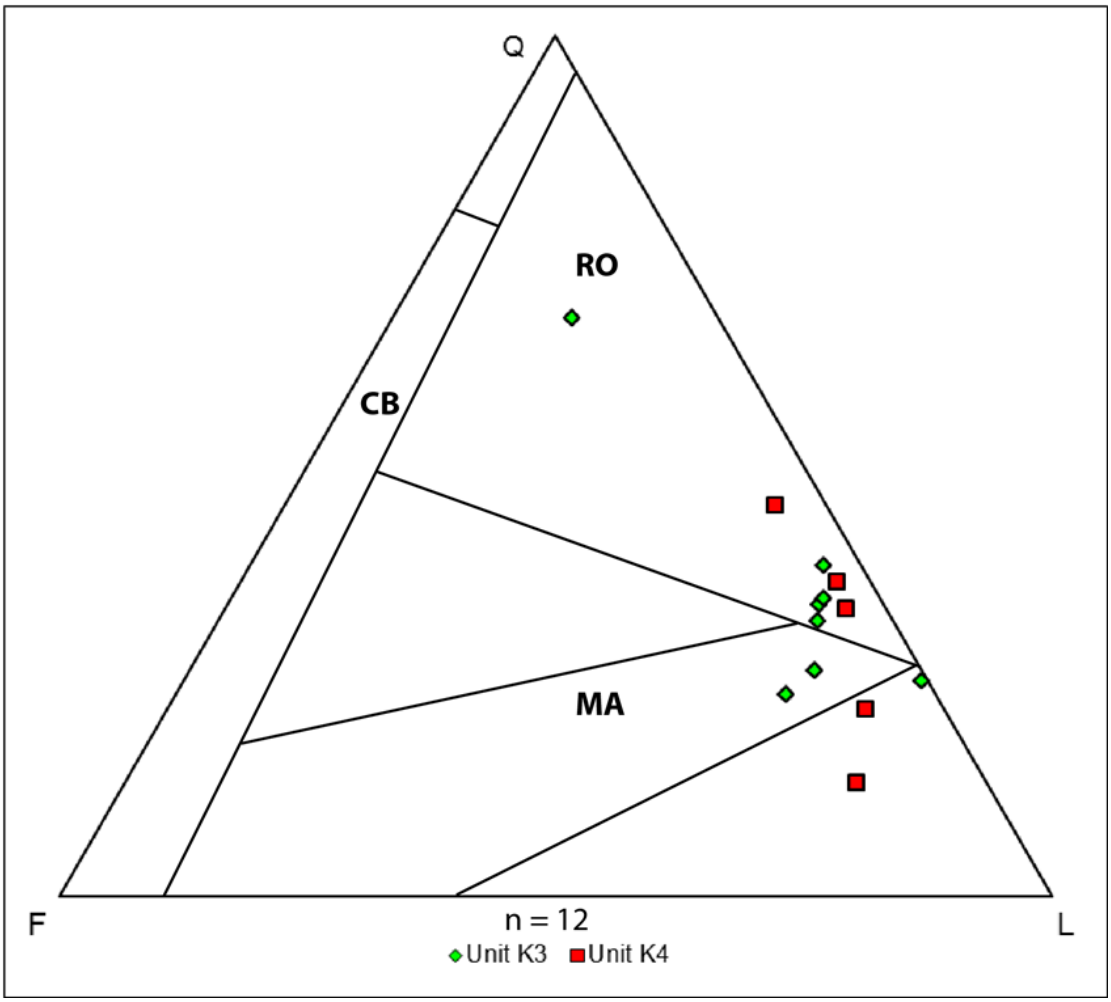

Figure 2-8: Results of the petrographic analysis of the Kerrouchen K3 and K4 formations. Samples from both formations show similar results and clastic compositions leading to their classification as quartzo-lithic or feldspatho-quartzo-lithic metamorphiclastic and volcanoclastic sandstones. The unique, quartz rich sample is the KH-20 sample from the middle-K3 member. This classification of sandstones is typically thought to be sourced from an undissected axial belt (Garzanti 2016) or a recycled orogenic belt (Dickinson 1985)

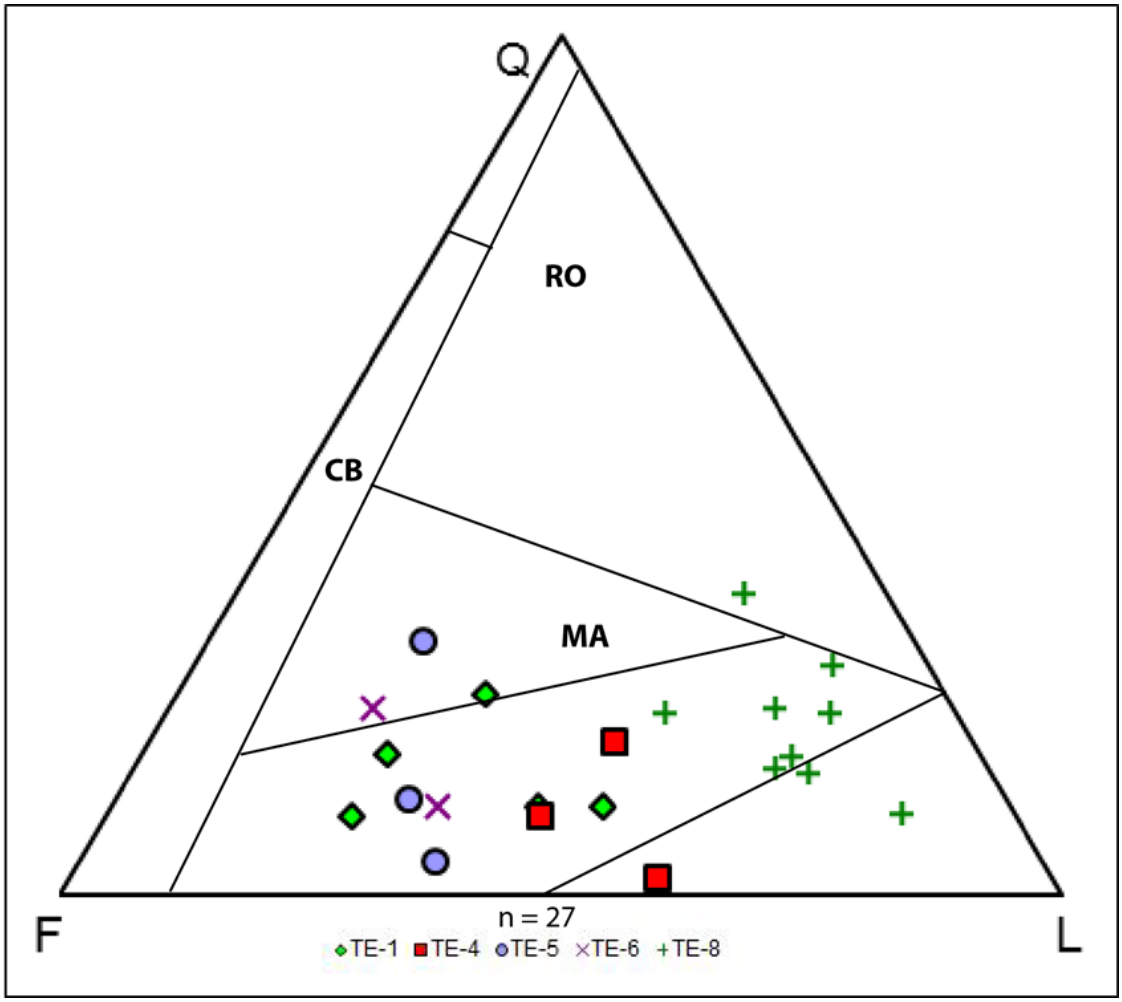

Figure 2-9: Results of the petrographic analysis of the Tendrara Field core samples. The majority of samples from the TE-1, 4, 5, 6 plots as litho-feldspathic to quartzo-litho-feldspathic plutoniclastic sandstones, with the TE-8 samples plotting as quartzo-feldspatho-lithic plutoniclastic or feldspatho-quartzo-lithic metamorphiclastic sands. The classification of the TE-1 to TE-6 sandstones is typical of a moderately dissected magmatic arc, whereas the TE-8 sands are more typical of a undissected magmatic arc or axial belt (Dickinson 1985; Garzanti 2016).

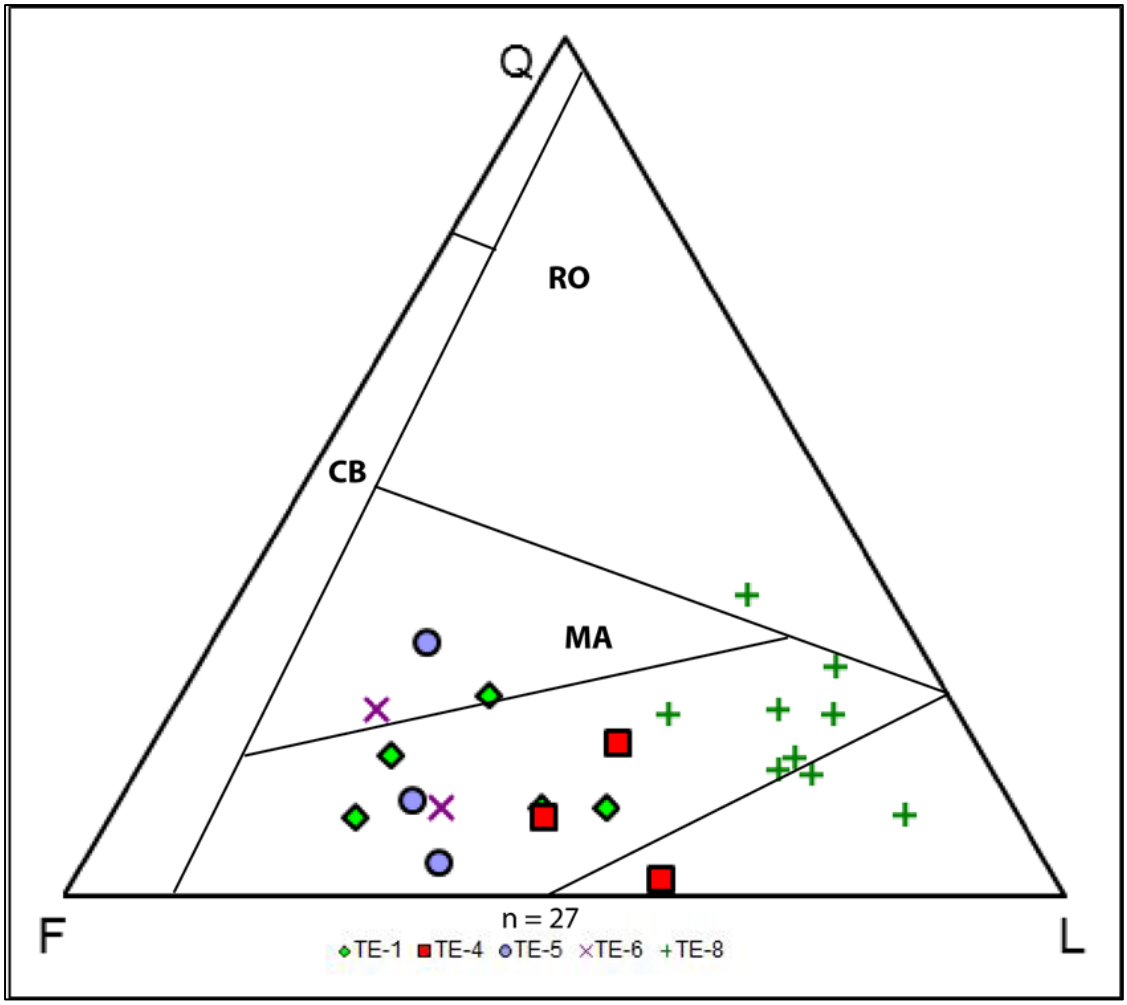

Figure 2-10: Results of the petrographic analysis of the facies of the F5 formation of the Oukaimeden Basin (Fabuel-Perez 2008, p. 165). The samples from all three facies plot predominantly as litho-quartzose to quartzose sands, typically interpreted to be from a recycled orogenic (Dickinson 1985) or recycled clastic provenance (Garzanti 2016).

2.5.2. Heavy Mineral Results

16 samples were chosen for heavy mineral analysis from across the 3 basins, with 4 from the F5 formation Oukaimeden, 5 form the K3 formation and 3 from the K4 formation of the Kerrouchen Basin, alongside 1 from TE-6 well and 3 from TE-8 wells from the Tendrara Field. The samples from the Oukaimeden and Kerrouchen Basin are from formations which represent the S2 formation, meaning they are likely to represent a similar depositional interval. When combined within the samples from Tendrara, they will provide insight into the likely reservoir quality and distribution in the Tendrara Field. Within the Tendrara Field, the TE-6 sample is from channel complex 1, with the three TE-8 samples from crevasse complexes thought to be correlated to the TE-6 channel complexes (Benvenuti 2017).

Within the Kerrouchen Basin, samples KH-10 to KH-64 *(Table 2.4)*, a low diversity heavy mineral assemblage is preserved, with TiO_2 polymorphs (rutile, anatase, brookite) dominating, comprising over 30% in 5 samples and over 20% in 7. Ilmenite is also a major component, 12-38% of the detrital heavy mineral assemblage of these 7 samples. Apatite forms a significant but variable component,0.8-31.7%, with lower values observed in samples interpreted to be from ephemeral or braided fluvial systems *(e.g. KH-10,11,31)* potentially due to the instability of Apatite in meteoric groundwater (Morton 1984; Morton & Hallsworth 2007). Zircon and hornblende form significant minor components in 7 of the samples, however hornblende is the major component of the heavy minerals within the KH-20 assemblage *(Table 2-D),* comprising over 50% of the heavy minerals. Hornblende also has an elevated in the uppermost K4 sample, KH-60, forming 26% of the assemblage. The KH-20 sample appears to be unique within the Kerrouchen Basin, as it is the only sample which is predominantly hornblende. The bulk heavy mineral assemblage of the Kerrouchen Basin is a relatively low stability assemblage, suggesting the basin has not been deeply buried, as low stability Ca-Amphiboles (e.g. hornblende) have been preserved alongside high stability minerals such as the TiO_2 polymorphs (Morton & Hallsworth 2007).

Within the four samples analysed from the lower and middle F5, Oukaimeden, a low diversity assemblage dominated by TiO_2 polymorphs (27-41%) with significant Ilmenite (20-37%), Apatite (14-16%) and Zircon (4.5-19.5%) components. Hornblende is a significant minor component in all samples, with ~4% present in all 4 samples with the MSC sample also contains a further 2.7% Actinolite. The assemblage preserved within the Oukaimeden Basin is similar to the assemblage of the Kerrouchen Basin, however the dominance of high stability minerals such as Zircon, TiO_2 polymorphs and Apatite indicates the basin may have been more deeply buried than the Kerrouchen Basin (Morton & Hallsworth 2007).

Within the Tendrara Field, 1 sample from the TE-6 well was analysed alongside 3 from the TE-8 well, with two distinct groupings observed. The first group comprises samples TE-6-77 and TE-8-80, which are dominated by TiO_2 minerals with significant Ilmenite (12-23%) and Hornblende (12-17%). The second group includes samples TE-8-73 and TE-8-65, which gave in excess of 60% Hornblende *(Table 2-D)* and Almandine garnet up to 9%. Both assemblage groupings are low diversity, however the first group is a moderate to high stability assemblage with the second preserving a much lower stability assemblage (Morton & Hallsworth 2007). As the difference in the detrital assemblage is seen within a basin, it is unlikely to be due to differing depths of burial. This implies that the differences in the preserved assemblages within the Tendrara field is due to a shift in provenance between the deposition of the TE-8-80 sample and the overlying TE-8-73 and TE-8-65 samples, as suggested by the petrographic results.

Table 2-D: QEMSCAN area percentage results of the major heavy minerals within the analysed samples

Sample	Formation	Actinolite	Al-Phosphate	Almandine	Apatite	Augite	Barite	Diopside	Glauconite	Hornblende	Ilmenite	Kutnohorite	Paragonite	Pargasite	Rutile	Zircon	Trace
KH-10	U-K3	2.5	1.7	3.1	2.3	2.0	0.5	0.0	0.4	14.1	12.1	0.0	0.0	0.0	50.7	10.0	0.6
KH-11	U-K3	0.1	1.8	2.4	2.9	0.1	0.1	0.0	0.5	15.9	15.6	0.0	0.1	0.0	49.9	10.2	0.4
KH-20	M-K3	2.4	0.0	0.0	31.7	4.0	0.5	0.8	2.5	51.8	0.0	4.1	0.0	0.2	1.7	0.1	0.1
KH-30	L-K3	2.8	0.0	0.7	16.5	3.3	1.2	0.2	0.9	4.7	36.5	0.0	0.2	0.0	28.0	4.7	0.3
KH-31	L-K3	0.1	0.7	1.0	0.8	0.0	8.1	0.0	5.3	17.6	12.5	0.0	1.1	0.0	49.0	3.5	0.1
KH-60	U-K4	0.5	0.6	1.0	14.0	0.8	0.2	0.2	2.9	26.1	25.3	0.4	0.6	0.0	21.9	4.9	0.6
KH-62	U-K4	0.3	0.1	0.2	8.2	0.4	0.0	0.1	0.6	3.8	30.9	0.3	0.3	0.0	46.0	8.7	0.1
KH-64	L-K4	0.3	0.1	0.2	8.2	0.4	0.0	0.1	0.6	3.8	38.9	0.3	0.3	0.0	38.0	8.8	0.1
ON-2	L-F5	0.0	0.0	0.5	14.5	0.0	0.0	0.0	0.7	4.4	22.0	0.0	0.1	0.0	37.7	19.6	0.3
ON-13	L-F5	0.0	0.0	0.6	14.4	0.0	0.0	0.0	0.7	4.5	22.1	0.0	0.1	0.0	37.5	19.7	0.4
ON-45	M-F5	0.0	0.1	3.0	15.7	0.0	0.0	0.0	0.7	4.4	24.5	0.0	0.2	0.0	41.8	9.5	0.2
MSC	M-F5	2.7	0.0	0.7	16.2	3.2	1.2	0.2	0.9	4.6	38.0	0.0	0.2	0.0	27.4	4.5	0.2
TE-6-77	-	0.1	0.7	1.1	0.7	0.0	8.1	0.0	5.3	17.7	12.7	0.0	1.2	0.0	48.6	3.6	0.1
TE-8-65	-	1.7	0.2	0.3	2.0	0.1	0.2	0.0	1.1	85.2	1.0	0.3	0.4	1.7	5.5	0.1	0.2
TE-8-73	-	0.8	0.2	9.1	7.4	0.2	1.2	0.0	1.6	62.0	4.2	0.4	0.2	1.6	8.8	1.3	0.7
TE-8-80	-	0.0	0.2	0.6	16.0	0.0	0.6	0.0	3.2	11.9	23.8	0.1	0.7	0.0	37.7	5.0	0.2

Provenance sensitive heavy mineral ratios were utilised to attempt to identify provenance variations between samples (Morton & Hallsworth 1994). Based on the heavy mineral assemblages from the samples only GZi and TiO_2:Zi were calculated *(Table 2-B)* with the results presented below and plotted against each other *(Figure 2-11).*

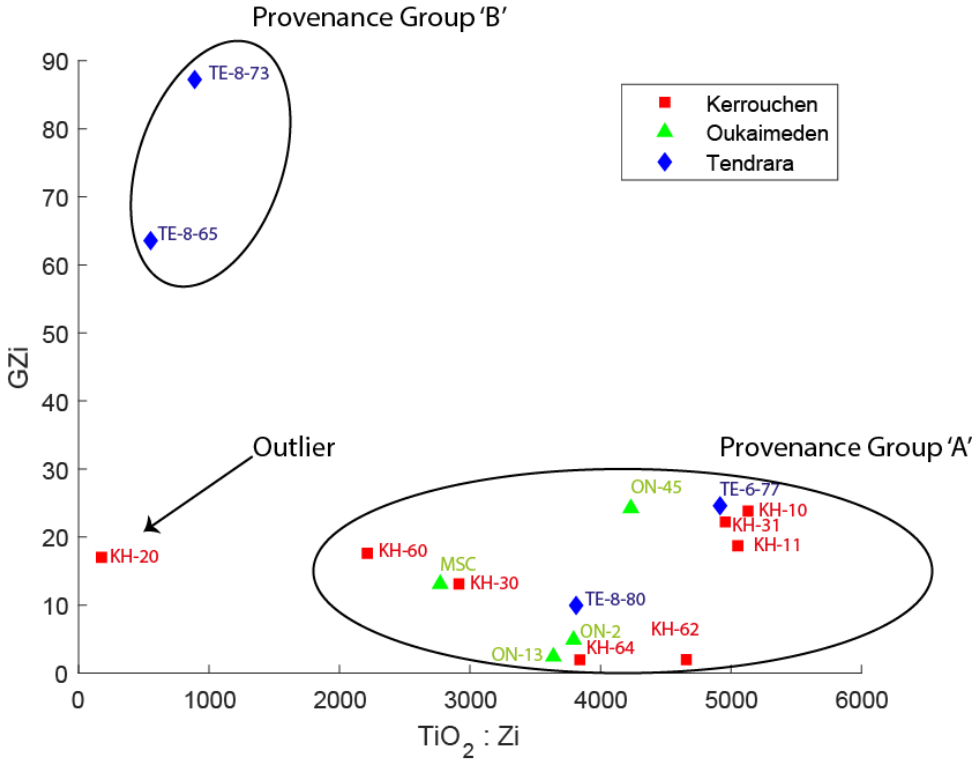

Figure 2-11: Plots of provenance sensitive heavy mineral ratios. The majority of samples cluster along the bottom right, with the TE-8-73, TE-8-65 and KH-20 samples displaying evidence of a different provenance

As can clearly be seen in Figure 2-11, 2 distinct groupings are present. The larger group, clustered in along the x-axis of the graph, contains samples from Kerrouchen, Oukaimeden and Tendrara. These samples are characterised by elevated TiO_2: Zi values and low G:Zi values. The second grouping clusters along the y-axis and is comprised of the TE-8-65 and 73 samples. This grouping is characterised by low TiO_2: Zi values and elevated G:Zi values. The KH-20 sample from the Kerrouchen Basin does not easily fit into either grouping, as it is both low G:Zi and low TiO_2:Zi.

These results indicate that at least two unique provenance groups are recorded within the analysed samples. The first is characterised by elevated TiO_2: Zi and is present across all basins. The second is characterised by elevated G:Zi and is only present within the TE-8 well of the Tendrara Field. The anomalous, KH-20 sample also indicates that a third, unique source may have been supplying sediment to the Kerrouchen Basin *(Figure 2-11).*

The final stage of provenance analysis performed on the samples was to utilise the heavy mineral indices of Garzanti and Ando (Garzanti & Andò 2007b) as shown in Table 2-B. From visual inspection of the heavy mineral indices shown in **Error! Reference source not found.**, it can be seen that all samples had low contributions from metamorphic terranes, as Garnet (Gt), Low grade Metamorphic (LgM) and High grade Metamorphic (HgM) are low in all samples. The low value of Olivine-Spinel (OS) and orthopyroxene (OPX) indicates that ultramafic sources are unlikely to form a significant contribution to the sediment. As a result of this, ZTR T&, Gt, CPX, Hb and &A were plotted in pie charts and underwent principal component analysis (PCA) utilising the R provenance package (Vermeesch *et al.* 2016).

Sample Number	Formation	ZTR,T&	Gt	LgM	HgM	CPX	OPX	OS	Hb	&A
KH-10	U-K3	74	4	0	0	2	0	0	16	3
KH-11	U-K3	77	3	0	0	0	0	0	19	0
KH-20	M-K3	35	0	0	0	5	0	0	53	7
KH-30	L-K3	81	1	0	0	6	0	0	7	5
KH-31	L-K3	77	1	0	0	0	0	0	22	0
KH-60	U-K4	58	1	0	0	1	0	0	37	1
KH-62	U-K4	92	0	0	0	1	0	0	6	1
KH-64	L-K4	91	0	0	0	1	0	0	6	1
ON-2	L-F5	93	1	0	0	0	0	0	6	0
ON-13	L-F5	93	1	0	0	0	0	0	6	0
ON-45	M-F5	90	4	0	0	0	0	0	6	0
MSC	M-F5	81	1	0	0	6	0	0	7	5
TE-6-77	-	76	1	0	0	0	0	0	22	0
TE-8-65	-	8	0	0	0	0	0	0	88	4
TE-8-73	-	20	10	1	0	0	0	0	66	3
TE-8-80	-	82	1	0	0	0	0	0	17	0

Table 2-E: HM Indices utilised to compare provenances and identify likely source terranes. Key to indices: ZTRT = Zircon, Tourmaline, Rutile, TiO_2-Minerals. Gt = Garnet. LgM = Low-grade metamorphic minerals. HgM = High grade metamorphic minerals. CPX = Clinopyroxene. OPX = Orthopyroxene. OS = Olivine-Spinel. Hb = Hornblende. &A = Non-hornblende amphiboles.

Within the Kerrouchen Basin, the heavy mineral assemblages are dominated by ZTR and T& minerals with the exception of the KH-20 which is dominated by hornblende. All the

samples contain a secondary component of hornblende, with garnet, clinopyroxene and other amphiboles present in varying amounts. The dominance of ZTR and T& minerals within the assemblage indicate that the sediment was sourced from a felsic igneous or reworked igneous source with a significant contribution from an intermediate to mafic source as seen by Hb, &A and CPX forming the secondary components within the samples. The presence of significant garnet (3-4%) within samples KH-10 and KH-11 suggests that the upper K3 may have had a contribution from a metamorphic source terrane *(Figure 2-12).*

The Oukaimeden Basin contains an assemblage dominated by ultrastable mineral indices with ZTR and T& comprising over 80% of the assemblage. The lower F5 contain 93% ZTR, T& and 6% Hb. The abundance of ZTR, T& decreases throughout the middle F5, reaching 81% in the MSC sample, with Hb, CPX and &A increasing in the middle F5. As seen in Figure 2-12, the assemblage preserved within the Oukaimeden Basin is dominated by minerals sourced from either felsic igneous or reworked sedimentary sources with increasing contributions from an intermediate to mafic source in the middle F5. The presence of minor Gt indicates a minor contribution from a metamorphic source, similar to that observed within the upper K3 of the Kerrouchen Basin.

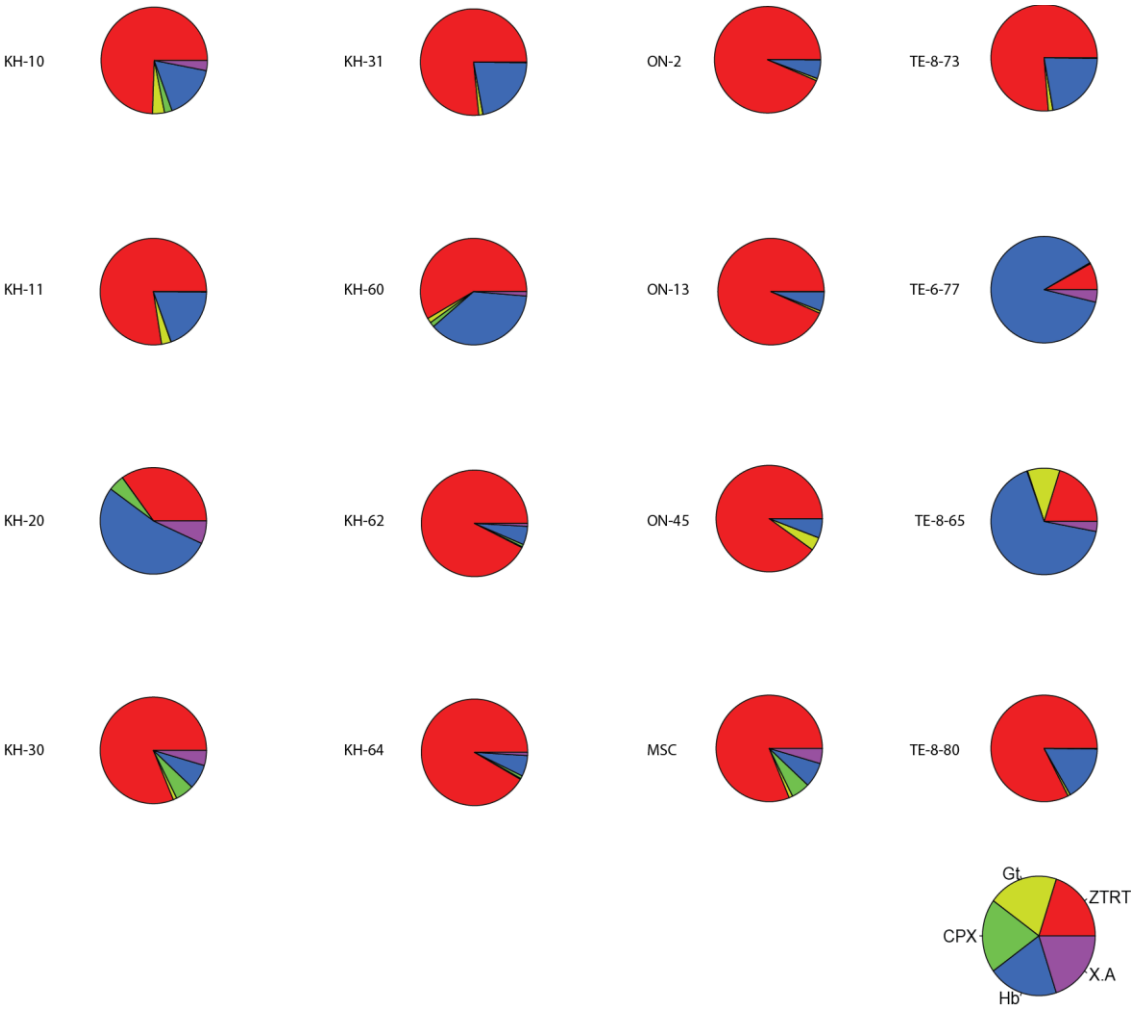

Figure 2-12: Heavy Mineral Indices pie chart plots from Kerrouchen, Oukaimeden and Tendrara. Produced using the R provenance package (Vermeesch et al. 2016). Key to indices: ZTRT = Zircon, Tourmaline, Rutile, TiO_2-Minerals. X.A = Non-hornblende amphiboles. Hb = Hornblende. CPX = Clinopyroxene. Gt = Garnet. For stratigraphic position of the samples please see Table 2E

The Tendrara Field contains two distinct signals, with the TE-8-80 and TE-6-77 containing mainly ZTR with secondary Hb and minor Gt. The secondary signal, seen in TE-8-73 and TE-8-65, has a major Hb component and minor ZTR and T& component *(Figure 2-12).* The TE-8-73 sample also contains a significant garnet component. These results support the observation of a distinct provenance for these 2 samples, as shown by the heavy mineral ratios *(Figure 2-11)* The heavy mineral indices allow us to identify the likely shift in source terrane responsible for these shifts, with the signal seen in TE-6-77 and TE-8-80 indicate a dominant felsic igneous or recycled sedimentary source with a contribution from an intermediate to mafic terrane. The signal seen in the TE-8-73 and TE-8-65 samples in contrast is predominantly sourced from an intermediate to mafic source with minor contributions from felsic igneous and metamorphic sources.

The PCA of the heavy mineral indices allows for the statistically rigorous identification of sample with similar provenances (Vermeesch *et al.* 2016; Garzanti *et al.* 2017). The most common provenance 'type-A' is seen clustered around the ZTR, T& pole *(Figure 2-13).*

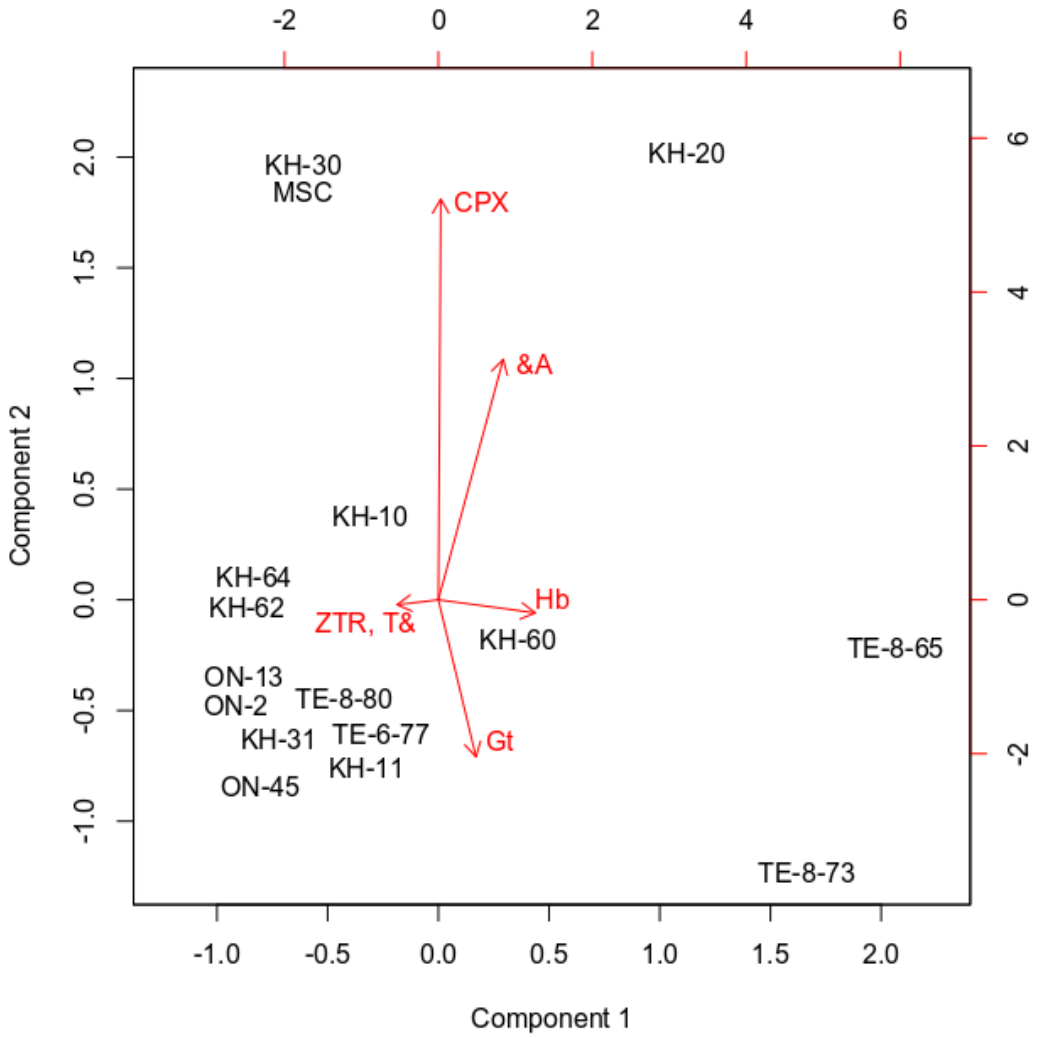

Figure 2-13: PCA of the Heavy Mineral Indices, highlighting the presence of multiple distinct provenances, both within in basins and across basins.

This grouping has minor contributions from Gt and CPX and is interpreted to record an igneous felsic or reworked sedimentary source with minor contributions from a metamorphic source for the majority of samples from Oukaimeden, Kerrouchen and Tendrara. The MSC and KH-30 samples share characteristics of the type A provenance, however they contained a more significant contribution from a mafic terrane than the other samples within the type A provenance.

The second provenance signal, type-B, is only observed within the TE-873 and TE-8-65 samples from the Tendrara field. This provenance type is dominated by hornblende, suggesting an intermediate to mafic igneous or meta-igneous source region for the

sediment. The KH-20 sample plots away from the other samples, and is unique due to its elevated &A, CPX indices alongside the high Hb value. This suggests that KH-20 was sourced from a unique mafic igneous or meta-igneous source and records a unique provenance. Sample KH-60 is also shown to be unique by the PCA, as it appears to be an intermediate between the type-A and type-B samples, potentially indicating a mixing of separate drainage systems.

Sample KH-20 could also be an anomalous sample. When comparing the heavy mineral data with the petrographic data *(Figure 2.8)* the anomalous data point which records a feldspatho-lithic-quartzose composition was KH-20. There are several possible explanations for this, which will be discussed below.

The heavy mineral ratios and indices utilised within this study both indicate at least two distinct provenances for the fluvial sands of the Middle to Late Triassic. One, provenance type-A, is likely to have been sourced from a felsic igneous or reworked sedimentary source, with type-B sourced from an intermediate to mafic source region. The type-A signal is present across all basins, whereas type-B is only present within the Tendrara Field. However, the type-B signal may also have contributed to the Kerrouchen Basin samples. When combined with the petrographic analysis, this presents several possible scenarios for the Triassic paleo-drainage across Morocco.

2.6. Discussion

Two main provenances have been recorded within the detrital heavy mineral assemblages preserved within the Triassic sands across Morocco. The first, A-type provenance, records a high stability heavy mineral assemblage likely sourced from a felsic igneous or reworked sedimentary source terrane. The second, B-type provenance, records a moderate stability heavy mineral assemblage interpreted to be sourced from an intermediate to mafic igneous or meta-igneous terrane. When viewed stratigraphically *(Figure 2-14).* it can be seen that there is a general tend from Type-A in at the base of each formation to Type-B in near the top of each formation. The only sample that does not fit this trend is the anomalous KH-20 sample from within the Kerrouchen Basin.

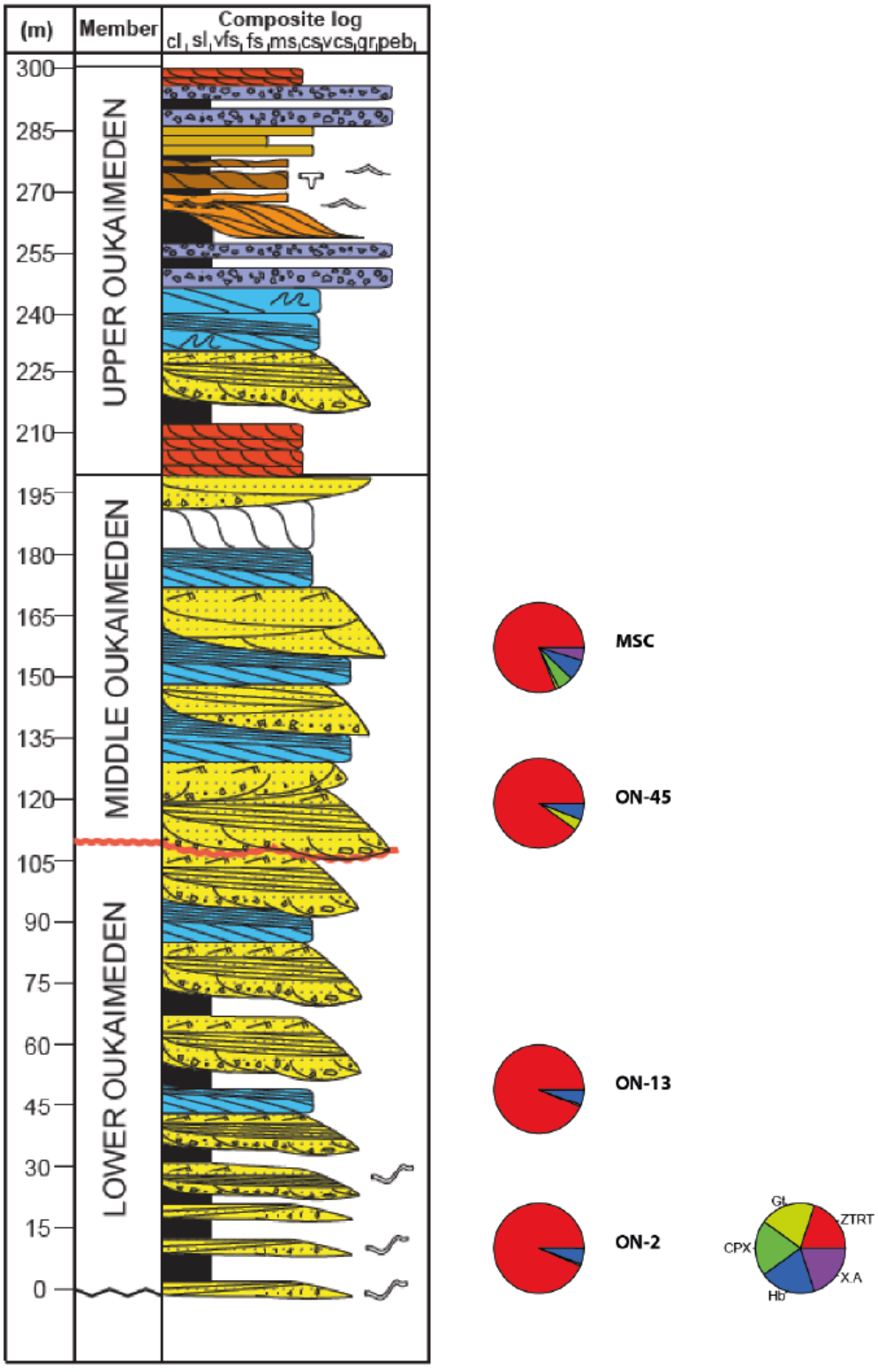

Figure 2-14: Showing the HMI pie chart variations within the stratigraphy of the F5 formation Oukaimeden Basin. The proportion of the mafic and metamorphic minerals increases as you move up through the stratigraphic units, indicating an increasing contribution from mafic source rocks which may be caused by stratigraphic unroofing.

There are several possible explanations for this anomalous sample. The first is that the sample is markedly different from the other samples within the Kerrouchen Basin due to environmental bias or local heterogeneity present within detrital assemblages. The second potential cause is that the KH-20 sample, located within a more axial setting, is sourced from a unique, regional source whereas the other samples from within the basin are sourced from more local, intra-basinal sources, potentially the uplifted regions on the basin margins *(Figure 2-14).* Within the Kerrouchen Basin, the two most hornblende rich samples, KH-20 and KH-60, are the most axial with lower hornblende in marginal positions within the basin. This suggests that the KH-20 and KH-60 sample may be representing a different drainage network to the other Kerrouchen samples *(Figure 2-15).*

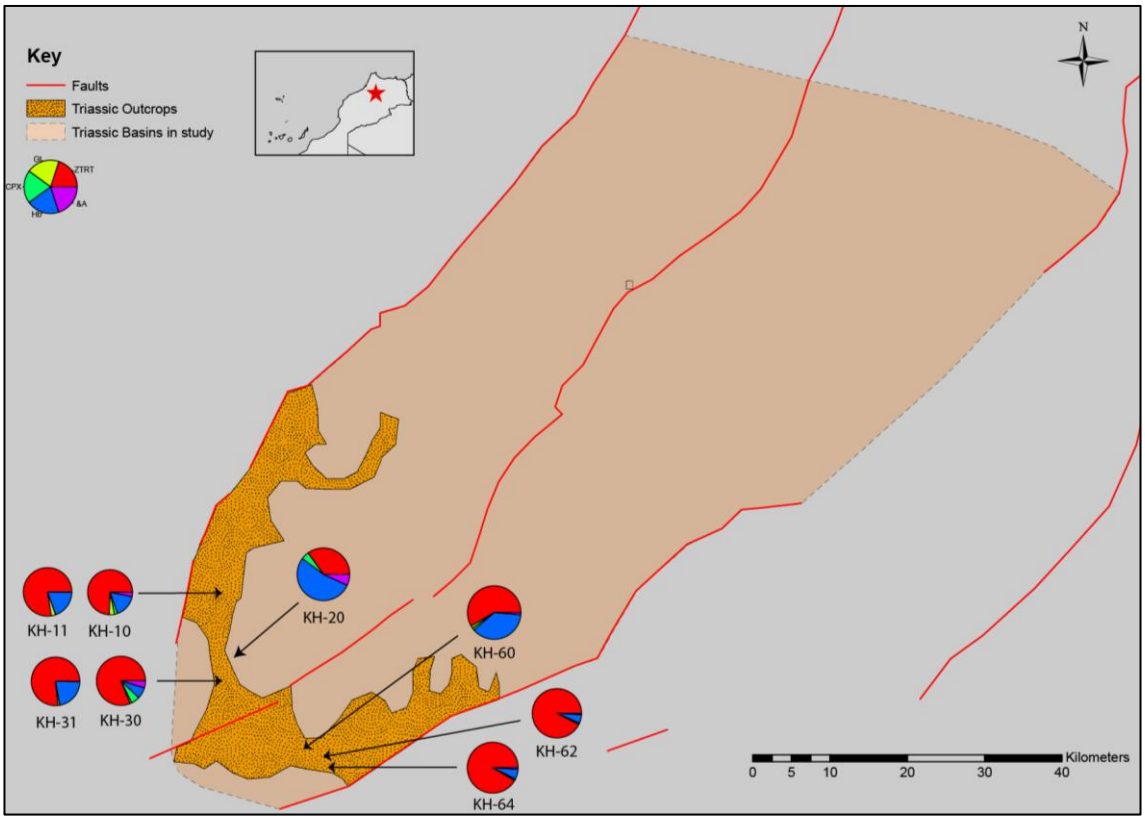

Figure 2-15: Spatial distribution of HMI results from the Kerrouchen Basin. The more hornblende rich facies are found in more axial settings, suggesting they represent a more regional drainage network. The KH-20 facies is from stacked fluvial sand, a likely stratigraphic representation of a regional drainage system; however the KH-60 sample is from silt-rich sandstone, which is unlikely to represent a regional system.

The third potential explanation is that the stratigraphic framework for the Kerrouchen Basin is incorrect, with the KH-20 stratigraphically younger than previously reported (Ouarhache *et al.* 2012). Whilst all three scenarios are possible, proving this would require resampling of the locality alongside remapping of the Kerrouchen Basin in order to further constrain the extent of the Triassic sandstone formations and their stratigraphic relation to each other.

Whilst the result from KH-20 shows that more work is needed, especially within the Middle Atlas, to fully understand the results of this study, the results can be used alongside previous work to propose some models for the hinterland evolution and Triassic regional drainage networks. The two models proposed here for the evolution of the source region build on recent thermochronometry work (Domènech *et al.* 2016; Charton *et al.* 2018) and hypothesise that the change in heavy mineral assemblage are the result of eiher hinterland unroofing or hinterland reorganisation leading to a change in the exposed lithology's available for erosion. Building of these hypotheses, likely source areas have been identified allowing for the development of source to sink models which can be tested for further study.

The hinterland reorganisation model suggests that during the Triassic, a new source area was uplifted, allowing for the erosion of different material resulting in the change in detrital assemblage preserved within the analysed samples. A period of tectonic uplift could also have resulted in the reorganisation of drainage networks resulting in the fluvial systems recording a shift in provenance, as seen in the north-west European Triassic (Tyrrell *et al.* 2012). This is considered to be unlikely in Morocco, as the thermal evolution models suggests the Triassic was a period of low uplift of the Anti-Atlas with subsidence of the Middle and High Atlas, continuing the post-Variscan trend (Gouiza *et al.* 2017; Charton *et al.* 2018). This suggests that it is unlikely for extensive reorganisation of the hinterland to have occurred during the Triassic allowing us to conclude that this model for the source region evolution is unlikely.

The second model for the change in provenance observed is that during the Triassic a period of hinterland unroofing occurred, where erosion reached new levels of the crust. In general, the continental crust has a sedimentary cover overlying felsic igneous rocks, with an intermediate to mafic igneous and meta-igneous middle crust overlying a high grade metamorphic and ultramafic deep crust (Wedepohl 1995). The erosion through these layers of the crust would therefore result in a change in the provenance signal despite the sediment being derived from the same locality. The thermochronometry models for the Anti-Atlas suggest that they were uplifted from the Late Triassic to the Middle Jurassic, resulting in the erosion of between 4.5 and 5.5 km (vertical profile models) (Domènech *et al.* 2016) and between 7.5 to 10km of sediment (Gouiza *et al.* 2017; Charton *et al.* 2018). During the Late Triassic, the primary source material eroded was Phanerozoic cover, however by the Middle Jurassic the Precambrian basement was exposed (Charton *et al.* 2018). Using this model, it the predicted heavy mineral signal would be one which goes from ultrastable, recycled sedimentary assemblage to one where more unstable, mafic and meta-igneous minerals are present. This model matches the observations seen within the Oukaimeden, Kerrouchen and Tendrara samples, suggesting that the variation in provenance recorded in these basins was the result of unroofing and erosion of the hinterland.

If this is correct, the source area for the sediment remained roughly constant throughout the Triassic, however erosion led to the exposure of new rocks leading to a change in the detrital heavy mineral assemblage. The recent thermochronometry studies focused on the Anti-Atlas and the Marrakech High Atlas, concluding that the Anti-Atlas and the Marrakech high Atlas were exhumed and eroded during the Triassic, acting as the rift shoulder to the subsiding Atlas rifts to the north (Domènech *et al.* 2016; Charton *et al.* 2018). The Central Meseta domain to the north was a slowly subsiding domain, outside of the rapidly subsiding rift basins (Domènech *et al.* 2016). Whilst uplift data from Eastern Meseta is sparse, the region was covered by thin evaporitic mudstones (Oujidi *et al.* 2000; Courel *et al.* 2003), suggesting that the region was slowly subsiding during the Triassic in a similar way to the Central Meseta.

Detrital zircons also provide evidence of where sediment was sourced from during the Triassic, although as they can survive multiple erosion-deposition-erosion cycles, they may record an initial source for the sediment that was not the source of sediment during the Triassic (Zimmermann *et al.* 2015; Andersen *et al.* 2016). Detrital zircons from the Triassic of the Ourika-Tizi n'Tacht basin have recorded input from the Reguibat Shield alongside the dominant input from the Anti-Atlas sedimentary cover and Pan-African basement (Domènech *et al.* 2018). Taken in combination with the thermochronometry data, the Anti-Atlas was probably the major source for sediment within the Triassic rift basins of Morocco, with contributions from the Reguibat shield to the south, with the Central and Eastern Meseta domains not providing a significant source of sediment.

The total sediment eroded during the Triassic is thought to be at least 2.5km (Domènech *et al.* 2016), with erosion beginning in the Palaeozoic cover and gradually unroofing more mafic rocks, as shown by the detrital heavy mineral assemblages and predicted by Charton (Charton *et al.* 2018).

Using this model for the evolution of the hinterland, we can make predictions about the paleo-drainage network which moved the sediment from source to sink and make predictions about the expected detrital geochronological signal which would be recorded within the basins. Based on the currently available data, it is unlikely that local drainage networks were the dominant systems in moving sediment from source to sink. A local drainage model would have the Triassic of the Oukaimeden Basin drained from local basement and the Anti-Atlas, the Kerrouchen Basin sourced from local basement and the Central or Eastern Meseta and the Tendrara field sourced from local basement and the Eastern Meseta *(Figure 2-16)*.

In this scenario, the Type-A provenance (felsic igneous or recycled sedimentary), could be sourced from the sedimentary cover or igneous intrusions exposed within fault planes, with erosion into through the cover resulting in the deposition of more mafic rich heavy mineral assemblages in the younger sediment. The shifts in provenance recorded in the sediment would just reflect unroofing of local basement in this scenario. The principal component analysis for the heavy mineral assemblage provides some support for this scenario*(Figure 2.10)*The PCA of the heavy mineral indices allows for the statistically rigorous identification of sample with similar provenances (Vermeesch *et al.* 2016; Garzanti *et al.* 2017). The most common provenance 'type-A' is seen clustered around the ZTR, T& pole *(Figure 2-13).*

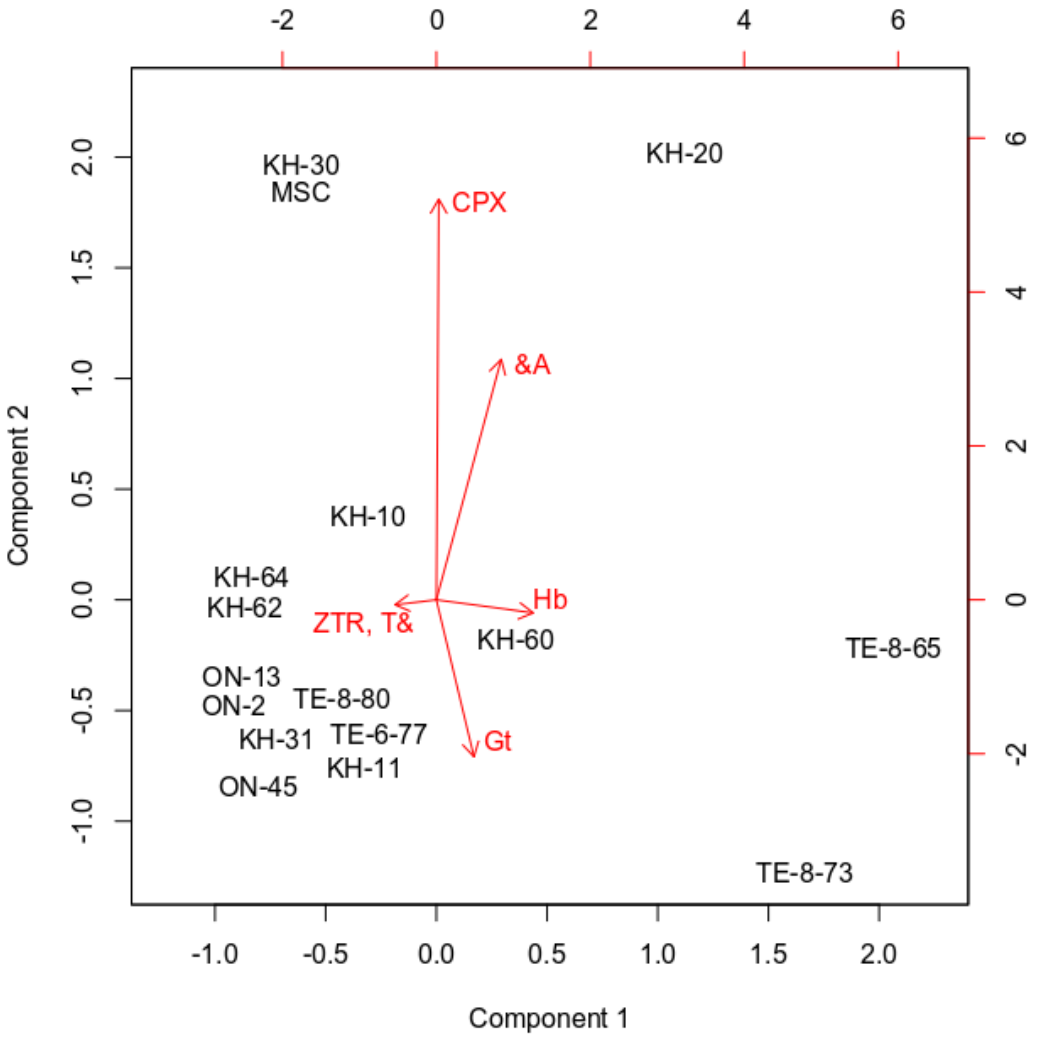

Figure 2-13, as while the sediment across all basins becomes more mafic with time; the transition in Oukaimeden is moderate, whereas in Kerrouchen it is fairly rapid. Both of these basins appear to be very different to Tendrara as it has the largest shift to a type-B provenance over the shortest stratigraphic distance *(Figure 2-13, Figure 2-14).* It is important to note that the Type B provenance is unique to Tendrara, with two samples from Kerrouchen (KH-20, KH-60) having traits of this provenance group (*Figure 2-13*). This suggests that the Type-B provenance may be unique to Kerrouchen and Tendrara, implying

that local drainage networks dominated the source to sink pathways in the Triassic. This model is supported from subsurface isopach data from the Tendrara field provided by Sound Energy shows the TAGI reservoir interval thickens to the south-west (Kape 2017), implying that the sediment was sourced from the north or north west (Hafid & Benaouiss 2010) supporting the idea that the Tendrara Field was locally sourced from the Eastern Meseta *(Figure 2-16)*.

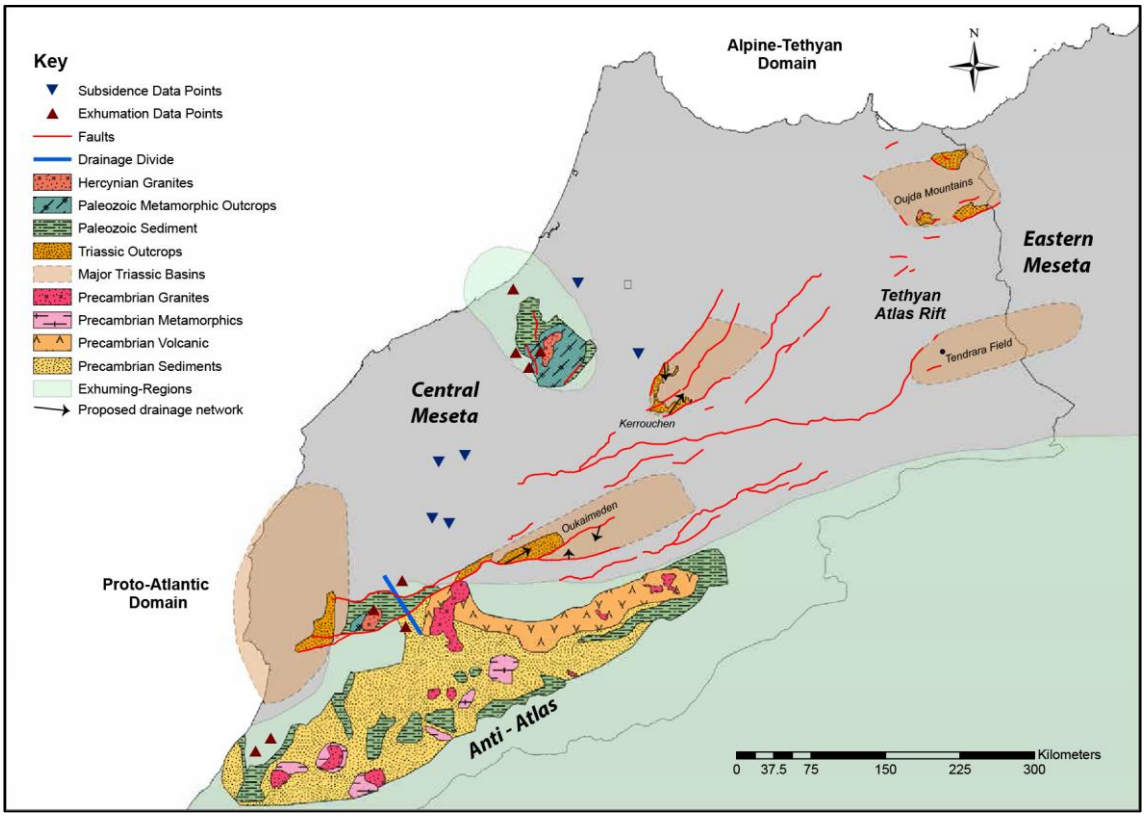

Figure 2-16: Local drainage network model. The three basins studied all have unique drainage networks with no communication between basins. The Central Meseta provided a source to the Kerrouchen Basin, the Eastern Meseta for the Tendrara Field and the Anti-Atlas to the Oukaimeden Basin.However, the uplift data does not support this model

This model appears to be contradicting the uplift data however, as it relies on the central and eastern Meseta providing source regions for the sediment. The uplift data and sedimentology from the Central and Eastern Meseta suggests that these regions were actually slowly subsiding during the Late Triassic, apart from a small area of uplift to the north-west of the Kerrouchen Basin (Oujidi *et al.* 2000; Domènech *et al.* 2016; Charton *et al.* 2018), meaning they are an unlikely source for the 600m of Triassic sediment in the Kerrouchen Basin. The absence of metamorphic heavy minerals ***(Error! Reference source not found.)*** within the Kerrouchen Basin means the uplifted region of the Central Meseta is unlikely to be a source as it is characterised by regional grade metamorphic rocks.

Furthermore, the paleoflows recorded within the Kerrouchen Basin suggest a source region to the south, not to the north, indicating that the uplifted region of the Central Meseta was unlikely to be a source for the Kerrouchen Basin in the Triassic.

In the future, detrital geochronology can be utilised to test this hypothesis. If basins were drained from local sources, there should be some discrepancies between the ages of the detrital assemblages. The Kerrouchen Basin and Tendrara Field, if sourced from the Central or Eastern Meseta, can be predicted to have a predominantly Pan-African detrital zircon U-Pb age, with first cycle zircons from the Variscan Orogeny (Domènech *et al.* 2018). As seen by the previous work, the detrital assemblage in the Oukaimeden Basin of the Central High Atlas should contain reworked Pan-African zircons from the Palaeozoic sediment of the Anti-Atlas, with detrital contributions from the Eburnean orogeny and the Paleoarchean of the Reguibat shield (Domènech *et al.* 2018).

The second model is one in which the basins progressively linked during the Triassic, with the S1 deposited in isolated basins with poorly developed depositional systems as shown by the random distribution of paleo-flows *(Figure 2-17).* During the deposition of the S2, middle syn-rift sequence, the Triassic rift basins were in communication and formed a wide, regional rift *(Figure 2-18).*

This model is supported by the shift in heavy mineral signal from the felsic sedimentary signal common to the older sediment of all basins to the intermediate to mafic heavy minerals present in the younger sediment, which could be a result of the basins being in communication during the unroofing of the uplifted source regions to the south. In this model, the trend for the heavy mineral assemblages to become more mafic in the younger sediment, is due to the basins sharing a common source area in the Anti-Atlas or another source further to the south (Domènech *et al.* 2018). The difference observed between the more mafic samples in the Kerrouchen Basin (KH-30, Kh-60), Oukaimeden Basin (MSC) and the Tendrara Field (TE-8-65, TE-8-73) is interpreted to be due to the Oukaimeden Basin undergoing deeper burial and as such losing more of the low stability mafic minerals which are present in the Kerrouchen and Tendrara Basins.

The three basins shared an initial common provenance, with sediment sourced from eroding the Palaeozoic cover, resulting in the deposition of an ultrastable heavy mineral assemblage across Morocco *(Figure 2-18).* As the source areas were eroded, more mafic rich units were exposed, resulting in the deposition of more mafic heavy mineral assemblages in the younger sediment of each basin. This unroofing trend is supported by the uplift data and erosional models developed using thermochronometry (Charton *et al.* 2018), with the Palaeozoic cover eroded during the middle to late Triassic to the extent that basement rocks where eroded during the Early to Middle Jurassic. The idea that the Triassic rift basins were

in communication has also been hypothesised *(Figure 2-18)* as some workers have proposed that the Tethyan and Atlantic rifts were in communication, with the Marrakech High Atlas providing a local drainage divide (Domènech *et al.* 2016).

Whilst this model does fit with the tectonic models and presumed source region evolution, the magnitude of the transition to mafic dominated heavy mineral assemblages is highly variable. The Oukaimeden Basin *(Figure 2-14)* shows a gradual, small increase in the abundance of mafic heavy minerals, whereas Kerrouchen has a much larger increase and Tendrara has a rapid, large magnitude increase in the proportion of mafic heavy minerals, specifically hornblende. This could potentially be due to the Tendrara field receiving sediment eroded from the Anti-Atlas east along the rift shoulder from the sediment at Oukaimeden. It is also important to recognise, that whilst the samples are from the 'S2' sequence, the time intervals over which this sequence was deposited is unknown, and the samples could have been deposited at significantly different times.

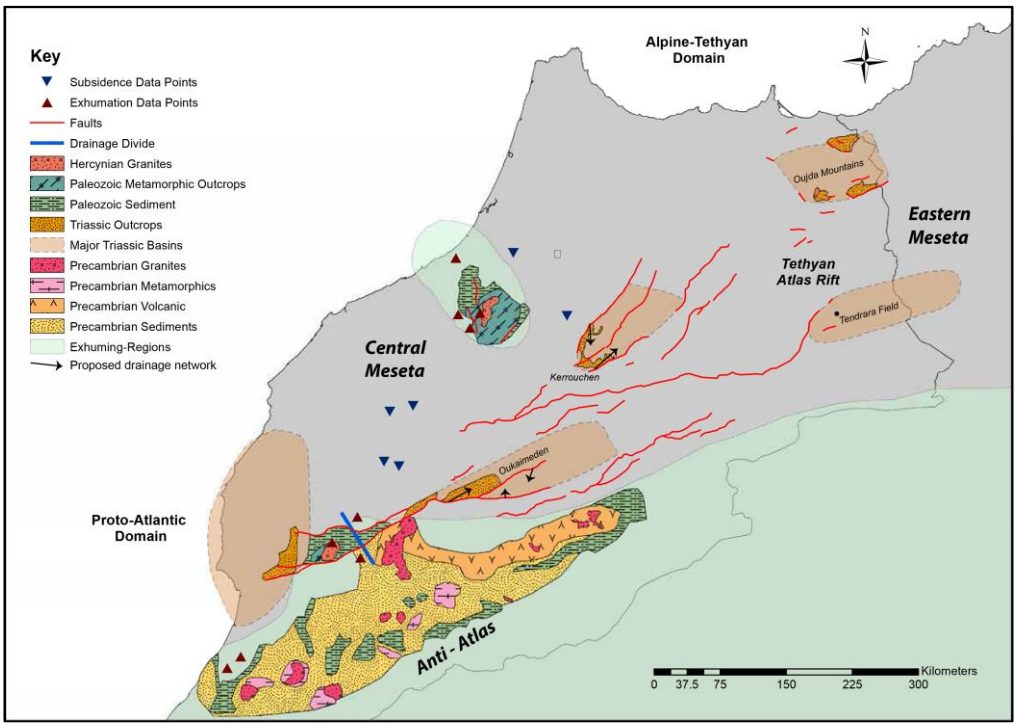

Figure 2-17: Early phase. The basins have small, intra-basinal, local drainage networks, with paleoflows from marginal basin highs towards the depocentres. The basins are not in communication during this phase.

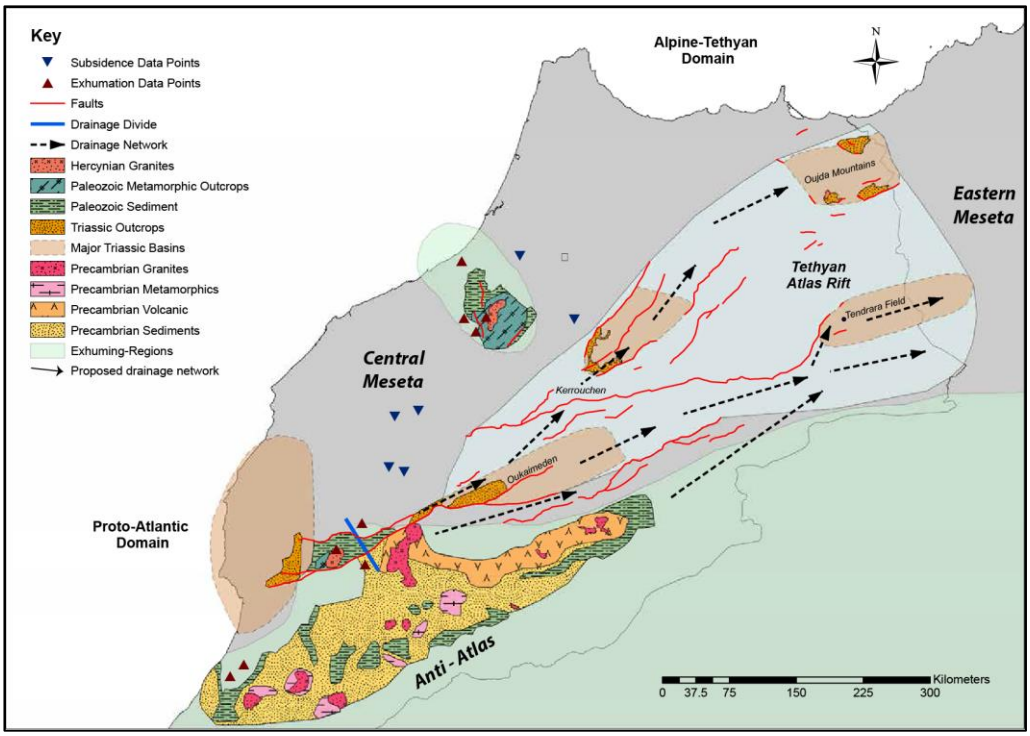

Figure 2-18: Late phase. The rift basins have grown and are in communication, with a regional drainage network dominating the source to sink systems. Sediment is fed through the Oukaimeden Basin to the Kerrouchen and High Plateaux to the north-east and into the Tethyan Ocean.

If this model is correct, the detrital ages should vary with the stratigraphic position of the sediment, reflecting the unroofing of crustal rocks. If this is the case the use of Pb-Pb dating of feldspar (Tyrrell *et al.* 2006) could be utilised to recognise distinctions between first and reworked detrital assemblages. The detrital zircon assemblage of all the basins should preserve a similar signal to that observed within the Ourika-Tizi n'Tacht basin, with a predominantly Pan-African signal with Eburnean and Paleo-Archean zircons (Domènech *et al.* 2018).

Whilst both of the proposed models are plausible, several key issues prevent a more valid hypothesis from being put forward. The first, issue is that the age of the samples is poorly constrained, limiting the ability to correlate them and increasing the risk of comparing samples of significantly different ages across basins. The second issue is that the stratigraphy of the Kerrouchen Basin may be poorly constrained, as the heavy mineral assemblage of the KH-20 sample demonstrates. If the published stratigraphy of the basin is correct, this sample records a rapid and large shift in provenance from type A provenance to type B provenance and back again. Whilst this is possible, it is more likely that the relationship between the middle-K3 member and the rest of the K3 formation needs to be redefined. Furthermore, the heavy mineral assemblages within the potential source regions are currently understudied, making identifying the ultimate source for the sediment deposited in the Triassic difficult to constrain beyond regions recognised as having been uplifted during this time period. The lack of metamorphic index minerals or similar diagnostic minerals which can only form under narrow conditions further limits the ability to constrain the source of the sediment further.

2.7. Implications for Reservoir Distribution and Quality

Provenance data can be utilised as a tool for assessing reservoir quality and distribution. The provenance of sand bodies provides a primary control on their composition and influences the likely diagenetic pathway the sand body will be subjected to, both of which provide a primary control on the reservoir quality (Vincent *et al.* 2013). Commonly, interest in provenance analysis during exploration and production has focused on identifying provenance derived compositional variation to assess diagenetic pathways (Ramm 2000). Heavy mineral analysis provides a useful insight into the extent of burial related diagenesis, as there is a well-established hierarchy of heavy mineral stability under deep burial (Morton 1984; Morton & Hallsworth 2007).

More recently, the insight of heavy mineral data into reservoir quality has been coupled with source to sink analysis and detrital geochronological work to identify the provenance of high reservoir quality quartz rich sandstones to better understand their distribution (Vincent *et al.* 2013). The use of a multitude of provenance sensitive techniques, for example petrography, heavy mineral analysis and detrital geochronology, can then identify both vertical and horizontal variations in reservoir quality (Vincent *et al.* 2013; Kilhams *et al.* 2014).

Within fluvial successions of monotonous sandstones with low fossil preservation such as the Triassic fields of the North Sea, heavy mineral analysis, alongside varietal heavy mineral analysis, has been utilised as tool for correlation between sand bodies (Maria A. Mange-Rajetzky 1995; Mouritzen *et al.* 2017). This is a highly useful tool for Triassic reservoir intervals globally, as they are commonly sparsely fossiliferous, making correlation of subsurface sand bodies difficult, hindering reservoir modelling and well planning. The use of source to sink analysis also allows for the prediction of facies distributions regionally and within a basin, which can help create GDE maps for use within exploration.

Within the analysed samples from the TE-6 and TE-8 wells of the Tendrara Field, the heavy mineral assemblage does not support the hypothesised correlation between the channel complexes of the TE-6 and TE-8 wells *(Figure 2-19).* The assemblage preserved in channel complex 1 is a predominantly ultrastable, type ‘A’ provenance, whereas in the correlated over-bank deposit has a type ‘B’ provenance *(Figure 2-19)* (Benvenuti 2017). To provide further evidence, more samples must be analysed from channel complexes 1, 2 and 3 to see if their assemblages correlate with crevasse complexes 1, 2 and 3. This highlights the use of heavy minerals as a way of testing well to well correlation. The variation observed within the heavy mineral signal in crevasse complexes 2 and 3 is similar to that observed in the petrographic data, with the upper portions of the TE-8 showing a compositional difference to the lower portion of the TE-8 and other wells. Whilst this study has only involved heavy mineral data from the TE-6 and TE-8 wells, it highlights the usefulness of

heavy mineral analysis as a basis for testing well to well correlation which could potentially be used across the Tendrara field.

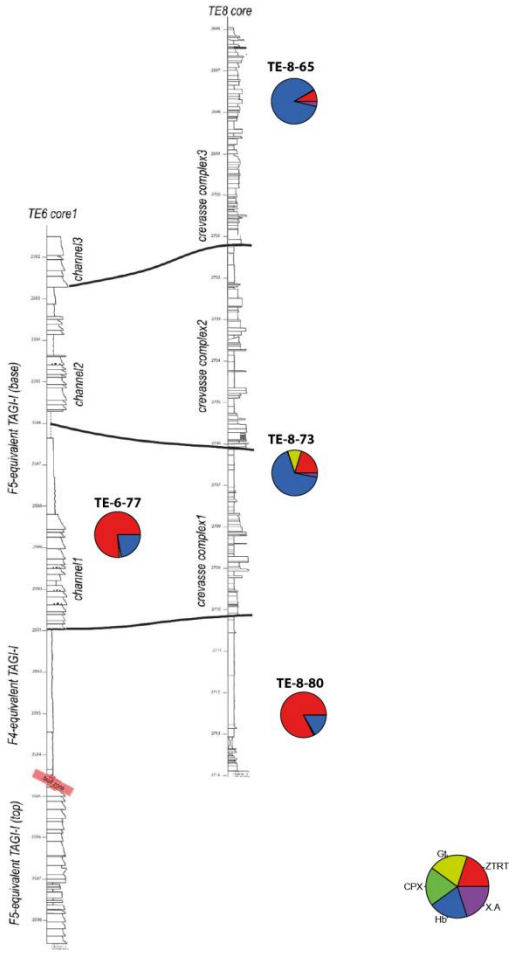

Figure 2-19: HMI pie charts and proposed correlation(Benvenuti 2017). The HMI results indicate that the correlation between channel complexes may not be correct, as channel complex 1 and crevasse complex 1 appear to have different provenances.

The composition of the heavy minerals preserved within the Tendrara field also provides insight into the reservoir quality of the sand bodies. Hornblende, and other amphiboles, make up a significant proportion of the detrital heavy mineral assemblage within the TE-8 well, despite being some of the least stable heavy minerals under burial diagenesis (Morton & Hallsworth 2007). The preservation of hornblende indicates that the Tendrara field has undergone a low extent of burial diagenesis and may have high reservoir quality as a result. However, as seen within the petrographic analysis, pedogenic carbonate cements are common, which could reduce reservoir quality without affecting the detrital assemblage.

As established in chapter 1, the Kerrouchen Basin could be an analogue for the Tendrara Field. Within the Kerrouchen Basin, the heavy mineral signal highlighted potential errors within the stratigraphic model of the Kerrouchen Basin, indicating again the usefulness of provenance data in correlating stratigraphic units. The highest net: gross sand body within

the Kerrouchen Basin is represented by the KH-20 sample of the middle-K3 *(Figure 1-10).* The KH-20 sample is more quartz rich *(Figure 2.8)* and preserves a unique, hornblende rich heavy mineral assemblage than the underlying and overlying samples *(Figure 2-12)*. This could be a result of a poorly constrained or understood stratigraphy or due to the KH-20 sample representing a unique signal related to an axial fluvial system. If the KH-20 sample does preserve a unique provenance signal which is present in the quartz-rich reservoir quality sands of the Moroccan Triassic, identifying this signal in the Tendrara Field will allow for the identification of the highest quality reservoirs. As the facies present in the TE-8 well are interpreted to be an over-bank deposit (Benvenuti 2017), similar to the KH-60 samples relation to the KH-20 sample *(Figure 2-15)*, this suggests that the TE-8 well is laterally equivalent to a high net to gross reservoir interval. As shown in Figure 2-19 however, the TE-6 well is unlikely to be the laterally equivalent high N: G reservoir.

Whilst the heavy mineral analysis only focused on the TE-6 and TE-8 wells, the petrographic analysis can help with assessing the likely distribution of the TAGI reservoir in all wells within Tendrara. The facies within the TE-8 well have been interpreted to be crevasse splay deposits, likely laterally equivalent to an axial fluvial system (Benvenuti 2017), which is supported by the petrographic and heavy mineral results presented here, as the petrographic and heavy mineral data show similarities to the sand rich fluvial intervals of the K3 and K4 formations. The TE-8 well appears to record the regional unroofing trend, with a marked increase in mafic components in younger samples *(Figure 2-19).* In contrast, the petrographic analysis of the TE-1 to TE-6 wells appears to record a unique provenance which is not seen in the Kerrouchen or Oukaimeden Basins. They may therefore reflect a local, transverse fluvial system as opposed to a regional, axial drainage system. If this is correct, they would form highly heterogeneous, low N: G reservoirs with high potential for pedogenic carbonates due to the ephemeral nature of such systems, as seen within the K4 formation.

The work undertaken here has highlighted the potential usefulness of provenance analysis for assessing the reservoir quality of syn-rift fluvial sandstones. There are several areas of future work that need to be undertaken to optimize the use of heavy minerals in assessing provenance and the reservoir quality within the Tendrara Field.

Firstly, the heavy minerals have been shown to be a basis of correlation for the TE-6 and TE-8 wells *(Figure 2-19)* and could be expanded to include the TE-1 to the TE-9 wells. There also needs to be analysis of more samples from within the TE-6 and TE-8 wells to allow for a more refined heavy mineral stratigraphy. Recent advances in methodologies allow for the rapid analysis of varietal heavy minerals alongside detrital geochronological data (Andò *et al.* 2009; Vermeesch *et al.* 2017). When used in combination, it will be possible via just two analysis to gather traditional heavy mineral data, varietal heavy mineral

data and geochronological data from a single sample. The use of these three complementary methods would represent an advance in utilising heavy mineral data to provide the basis of correlations within homogenous successions of sparsely fossiliferous sandstones (Maria A. Mange-Rajetzky 1995).

The resampling of the Tendrara field would be undertaken alongside remapping and resampling of the Kerrouchen Basin. The remapping of this basin will allow for greater insight into its suitability as an analogue of the Tendrara Field and allow for the heavy mineral analysis to be better constrained within the Tendrara Field. By having a better understanding of the depositional systems and the heavy mineral variation within the Kerrouchen Basin, it may be possible to use heavy minerals to predict the extent of depositional systems within Tendrara (Kilhams *et al.* 2014).

A third area of future work will be to utilise outcrop and depositional modelling within the Kerrouchen Basin similar to that undertaken within the Oukaimeden Basin (Fabuel-Perez 2008; Fabuel-Perez *et al.* 2010). The heavy mineral analysis will provide a basis for correlation between genetically linked facies, as well as indicating the lateral and stratigraphic variations within the reservoir quality which will be able to be incorporated into the digital outcrop model. These models can then be combined with the subsurface heavy mineral data and core analysis of the Tendrara Field to provide a reservoir model for the TAGI within Tendrara.

2.7. Conclusions

Based on the work presented here several conclusions can be drawn, however there are severe limitations to their strength due to the constraints of this study. Only 5 days of fieldwork was conducted, reducing the confidence in the conclusions drawn. The petrographic and heavy mineral datasets, whilst presenting new data, are limited by sample density, especially the heavy mineral dataset from the Tendrara Field. However, with these limitations accounted for, the following conclusions are proposed:

1. A new lithofacies scheme is proposed for the Kerrouchen Basin based upon the recognition of variations in both sedimentology and fluvial architecture. Four key lithofacies associations are described, forming formations and members within the Kerrouchen Basin. These lithofacies appear to be spatially limited within the basin, with sand-rich facies distributed near the basin axis, with conglomerates and mudstones more prevalent near the basin margin.

2. Core analysis of the TE-6 and TE-8 wells from the Tendrara Field highlights the similarity between the TAGI interval in the Tendrara Field and the key lithofacies observed within the Kerrouchen Basin. Whilst this comparison is based on logging of only two core sections, it suggests that higher quality reservoir intervals will be orientated roughly parallel to the major basin faults, a conclusion in agreement with work done within the Oukaimeden Basin (Baudon *et al.* 2009).

3. The petrographic and heavy mineral datasets provides the first quantative data on the composition of the Triassic of the Kerrouchen Basin . The heavy mineral data presented here provides the first heavy mineral dataset from the Triassic of the Oukaimeden, Kerrouchen and Tendrara Basins. Using both heavy mineral ratios and indices together with more advanced statistical techniques has led to the identification of two potential provenance populations within the dataset, one from a reworked sedimentary or felsic igneous source and one from an intermediate or mafic igneous or meta-igneous source. This result correlate with changes identified within the petrographic datasets collected from the CHA and MHA rift basins, suggesting a regional change in drainage networks is recorded within the analysed samples.

4. The provenance groupings observed within the heavy mineral and petrographic datasets are common to multiple basins, observed within the Oukaimeden and Kerrouchen Basin. The Kerrouchen Basin and TE-8 well also share some petrographic similarities.

5. The petrographic and heavy mineral data in the three basins can be correlated with published uplift models (e.g. Charton *et al.* 2018) that indicate the main source of sediments was the Anti-Atlas and Massif Ancien. During the Triassic, the heavy mineral data suggest a connection between the Central High Atlas Rift to the Middle High Atlas Rift and the Eastern Meseta. The Oukaimeden Basin is located to the east of a drainage divide, and served as the first of a series of intra-montane rift basins through which a regional drainage network fed sediment from a southerly source in the Anti-Atlas or beyond, to the northeast through the Kerrouchen Basin and Tendrara Field into the proto-Tethyan Ocean.

6. Within the Tendrara field, the samples taken for heavy mineral analysis from the TAGI interval highlights the potential of using heavy minerals to correlate sparsely fossiliferous continental successions. The proposed correlation of the TAGI interval between the TE-6 and TE-8 well is not supported by the heavy mineral data. Genetically linked sand bodies should share a provenance and have similar heavy

mineral assemblages. The new data suggest quite different populations, indicating they sands were not be part of the same drainage network.

7. This study has also important implications for exploration of the TAGI play in the Tendrara block, as well as wider implications for the distribution of the TAGI reservoir across Morocco. In the Kerrouchen and Oukaimeden Basins, the high N:G fluvial sands, such as the Oukaimeden F5 formation, are found in an axial position within the basin, orientated sub-parallel to the major structural trend of the basin, implying that better quality reservoir could be found within the TAGI interval in a basinward position from the TE-8 well.

2.8. Future Work

The results discussed in this thesis are based in limited reconnaissance fieldwork and sample analysis. The speculative nature of some of the conclusions discussed above highlight the need for extensive further work on to better understand the syn-rift depositional processes and source to sink systems which operated during the Triassic break up of Pangea leading to the deposition of the economically significant TAGI reservoir.

1. The Triassic stratigraphy of the Kerrouchen Basin is poorly constrained, and the distribution and extent of the lithofacies and formations identified in the reconnaissance fieldwork still needs to be further verified. Further fieldwork is required in order to map out the syn-rift sequence exposed within the basin in order to improve the stratigraphic framework and the paleogeographic models for the Middle Atlas Rift during the Triassic. This field study should be undertaken alongside facies analysis of subsurface well data, logging and sampling cores drilled from the Tendrara Field, as this will help constrain paleogeographic reconstructions and models of the Tendrara Field.

2. This field study should be undertaken alongside facies analysis of subsurface well data, logging and sampling cores drilled from the Tendrara Field, as this will help constrain paleogeographic reconstructions and models of the Tendrara Field. The study of the wells across the region may allow for improved identification of the early, middle and late syn-rift sequences within the Tendrara field, and an integrated chrono-stratigraphic study could improve the biostratigraphic or chemo-stratigraphic framework in order to correlate horizons and sequences between basins.

3. The logging of further core data from Tendrara and mapping of the Kerrouchen Basin should be done concurrently with a resampling of sand rich horizons in order for further heavy mineral and detrital geochronology analysis to be completed. The heavy minerals should be analysed using a micro-Raman spectrometer, in order to identify varietal data which can be used to build well to well correlations (Maria A. Mange-Rajetzky 1995; Andò *et al.* 2014), as well as utilising the provenance sensitive heavy mineral ratios to constrain the likely source regions (Garzanti & Andò 2007b). Within this provenance study, it will be important to calculate the source rock density as a further way of constraining the likely source rocks (Garzanti & Andò 2007a). Once this has been calculated, the lithologies available for erosion in the likely source terranes can be sampled in order to develop a database with their heavy mineral and the geochronological age.

4. Once this has been undertaken, the detrital samples collected from the Triassic rift basins should be analysed for detrital geochronological ages, targeting zircons and feldspars for dating. The dating of the zircons will allow us to identify the original source for the sediment, whereas dating feldspar will allow for the identification of the first cycle sediment (Tyrrell *et al.* 2006). The identification of the reworked component alongside the first cycle sediment will allow for the recognition of the most recent source to sink system which transported the sediment.

5. Once all samples have been analysed for petrographic, heavy mineral, detrital zircon and k-feldspar ages, variations in provenance will be identified. By combining the provenance study with the stratigraphic study, variations in provenance can be related to the depositional system and spatial or temporal variations. This will allow for a high quality paleogeographic reconstruction, identifying both local and regional drainage networks and the interaction between them.

6. The results of this study will also have important implications for chasing the TAGI play across Morocco and Western Algeria. Firstly, the regional paleogeographic study will allow for the identification of regional sand distribution, highlighting areas for exploration to target. The regional provenance signal can then be utilised within the sub-surface rift basins, in order to identify whether the depositional systems are locally or regionally sourced.

7. The work undertaken in the Kerrouchen and Tendrara Fields will help identify specific characteristics of the local and regional systems in order to help model variations in reservoir architecture and quality. If aeolian deposits similar to the upper-F5 formation or those found in the Argana Valley (Fabuel-Perez *et al.* 2009; Mader & Redfern 2011) are identified and a provenance profile recognised, the provenance profile from well data could also allow for the recognition of fluvial vs aeolian systems. The provenance profiles from the Tendrara Field could also be combined with petrophysical data, in order to assess whether there is a systematic change in reservoir properties that correlates with provenance variations.

In summary, there is still a large contribution to be made to the understanding of the TAGI play in Morocco from both field and provenance analysis. Fieldwork in the Middle High Atlas will allow for a greater understanding on the nature of the source to sink systems responsible for the deposition of the TAGI reservoir's, with provenance analysis providing a tool for understanding their distribution on a regional scale and correlating the TAGI intervals within a basin.

2.9. Acknowledgements

I would like to thank the all the sponsors of the NARG, with special thanks to ONHYM for providing field guides and identifying key sections within the Kerrouchen Basin and Sound Energy for providing access to the TE-6 and TE-8 core as well as samples and thin sections. I would also like to thank Jason Canning and John Argent, Sound Energy for the helpful discussions and sharing of data. I gratefully acknowledge all the other students in the NARG for their help and support, as well as my supervisor, Professor Jonathan Redfern. I would also like to thank Professor Mostafa Oujidi from the University Mohammed Premier for his assistance in the field.

2.10. References

Amorosi, A. & Sammartino, I. 2018. Shifts in sediment provenance across a hierarchy of bounding surfaces: A sequence-stratigraphic perspective from bulk-sediment geochemistry. *Sedimentary Geology*, https://doi.org/10.1016/j.sedgeo.2017.09.017.

Andersen, T., Kristoffersen, M. & Elburg, M.A. 2016. How far can we trust provenance and crustal evolution information from detrital zircons? A South African case study. *Gondwana Research*, https://doi.org/10.1016/j.gr.2016.03.003.

Andò, S., Bersani, D., Vignola, P. & Garzanti, E. 2009. Raman spectroscopy as an effective tool for high-resolution heavy-mineral analysis: Examples from major Himalayan and Alpine fluvio-deltaic systems. *Spectrochimica Acta - Part A: Molecular and Biomolecular Spectroscopy*, **73**, 450–455, https://doi.org/10.1016/j.saa.2008.11.005.

Andò, S., Vignola, P. & Garzanti, E. 2011. Raman counting: A new method to determine provenance of silt. *Rendiconti Lincei*, **22**, 327–347, https://doi.org/10.1007/s12210-011-0142-4.

Andò, S., Garzanti, E., Padoan, M. & Limonta, M. 2012. Corrosion of heavy minerals during weathering and diagenesis: A catalog for optical analysis. *Sedimentary Geology*, **280**, 165–178, https://doi.org/10.1016/j.sedgeo.2012.03.023.

Andò, S., Morton, A. & Garzanti, E. 2014. Metamorphic grade of source rocks revealed by chemical fingerprints of detrital amphibole and garnet. *Geological Society, London, Special Publications*, **386**, https://doi.org/10.1144/SP386.5.

Arche, A. & López-Gómez, J. 2014. The Carnian Pluvial Event in Western Europe: New data from Iberia and correlation with the Western Neotethys and Eastern North America-NW Africa regions. *Earth-Science Reviews*, **128**, 196–231, https://doi.org/10.1016/j.earscirev.2013.10.012.

Baudon, C., Fabuel-Perez, I. & Redfern, J. 2009. Structural style and evolution of a Late Triassic rift basin in the Central High Atlas, Morocco: controls on sediment deposition. *Geological Journal*, https://doi.org/Doi 10.1002/Gj.1195.

Baudon, C., Redfern, J. & Van Den Driessche, J. 2012. Permo-Triassic structural evolution of the Argana Valley, impact of the Atlantic rifting in the High Atlas, Morocco. *Journal of African Earth Sciences*, **65**, 91–104, https://doi.org/10.1016/j.jafrearsci.2012.02.002.

Beauchamp, J. 1988. Triassic sedimentation and rifting in the High Atlas (Morocco). *Developments in Geotectonics*, **22**, 477–497, https://doi.org/10.1016/B978-0-444-42903-2.50025-7.

Benaouiss, N., Courel, L. & Beauchamp, J. 1996. Rift-controlled fluvial / tidal transitional series in the Oukdimeden Sandstones , High Atlas of Marrakesh (Morocco). *Sedimentary Geology*, **107**, 21–36, https://doi.org/10.1016/S0037-0738(96)00013-9.

Benvenuti, M. (Dipartimento di S. della T.U. di F. 2016. *Interim Report on the Sedimentological and Stratigraphic Analysis of the TE6 Well-Core1*.

Benvenuti, M. (Dipartimento di S. della T.U. di F. 2017. *Report on the Sedimentological and*

Stratigraphic Analysis of the TE8 Well-Core.

Brown, R. 1980. Triassic rocks of Argana Valley, southern Morocco, and their regional structural implications. *AAPG Bulletin*, **64**, 988–1003, https://doi.org/10.1306/2F919418-16CE-11D7-8645000102C1865D.

Charriere, A., Ibouh, H. & Haddoumi, H. 2011. *The Central High Atlas from Beni Mellal to Imilchil*, Volume 4. Service Geologique du Maroc.

Charton, R., Bertotti, G., Arantegui, A. & Bulot, L.G. 2018. The Sidi Ifni transect across the rifted margin of Morocco (Central Atlantic): Vertical movements constrained by low-temperature thermochronology. *Journal of African Earth Sciences*.

Courel, L., Aït Salem, H., et al. 2003. Mid-Triassic to Early Liassic clastic/evaporitic deposits over the Maghreb Platform. *Palaeogeography, Palaeoclimatology, Palaeoecology*, **196**, 157–176, https://doi.org/10.1016/S0031-0182(03)00317-1.

Dickinson, W.R. 1970. Interpreting detrital modes of greywackes and arkose. *Journal of Sedimentary Petrology*, **40**, 695–707.

Dickinson, W.R. 1985. Interpreting provenance relations from detrital modes of sandstones. *In*: *Provenance of Arenites*. 333–361.

Dickinson, W.R., Beard, L.S., et al. 1983. Provenance of North American Phanerozoic sandstones in relation to tectonic setting Provenance of North American Phanerozoic sandstones in relation to tectonic setting. *Geological Society of America Bulletin*, 222–235, https://doi.org/10.1130/0016-7606(1983)94<222.

Domènech, M., Teixell, A., Babault, J. & Arboleya, M.L. 2015. The inverted Triassic rift of the Marrakech High Atlas: A reappraisal of basin geometries and faulting histories. *Tectonophysics*, **663**, 177–191, https://doi.org/10.1016/j.tecto.2015.03.017.

Domènech, M., Teixell, A. & Stockli, D.F. 2016. Magnitude of rift-related burial and orogenic contraction in the Marrakech High Atlas revealed by zircon (U-Th)/He thermochronology and thermal modeling. *Tectonics*, **35**, 2609–2635, https://doi.org/10.1002/2016TC004283.

Domènech, M., Stockli, D.F., Teixell, A. & Geologia, D. 2018. Detrital zircon U-Pb provenance and paleogeography of Triassic rift basins in the Marrakech High Atlas. 0–2, https://doi.org/10.1111/ter.12340.

Ellouz, N., Patriat, M., Gaulier, J.M., Bouatmani, R. & Sabounji, S. 2003. From rifting to Alpine inversion: Mesooic and Cenozoic subsidence history of some Moroccan basins. *Sedimentary Geology*, **156**, 185–212, https://doi.org/10.1016/S0037-0738(02)00288-9.

Fabuel-Perez, I. 2008. *3D Reservoir Modeling of Upper Triassic Continental Mixed Systems: Integration of Digital Outcrop Models (DOMs) and High Resolution Sedimentology. The Oukaimeden Sandstone Formation, Central High Atlas, Morocco*. University of Manchester.

Fabuel-Perez, I., Hodgetts, D. & Redfern, J. 2009. A new approach for outcrop characterization and geostatistical analysis of a low-sinuosity fluvial-dominated succession using digital outcrop models: Upper triassic oukaimeden sandstone

formation, central high Atlas, Morocco. *AAPG Bulletin*, **93**, 795–827, https://doi.org/10.1306/02230908102.

Fabuel-Perez, I., Redfern, J. & Hodgetts, D. 2009. Sedimentology of an intra-montane rift-controlled fluvial dominated succession: The Upper Triassic Oukaimeden Sandstone Formation, Central High Atlas, Morocco. *Sedimentary Geology*, **218**, 103–140, https://doi.org/10.1016/j.sedgeo.2009.04.006.

Fabuel-Perez, I., Hodgetts, D. & Redfern, J. 2010. Integration of digital outcrop models (DOMs) and high resolution sedimentology–workflow and implications for geological modelling: Oukaimeden Sandstone Formation, High Atlas (Morocco). *Petroleum Geoscience*, **16**, 133–154, https://doi.org/10.1144/1354-079309-820.

Fiechtner, L., Friedrichsen, H. & Hammerschmidt, K. 1992. Geochemistry and geochronology of Early Mesozoic tholeiites from Central Morocco. *Geologische Rundschau*, **81**, 45–62, https://doi.org/10.1007/BF01764538.

Flint, S.S., Payenberg, T., Hildred, G.V., Ratcliffe, K.T., Rittersbacher, A. & Wilson, A. 2015. Ground trothing chemostratigraphic correlations in fluvial systems. *AAPG Bulletin*, https://doi.org/10.1306/06051413120.

Ford, D. & Golonka, J. 2003. *Phanerozoic Paleogeography, Paleoenvironment and Lithofacies Maps of the Circum-Atlantic Margins*, https://doi.org/10.1016/S0264-8172(03)00041-2.

Galeazzi, S., Point, O., Haddadi, N., Mather, J. & Druesne, D. 2010. Regional geology and petroleum systems of the Illizi-Berkine area of the Algerian Saharan Platform: An overview. *Marine and Petroleum Geology*, **27**, 143–178, https://doi.org/10.1016/j.marpetgeo.2008.10.002.

Galehouse, J. 1971. Point counting. *In*: *Procedures in Sedimentary Petrology*. 385–407.

Garzanti, E. 2016. From static to dynamic provenance analysis-Sedimentary petrology upgraded. *Sedimentary Geology*, **336**, 3–13, https://doi.org/10.1016/j.sedgeo.2015.07.010.

Garzanti, E. & Andò, S. 2007a. Chapter 20 Heavy Mineral Concentration in Modern Sands: Implications for Provenance Interpretation. *Developments in Sedimentology*, **58**, 517–545, https://doi.org/10.1016/S0070-4571(07)58020-9.

Garzanti, E. & Andò, S. 2007b. Chapter 29 Plate Tectonics and Heavy Mineral Suites of Modern Sands. *Developments in Sedimentology*, **58**, 741–763, https://doi.org/10.1016/S0070-4571(07)58029-5.

Garzanti, E., Andò, S. & Vezzoli, G. 2008. Settling equivalence of detrital minerals and grain-size dependence of sediment composition. *Earth and Planetary Science Letters*, **273**, 138–151, https://doi.org/10.1016/j.epsl.2008.06.020.

Garzanti, E., Andò, S. & Vezzoli, G. 2009. Grain-size dependence of sediment composition and environmental bias in provenance studies. *Earth and Planetary Science Letters*, **277**, 422–432, https://doi.org/10.1016/j.epsl.2008.11.007.

Garzanti, E., Resentini, A., Vezzoli, G., Andò, S., Malusà, M.G., Padoan, M. & Paparella, P.

2010. Detrital Fingerprints of Fossil Continental-Subduction Zones (Axial Belt Provenance, European Alps). *The Journal of Geology*, **118**, 341–362, https://doi.org/10.1086/652720.

Garzanti, E., Al-Juboury, A.I., et al. 2016. The Euphrates-Tigris-Karun river system: Provenance, recycling and dispersal of quartz-poor foreland-basin sediments in arid climate. *Earth-Science Reviews*, **162**, 107–128, https://doi.org/10.1016/j.earscirev.2016.09.009.

Garzanti, E., Dinis, P., et al. 2017. Sedimentary processes controlling ultralong cells of littoral transport: Placer formation and termination of the Orange sand highway in southern Angola. *Sedimentology*, https://doi.org/10.1111/sed.12387.

Golonka, J. & Ford, D. 2000. Pangean (Late Carboniferous-Middle Jurassic) paleoenvironment and lithofacies. *Palaeogeography, Palaeoclimatology, Palaeoecology*, **161**, 1–34, https://doi.org/10.1016/S0031-0182(00)00115-2.

Gouiza, M., Charton, R., Bertotti, G., Andriessen, P. & Storms, J.E.A. 2017. Post-Variscan evolution of the Anti-Atlas belt of Morocco constrained from low-temperature geochronology. *International Journal of Earth Sciences*, **106**, 593–616, https://doi.org/10.1007/s00531-016-1325-0.

Guiraud, R. 1998. Mesozoic rifting and basin inversion along the northern African Tethyan margin: an overview. *Geological Society, London, Special Publications*, **132**, 217–229, https://doi.org/10.1144/GSL.SP.1998.132.01.13.

Hafid, M. & Benaouiss, N. 2010. *Structural, Sedimentological and Diagenetic Analysis of the Triassic Formations of the Tendrara 3D Seismic Survey Area*.

Hoepffner, C., Soulaimani, A. & Piqué, A. 2005. The Moroccan Hercynides. *Journal of African Earth Sciences*, **43**, 144–165, https://doi.org/10.1016/j.jafrearsci.2005.09.002.

Hofmann, A., Tourani, A. & Gaupp, R. 2000. Cyclicity of Triassic to Lower Jurassic continental red beds of the Argana Valley, Morocco: Implications for palaeoclimate and basin evolution. *Palaeogeography, Palaeoclimatology, Palaeoecology*, **161**, 229–266, https://doi.org/10.1016/S0031-0182(00)00125-5.

Hubert, J.. 1971. Analysis of heavy mineral assemblages. *In*: Carver, R. E. (ed.) *Procedures in Sedimentary Petrology*. Wiley, 453–478.

Hubert, J.F. 1962. A zircon-tourmaline-rutile maturity index and the interdependence of the composition of heavy mineral assemblages with the gross composition and texture of sandstones. *Journal of Sedimentary Research*, **32**, 440–450, https://doi.org/10.1306/74D70CE5-2B21-11D7-8648000102C1865D.

Hurst, A. & Morton, A. 2014. Provenance models: the role of sandstone mineral-chemical stratigraphy. *Geological Society, London, Special Publications*, **386**, 7–26, https://doi.org/10.1144/SP386.11.

Kape, S. 2017. *Tendrara - Preliminary Report for Sound Energy*.

Kilhams, B., Morton, A., Borella, R., Wilkins, A. & Hurst, A. 2014. Understanding the provenance and reservoir quality of the Sele Formation sandstones of the UK Central

Graben utilizing detrital garnet suites. *Sediment Provenance Studies in Hydrocarbon Exploration and Production*, https://doi.org/10.1144/SP386.16.

Komar, P.D., Clemens, K.E., Li, Z. & Shih, S.-M. 1989. The Effects of Selective Sorting on Factor Analyses of Heavy-mineral Assemblages. *Journal of Sedimentary Research*, **Vol. 59**, 590–596, https://doi.org/10.1306/212F8FF8-2B24-11D7-8648000102C1865D.

Lachkar, G., Ouarhache, D. & Charriere, A. 2000. New palynological data on sedimentary formations associated with Triassic Basalts of the Middle Atlas and High Moulouya (Morocco). *Revue De Micropaleontologie*, **43**, 281–299.

Laville, E., Pique, A., Amrhar, M. & Charroud, M. 2004. A restatement of the Mesozoic Atlasic Rifting (Morocco). *Journal of African Earth Sciences*, **38**, 145–153, https://doi.org/10.1016/j.jafrearsci.2003.12.003.

Le Roy, P. & Piqué, A. 2001. Triassic-Liassic western Moroccan synrift basins in relation to the Central Atlantic opening. *Marine Geology*, **172**, 359–381, https://doi.org/10.1016/S0025-3227(00)00130-4.

Lorenz, J. 1976. Triassic sediments and basin structure of the Kerrouchen Basin, Central Morocco. **46**, 897–905.

Lorenz, J.C. 1988. Synthesis of Late Paleozoic and Triassic redbed sedimentation in Morocco. *The Atlas System of Morocco, vol. 15*, **15**, 139–168.

Mackie, W. 1923. The principles that regulate the distribution of particles of heavy minerals in sedimentary rocks, as illustrated by the sandstones of the north-east of Scotland. *Edinburgh Geological Society Transcripts*, **11**, 138–164.

Mader, N.K. 2005. Sedimentology and sediment distribution of Upper Triassic fluvio-aeolian reservoirs on a regional scale (Central Algeria , SW Morocco , NE Canada): an integrated approach unravelling the influence of climate versus tectonics on reservoir architecture Vo. **I**.

Mader, N.K. & Redfern, J. 2011. A sedimentological model for the continental upper triassic tadrart ouadou sandstone member: Recording an interplay of climate and tectonics (Argana valley; south-west Morocco). *Sedimentology*, **58**, 1247–1282, https://doi.org/10.1111/j.1365-3091.2010.01204.x.

Mader, N.K., Redfern, J. & El Ouataoui, M. 2017. Sedimentology of the Essaouira Basin (Meskala Field) in context of regional sediment distribution patterns during upper Triassic pluvial events. *Journal of African Earth Sciences*, **130**, 293–318, https://doi.org/10.1016/j.jafrearsci.2017.02.012.

Malusà, M.G., Resentini, A. & Garzanti, E. 2016. Hydraulic sorting and mineral fertility bias in detrital geochronology. *Gondwana Research*, **31**, https://doi.org/10.1016/j.gr.2015.09.002.

Mange-Rajetzky, M.A. 1995. Subdivision and correlation of monotonous sandstone sequences using high-resolution heavy mineral analysis, a case study: the Triassic of the Central Graben. *Geological Society, London, Special Publications*, **89**, 23–30, https://doi.org/10.1144/GSL.SP.1995.089.01.03.

Mange-Rajetzky, M.A. 1995. Subdivision and correlation of monotonous sandstone sequences using high resolution heavymineral analysis, a case study: the Triassic of the Central Graben. *Non-biostratigraphical Methods of Dating and Correlation*, **89**, 23–30, https://doi.org/10.1144/GSL.SP.1995.089.01.03.

Mange, M.A. & Morton, A.C. 2007. Chapter 13 Geochemistry of Heavy Minerals. *Developments in Sedimentology*, **58**, 345–391, https://doi.org/10.1016/S0070-4571(07)58013-1.

Mckie, T. 2014. Climatic and tectonic controls on Triassic dryland terminal fluvial system architecture, central North Sea. *From Depositional Systems to Sedimentary Successions on the Norwegian Continental Margin*, 19–57, https://doi.org/10.1002/9781118920435.ch2.

Michard, A., Hoepffner, C., Soulaimani, A. & Baidder, L. 2008. The variscan belt. *Lecture Notes in Earth Sciences*, **116**, 65–132, https://doi.org/10.1007/978-3-540-77076-3_3.

Morton, A., O'B. Knox, R.W. & Hallsworth, C. 2002. Correlation of reservoir sandstones using quantitative heavy mineral analysis. *Petroleum Geoscience*, **8**, 251–262, https://doi.org/10.1144/petgeo.8.3.251.

Morton, A., Hallsworth, C. & Chalton, B. 2004. Garnet compositions in Scottish and Norwegian basement terrains: A framework for interpretation of North Sea sandstone provenance. *Marine and Petroleum Geology*, **21**, 393–410, https://doi.org/10.1016/j.marpetgeo.2004.01.001.

Morton, A.C. 1984. Stability of detrital heavy tertiary sandstones from sea basin minerals in the north. *Clay Minerals*, **19**, 287–308, https://doi.org/10.1180/claymin.1984.019.3.04.

Morton, A.C. & Hallsworth, C. 1994. Identifying provenance-specific features of detrital heavy mineral assemblages in sandstones. *Sedimentary Geology*, **90**, 241–256, https://doi.org/10.1016/0037-0738(94)90041-8.

Morton, A.C. & Hallsworth, C. 2007. Chapter 7 Stability of Detrital Heavy Minerals During Burial Diagenesis. *Developments in Sedimentology*, **58**, 215–245, https://doi.org/10.1016/S0070-4571(07)58007-6.

Morton, A.C. & Hallsworth, C.R. 1999. Processes controlling the composition of heavy mineral assemblages in sandstones. *Sedimentary Geology*, **124**, 3–29, https://doi.org/10.1016/S0037-0738(98)00118-3.

Mouritzen, C., Farris, M.A., Morton, A. & Mathews, S. 2017. Integrated Triassic stratigraphy of the greater Culzean area, UK Central North Sea. *Petroleum Geoscience*, **24**, 197–207, https://doi.org/10.1144/petgeo2017-039.

Ouarhache, D., Charriere, A., Chalot-Prat, F. & El-Wartiti, M. 2000. Sédimentation détritique continentale synchrone d'un volcanisme explosif dans le Trias terminal à infra-Lias du domaine atlasique (Haute Moulouya, Maroc) (Late Triassic to infra-Liassic continental detrital sedimentation synchronous with an explosive volc. *Journal of African Earth Sciences*, **31**, 555–570, https://doi.org/http://dx.doi.org/10.1016/S0899-5362(00)80007-X.

Ouarhache, D., Charriere, A., Chalot-Prat, F. & El Wartiti, M. 2012. Chronologie et modalités du rifting triasico-liasique à la marge sud-ouest de la Téthys alpine (Moyen Atlas et Haute Moulouya, Maroc); corrélations avec le rifting atlantique: Simultané ité et diachronisme. *Bulletin de la Societe Geologique de France*, https://doi.org/10.2113/gssgfbull.183.3.233.

Ouijidi, M. 2000. Triassic marine onlap in the south-western peritethyan domain, example of Oujda Mountains (Eastern Morocco).pdf. 1243–1268.

Ouijidi, M., Courel, L., Benaouiss, N., El Mostaine, M., Ouarhache, D., Sabaoui, A. & Tourani, A.-I. 2000. Moroccan Paleogeographic maps during Early Mesozoic times. *In*: *Le Permian et Le Trias Du Maroc*. Oujda, 15–24.

Oujidi, M., Courel, L., et al. 2000. Triassic series of Morocco: stratigraphy, palaeogeography and structuring of the Southwestern Peri-Tethyan platform. An overview. *Peri-Tethys Memoir 5: new data on Peri-Tethyan sedimentary basins*.

Parrish, J.T. 2016. Climate of the Supercontinent Pangea Author (s): Judith Totman Parrish Source : The Journal of Geology , Vol . 101 , No . 2 , 100th Anniversary Symposium : Evolution of the Earth ' s Surface (Mar ., 1993), pp . 215-233 Published by : The University of. **101**, 215–233.

Pettijohn, F.J. 1941. Persistence of Heavy Minerals and Geologic Age. *The Journal of Geology*, https://doi.org/10.2307/30079640.

Pique, A., Le Roy, P. & Amrhar, M. 1998. Transtensive synsedimentary tectonics associated with ocean opening: the Essaouira-Agadir segment of the Moroccan Atlantic margin. *Journal of the Geological Society*, **155**, 913–928, https://doi.org/10.1144/gsjgs.155.6.0913.

Ramm, M. 2000. Reservoir quality and its relationship to facies and provenance in Middle to Upper Jurassic sequences, northeastern North Sea. *Clay Minerals*, https://doi.org/10.1180/000985500546747.

Rossi, C., Kälin, O., Arribas, J. & Tortosa, A. 2002. Diagenesis, provenance and reservoir quality of Triassic TAGI sandstones from Ourhoud field, Berkine (Ghadames) Basin, Algeria. *Marine and Petroleum Geology*, **19**, 117–142, https://doi.org/10.1016/S0264-8172(02)00004-1.

Rubey, W. 1933. The size distribution of heavy minerals within a water-laid sandstone. **3**, 3–29.

Soulaimani, A., Michard, A., Ouanaimi, H., Baidder, L., Raddi, Y., Saddiqi, O. & Rjimati, E.C. 2014. Late Ediacaran-Cambrian structures and their reactivation during the Variscan and Alpine cycles in the Anti-Atlas (Morocco). *Journal of African Earth Sciences*, **98**, https://doi.org/10.1016/j.jafrearsci.2014.04.025.

Tyrrell, S., Haughton, P.D.W., Daly, J.S., Kokfelt, T.F. & Gagnevin, D. 2006. The Use of the Common Pb Isotope Composition of Detrital K-Feldspar Grains as a Provenance Tool and Its Application to Upper Carboniferous Paleodrainage, Northern England. *Journal of Sedimentary Research*, **76**, 324–345, https://doi.org/10.2110/jsr.2006.023.

Tyrrell, S., Haughton, P.D.W. & Daly, J.S. 2007. Drainage reorganization during breakup of Pangea revealed by in-situ Pb isotopic analysis of detrital K-feldspar. *Geology*, **35**, 971–974, https://doi.org/10.1130/G4123A.1.

Tyrrell, S., Haughton, P.D.W., Souders, A.K., Daly, J.S. & Shannon, P.M. 2012. Large-scale, linked drainage systems in the NW European Triassic: insights from the Pb isotopic composition of detrital K-feldspar. *Journal of the Geological Society*, **169**, 279–295, https://doi.org/10.1144/0016-76492011-104.

Vermeesch, P. & Garzanti, E. 2015. Making geological sense of 'Big Data' in sedimentary provenance analysis. *Chemical Geology*, **409**, 20–27, https://doi.org/10.1016/j.chemgeo.2015.05.004.

Vermeesch, P., Resentini, A. & Garzanti, E. 2016. An R package for statistical provenance analysis. *Sedimentary Geology*, **336**, 14–25, https://doi.org/10.1016/j.sedgeo.2016.01.009.

Vermeesch, P., Rittner, M., Petrou, E., Omma, J., Mattinson, C. & Garzanti, E. 2017. High Throughput Petrochronology and Sedimentary Provenance Analysis by Automated Phase Mapping and LAICPMS. *Geochemistry, Geophysics, Geosystems*, **18**, 4096–4109, https://doi.org/10.1002/2017GC007109.

Vincent, S.J., Morton, A.C., Hyden, F. & Fanning, M. 2013. Insights from petrography, mineralogy and U-Pb zircon geochronology into the provenance and reservoir potential of Cenozoic siliciclastic depositional systems supplying the northern margin of the Eastern Black Sea. *Marine and Petroleum Geology*, https://doi.org/10.1016/j.marpetgeo.2013.04.002.

Wedepohl, K.H. 1995. INGERSON LECTURE The composition of the continental crust. *Geochimica et Cosmochimica Acta*, https://doi.org/10.1016/0016-7037(95)00038-2.

Weissmann, G.S., Hartley, a. J., Nichols, G.J., Scuderi, L. a., Olson, M., Buehler, H. & Banteah, R. 2010. Fluvial form in modern continental sedimentary basins: Distributive fluvial systems. *Geology*, **38**, 39–42, https://doi.org/10.1130/G30242.1.

Zimmermann, U., Andersen, T., Madland, M.V. & Larsen, I.S. 2015. The role of U-Pb ages of detrital zircons in sedimentology-An alarming case study for the impact of sampling for provenance interpretation. *Sedimentary Geology*, https://doi.org/10.1016/j.sedgeo.2015.02.006.

Appendix A: – Summary of Fieldwork Undertaken

As part of this study, fieldwork was undertaken from the 20th – 25th November 2017, 3 days of fieldwork were undertaken in the Kerrouchen Basin to log key sections and collect samples for petrographic and heavy mineral analysis. This was followed up by 2 days of reconnaissance fieldwork within the Oujda Mountains with Professor Mostafa Oujidi to help with understanding the paleogeography of Morocco during the Triassic.

Appendix B: – Petrographic Database

Sample	Basin	Quartz %	Feldspar %	Lithic %
KH-10	Kerrouchen	31.84	7.46	60.7
KH-11	Kerrouchen	23.2	14.95	61.86
KH-20	Kerrouchen	67	14.56	18.44
KH-21	Kerrouchen	38.17	3.76	58.07
KH-30	Kerrouchen	33.64	6.45	59.91
KH-31	Kerrouchen	24.87	0.5	74.61
KH-32	Kerrouchen	34.5	5.5	60
KH-40	Kerrouchen	26.04	10.65	63.31
KH-50	Kerrouchen	21.67	7.88	70.45
KH-60	Kerrouchen	33.33	4.02	62.65
KH-62	Kerrouchen	36.49	3.32	60.19
KH-63	Kerrouchen	45.33	5.14	49.53
KH-64	Kerrouchen	13.1	13.1	73.8
TE-1-1	Tendrara	10.18	40.74	49.07
TE-1-2	Tendrara	10.09	47.25	42.66
TE-1-3	Tendrara	8.96	66.42	24.63
TE-2-5	Tendrara	16.2	59.15	24.64
TE-2-7	Tendrara	23.16	45.79	31.05
TE-4-9	Tendrara	17.58	35.76	46.66
TE-4-11	Tendrara	1.68	39.5	58.82
TE-4-15	Tendrara	9	47.5	43.5
TE-5-17	Tendrara	3.76	60.56	35.68
TE-5-18	Tendrara	29.2	49.1	21.6
TE-5-23	Tendrara	11.06	59.57	29.36
TE-6-2	Tendrara	10.05	57.29	32.66
TE-6-12H	Tendrara	21.43	58.04	20.5
TE-8 #1H	Tendrara	21.05	28.95	50
TE-8 #7H	Tendrara	21.5	17.74	60.75
TE-8 #13H	Tendrara	34.82	14.29	50.89
TE-8 #19H	Tendrara	20.91	12.73	66.36
TE-8 #31H	Tendrara	26.6	9.57	63.83
TE-8 #43H	Tendrara	16	19	65
TE-8 #49H	Tendrara	13.89	18.33	67.78
TE-8 #54H	Tendrara	9.23	11.28	79.48
TE-8 #63H	Tendrara	14.47	21.38	64.15

The thin sections from the Tendrara Field were kindly provided by Sound Energy.

Appendix C: – Heavy Mineral Database

Sample	Basin	Actinolite	Al-Phosphate	Almandine	Apatite	Augite	Barite	Diopside	Glauconite	Hornblende	Ilmenite	Kutnohorite	Paragonite	Pargasite	Rutile	Zircon	Trace
KH-10	Kerrouchen	*2.5*	*1.7*	*3.1*	*2.3*	*2.0*	*0.5*	*0.0*	*0.4*	*14.1*	*12.1*	*0.0*	*0.0*	*0.0*	*50.7*	*10.0*	*0.6*
KH-11	Kerrouchen	*0.1*	*1.8*	*2.4*	*2.9*	*0.1*	*0.1*	*0.0*	*0.5*	*15.9*	*15.6*	*0.0*	*0.1*	*0.0*	*49.9*	*10.2*	*0.4*
KH-20	Kerrouchen	*2.4*	*0.0*	*0.0*	*31.7*	*4.0*	*0.5*	*0.8*	*2.5*	*51.8*	*0.0*	*4.1*	*0.0*	*0.2*	*1.7*	*0.1*	*0.1*
KH-30	Kerrouchen	*2.8*	*0.0*	*0.7*	*16.5*	*3.3*	*1.2*	*0.2*	*0.9*	*4.7*	*36.5*	*0.0*	*0.2*	*0.0*	*28.0*	*4.7*	*0.3*
KH-31	Kerrouchen	*0.1*	*0.7*	*1.0*	*0.8*	*0.0*	*8.1*	*0.0*	*5.3*	*17.6*	*12.5*	*0.0*	*1.1*	*0.0*	*49.0*	*3.5*	*0.1*
KH-60	Kerrouchen	*0.5*	*0.6*	*1.0*	*14.0*	*0.8*	*0.2*	*0.2*	*2.9*	*26.1*	*25.3*	*0.4*	*0.6*	*0.0*	*21.9*	*4.9*	*0.6*
KH-62	Kerrouchen	*0.3*	*0.1*	*0.2*	*8.2*	*0.4*	*0.0*	*0.1*	*0.6*	*3.8*	*30.9*	*0.3*	*0.3*	*0.0*	*46.0*	*8.7*	*0.1*
KH-64	Kerrouchen	*0.3*	*0.1*	*0.2*	*8.2*	*0.4*	*0.0*	*0.1*	*0.6*	*3.8*	*38.9*	*0.3*	*0.3*	*0.0*	*38.0*	*8.8*	*0.1*
ON-2	Oukaimeden	*0.0*	*0.0*	*0.5*	*14.5*	*0.0*	*0.0*	*0.0*	*0.7*	*4.4*	*22.0*	*0.0*	*0.1*	*0.0*	*37.7*	*19.6*	*0.3*
ON-13	Oukaimeden	*0.0*	*0.0*	*0.6*	*14.4*	*0.0*	*0.0*	*0.0*	*0.7*	*4.5*	*22.1*	*0.0*	*0.1*	*0.0*	*37.5*	*19.7*	*0.4*
ON-45	Oukaimeden	*0.0*	*0.1*	*3.0*	*15.7*	*0.0*	*0.0*	*0.0*	*0.7*	*4.4*	*24.5*	*0.0*	*0.2*	*0.0*	*41.8*	*9.5*	*0.2*
MSC	Oukaimeden	*2.7*	*0.0*	*0.7*	*16.2*	*3.2*	*1.2*	*0.2*	*0.9*	*4.6*	*38.0*	*0.0*	*0.2*	*0.0*	*27.4*	*4.5*	*0.2*
TE-6-77	Tendrara	*0.1*	*0.7*	*1.1*	*0.7*	*0.0*	*8.1*	*0.0*	*5.3*	*17.7*	*12.7*	*0.0*	*1.2*	*0.0*	*48.6*	*3.6*	*0.1*
TE-8-65	Tendrara	*1.7*	*0.2*	*0.3*	*2.0*	*0.1*	*0.2*	*0.0*	*1.1*	*85.2*	*1.0*	*0.3*	*0.4*	*1.7*	*5.5*	*0.1*	*0.2*
TE-8-73	Tendrara	*0.8*	*0.2*	*9.1*	*7.4*	*0.2*	*1.2*	*0.0*	*1.6*	*62.0*	*4.2*	*0.4*	*0.2*	*1.6*	*8.8*	*1.3*	*0.7*
TE-8-80	Tendrara	*0.0*	*0.2*	*0.6*	*16.0*	*0.0*	*0.6*	*0.0*	*3.2*	*11.9*	*23.8*	*0.1*	*0.7*	*0.0*	*37.7*	*5.0*	*0.2*

The samples TE-8-80, TE-8-73, TE-8-65 and TE-6-77 were provided by Sound Energy from cores drilled within the Tendrara Field. Sample ON-2, ON-13, ON-45 were collected by Ivan Fabuel-Perez as part of his PhD from the Oukaimeden Basin.

Processed heavy mineral images, with non-provenance sensitive heavy minerals removed from the images.

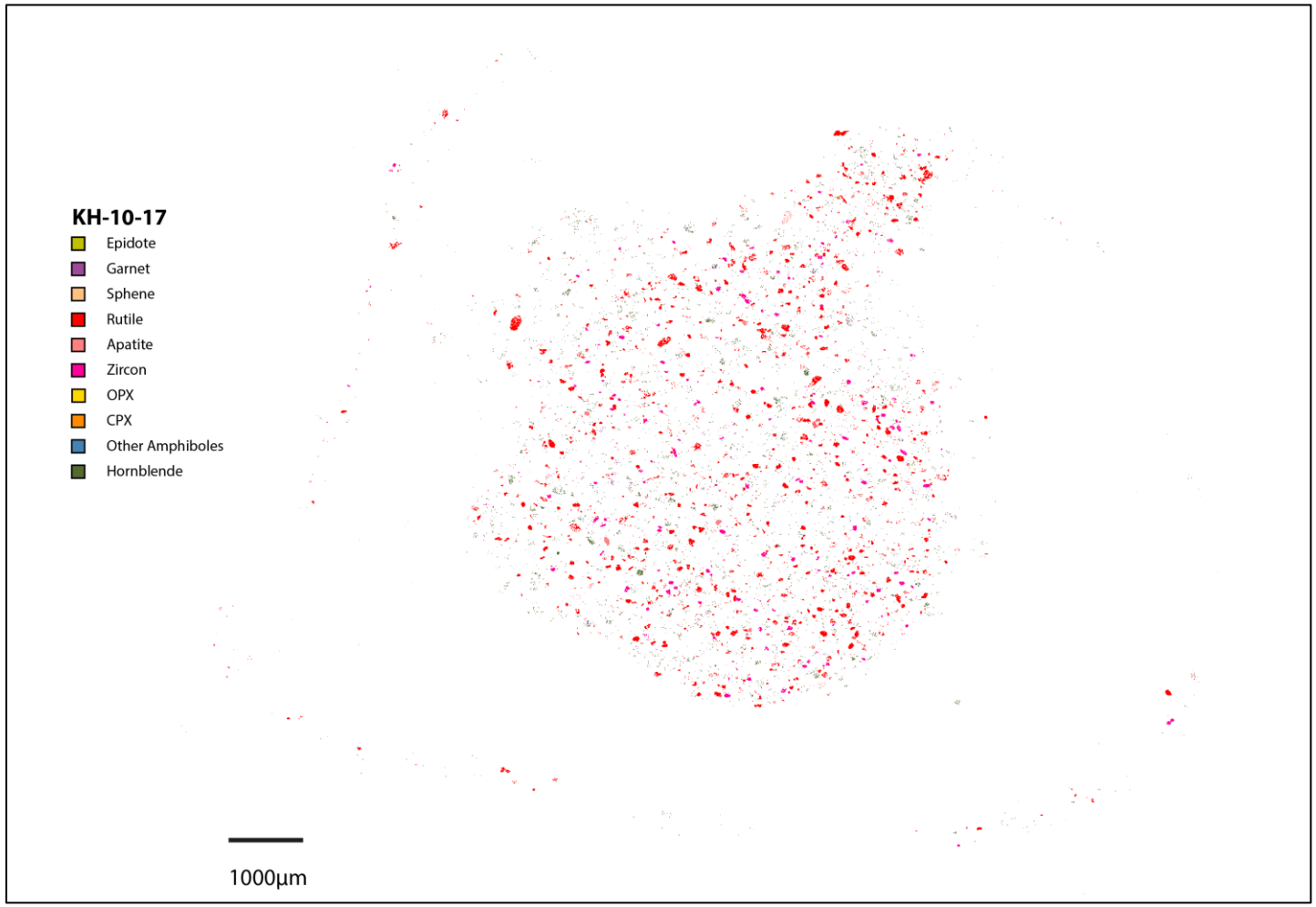

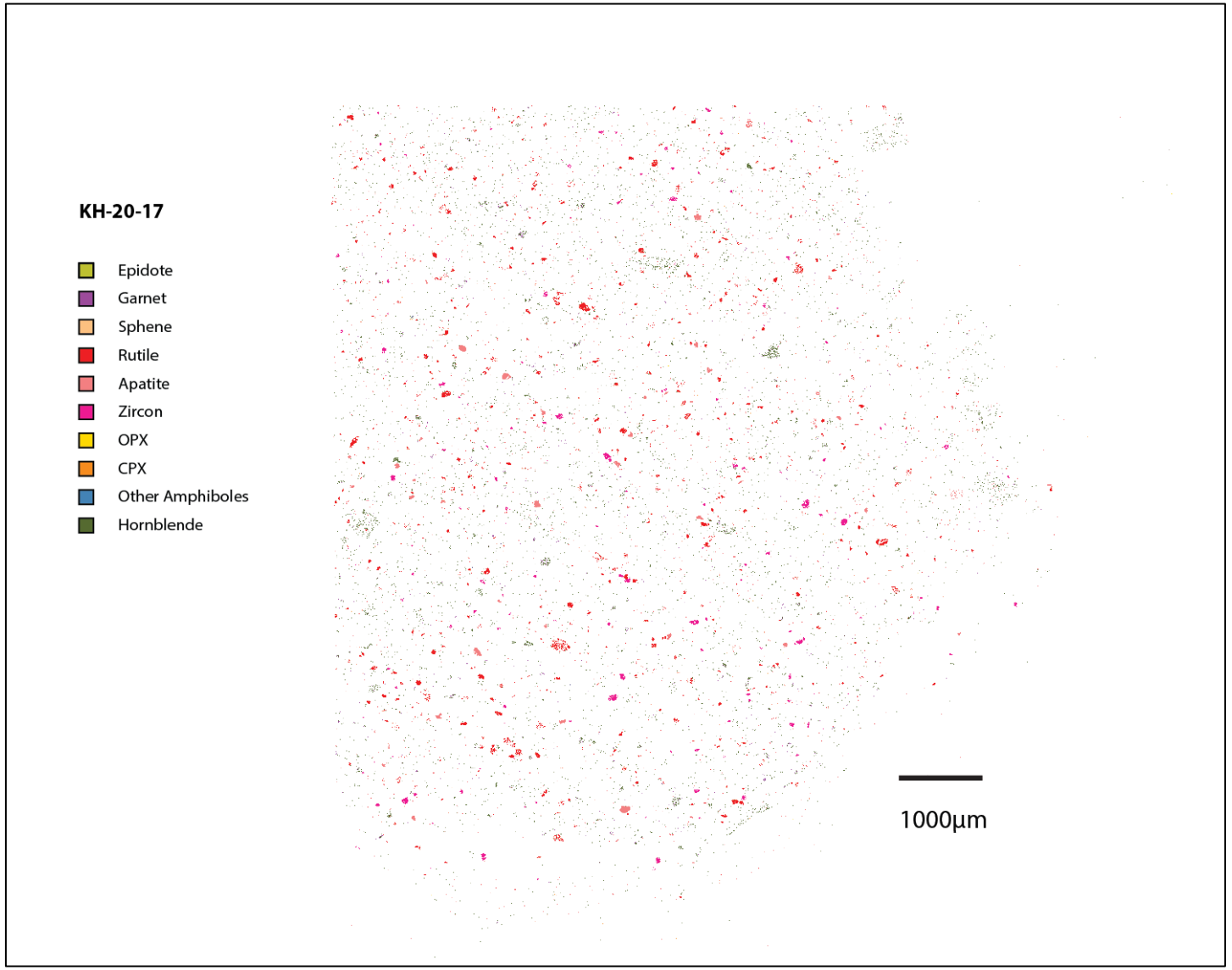
KH-20-17
Epidote
Garnet
Sphene
Rutile
Apatite
Zircon
OPX
CPX
Other Amphiboles
Hornblende
1000µm

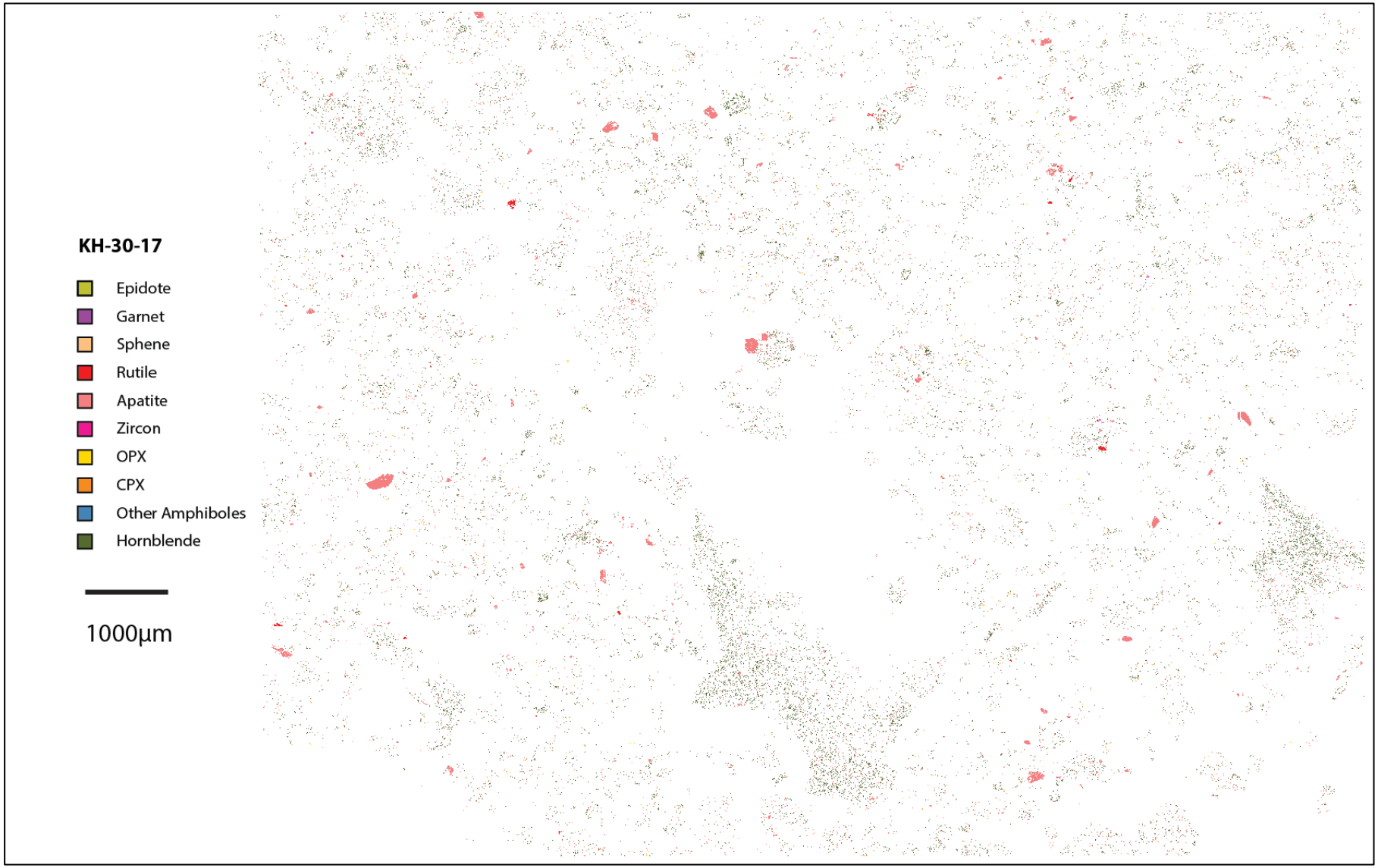
KH-30-17
Epidote
Garnet
Sphene
Rutile
Apatite
Zircon
OPX
CPX
Other Amphiboles
Hornblende
1000µm


KH-31-17
Epidote
Garnet
Sphene
Rutile
Apatite
Zircon
OPX
CPX
Other Amphiboles
Hornblende
1000µm

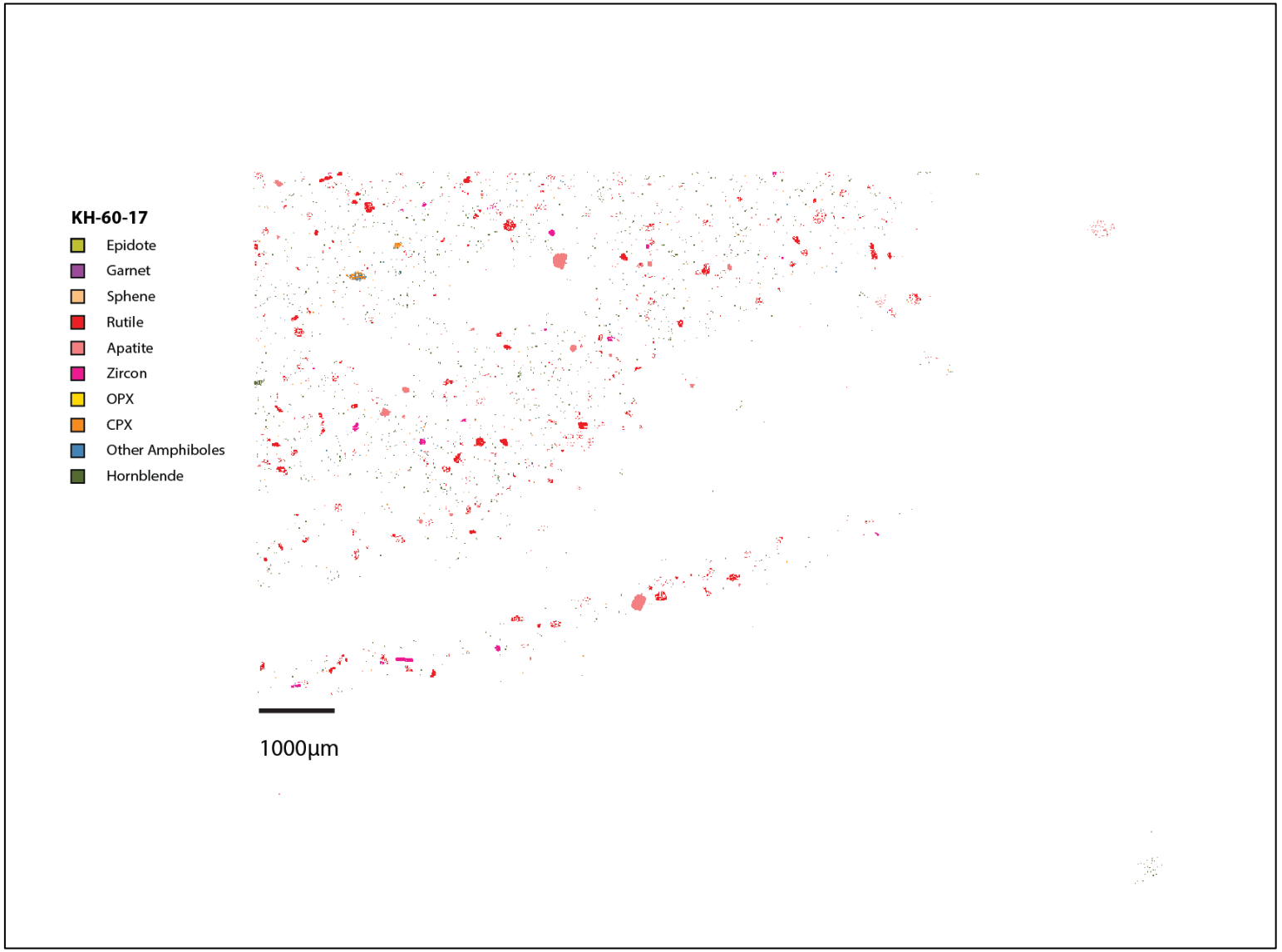
KH-60-17
Epidote
Garnet
Sphene
Rutile
Apatite
Zircon
OPX
CPX
Other Amphiboles
Hornblende
1000µm

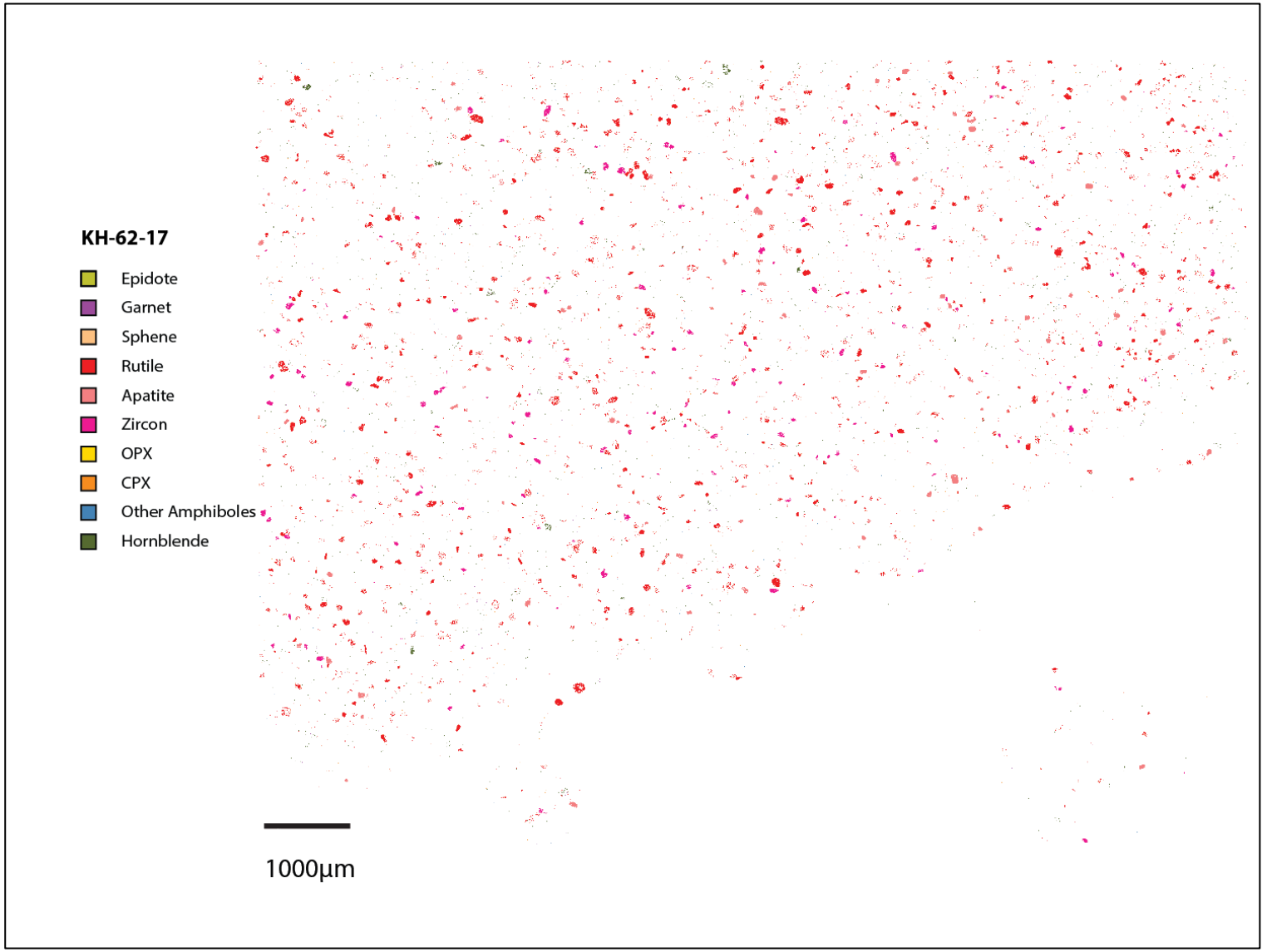
KH-62-17
Epidote
Garnet
Sphene
Rutile
Apatite
Zircon
OPX
CPX
Other Amphiboles
Hornblende
1000µm

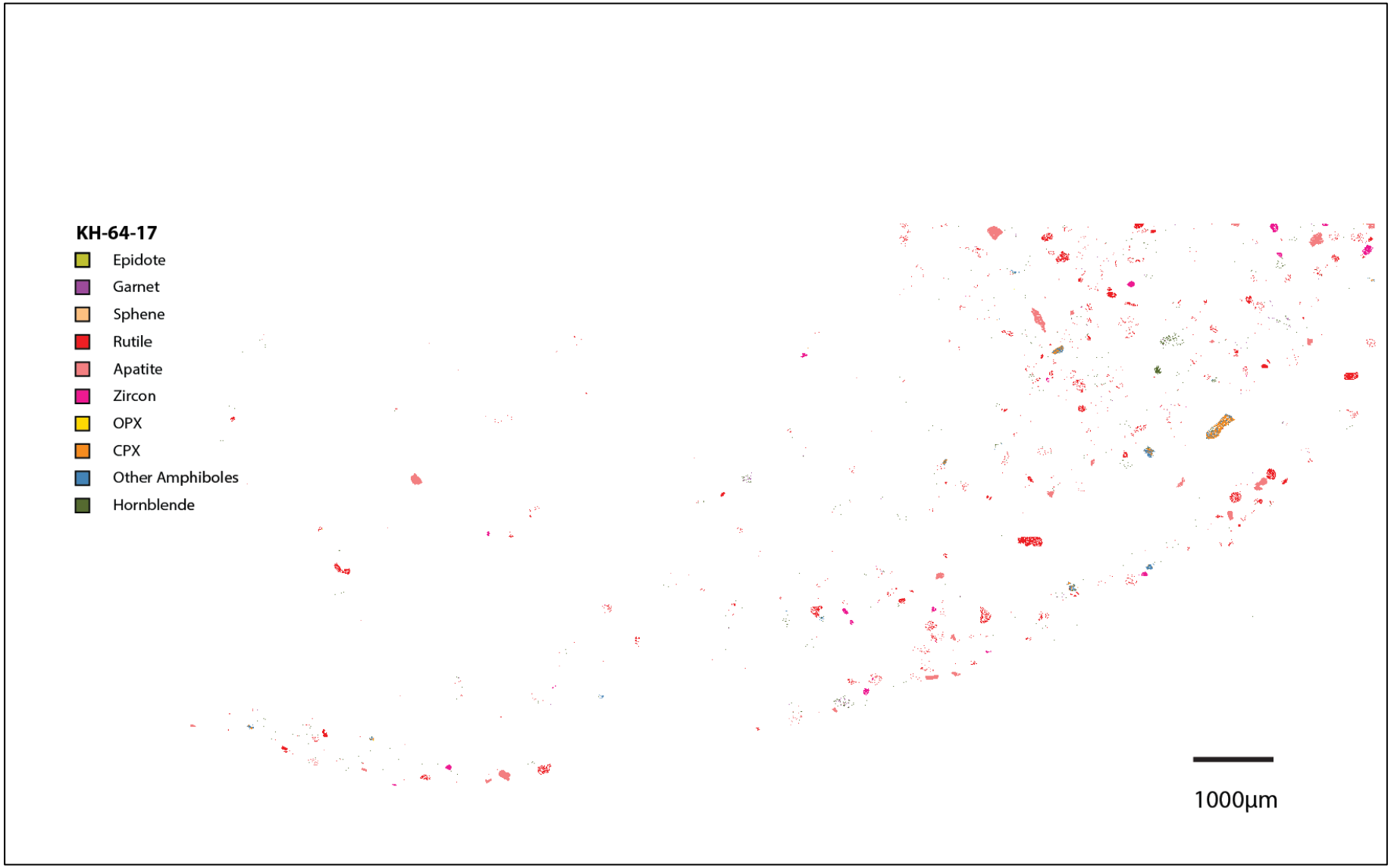
KH-64-17
Epidote
Garnet
Sphene
Rutile
Apatite
Zircon
OPX
CPX
Other Amphiboles
Hornblende
1000µm

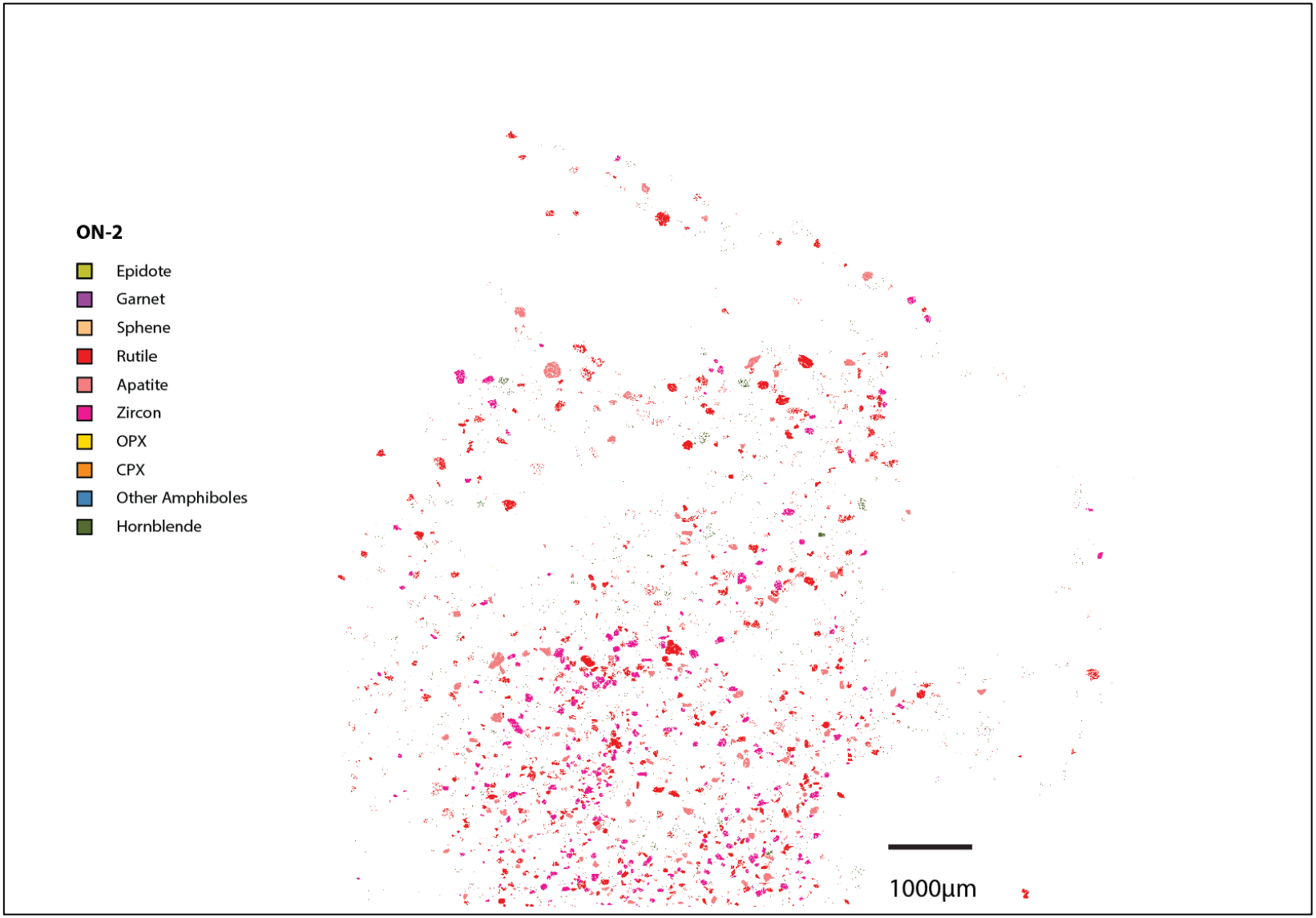
ON-2
Epidote
Garnet
Sphene
Rutile
Apatite
Zircon
OPX
CPX
Other Amphiboles
Hornblende
1000µm

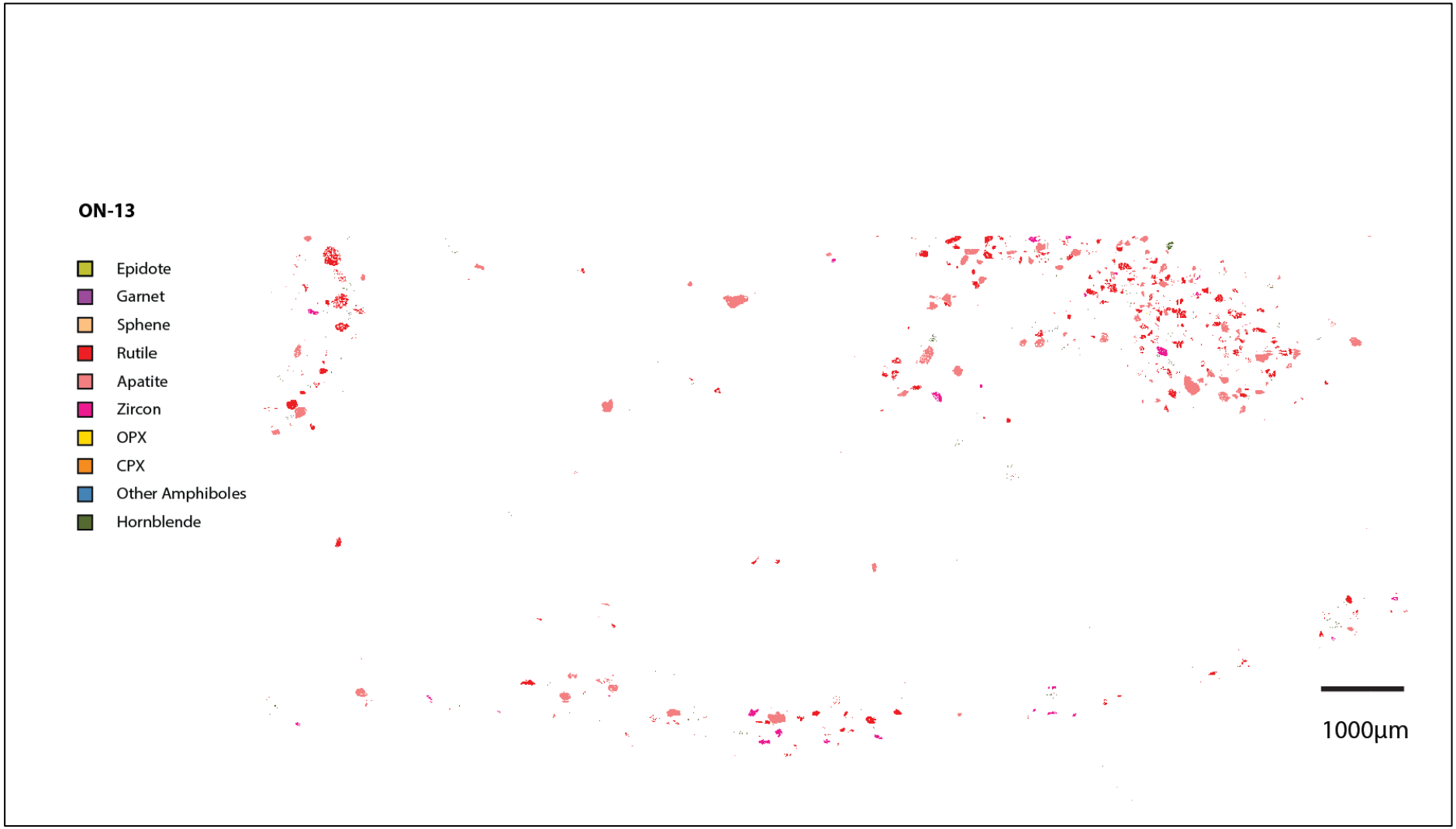
ON-13
Epidote
Garnet
Sphene
Rutile
Apatite
Zircon
OPX
CPX
Other Amphiboles
Hornblende
1000µm

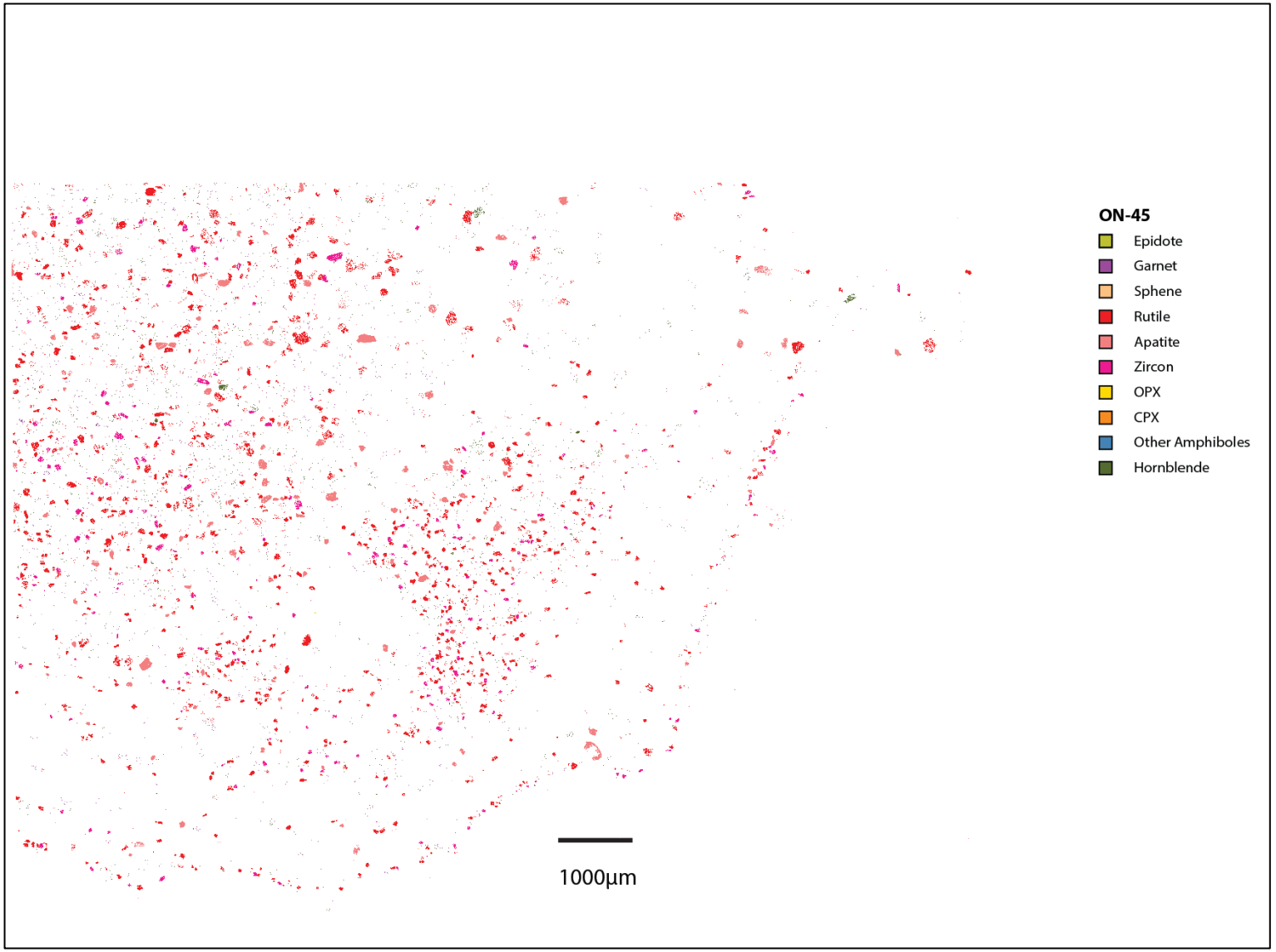
ON-45
Epidote
Garnet
Sphene
Rutile
Apatite
Zircon
OPX
CPX
Other Amphiboles
Hornblende
1000µm

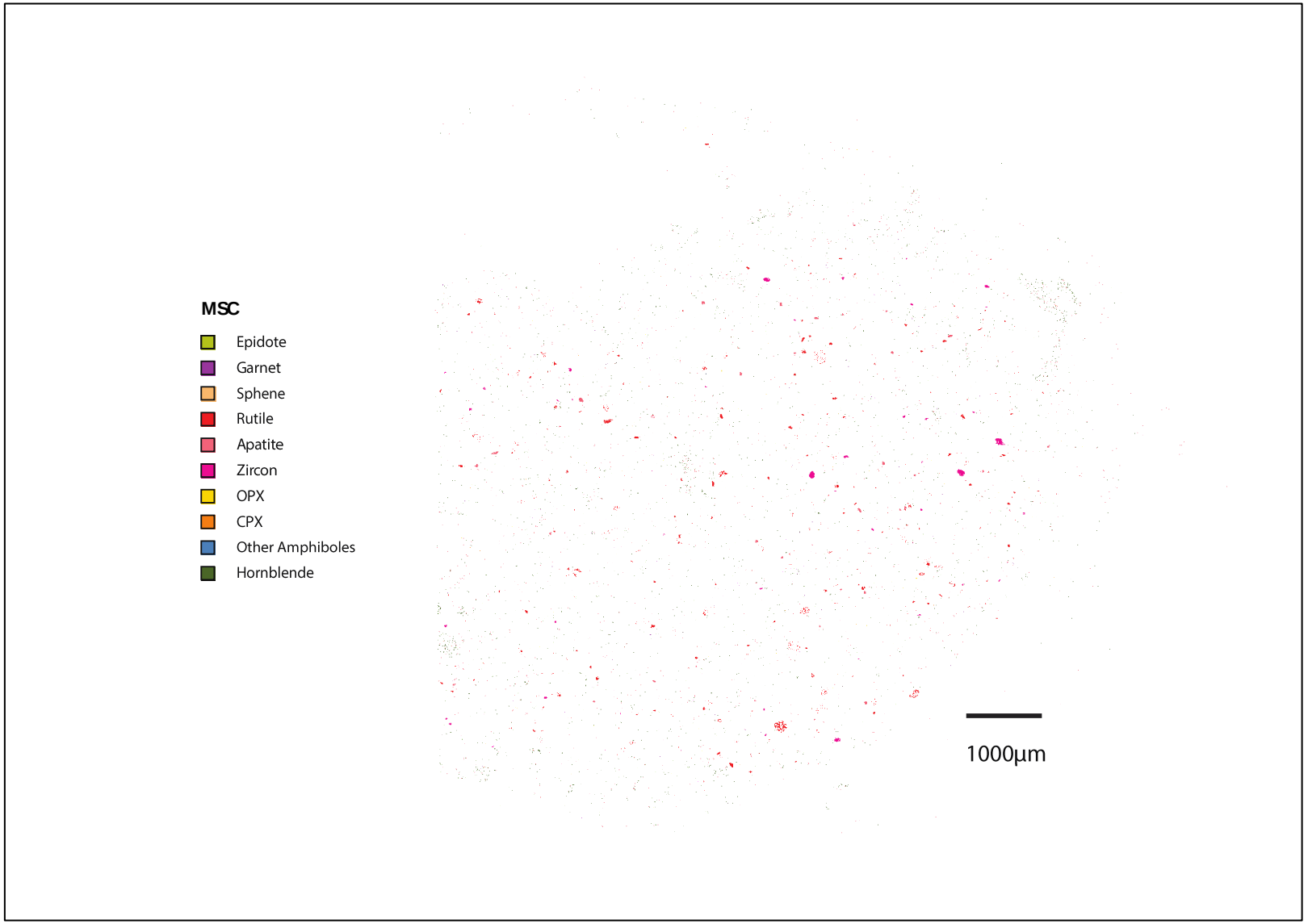
MSC
Epidote
Garnet
Sphene
Rutile
Apatite
Zircon
OPX
CPX
Other Amphiboles
Hornblende
1000µm

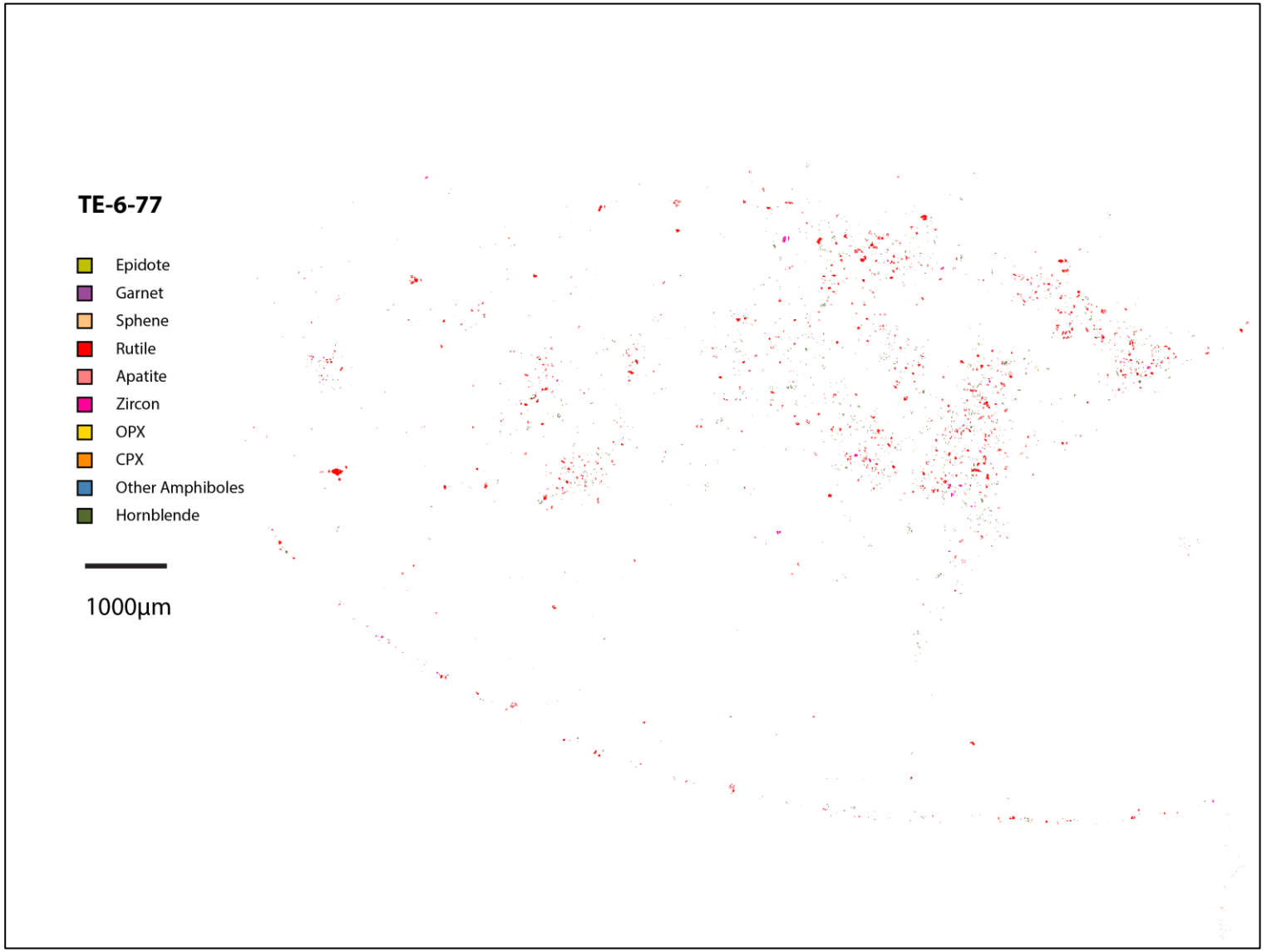
TE-6-77
Epidote
Garnet
Sphene
Rutile
Apatite
Zircon
OPX
CPX
Other Amphiboles
Hornblende
1000µm

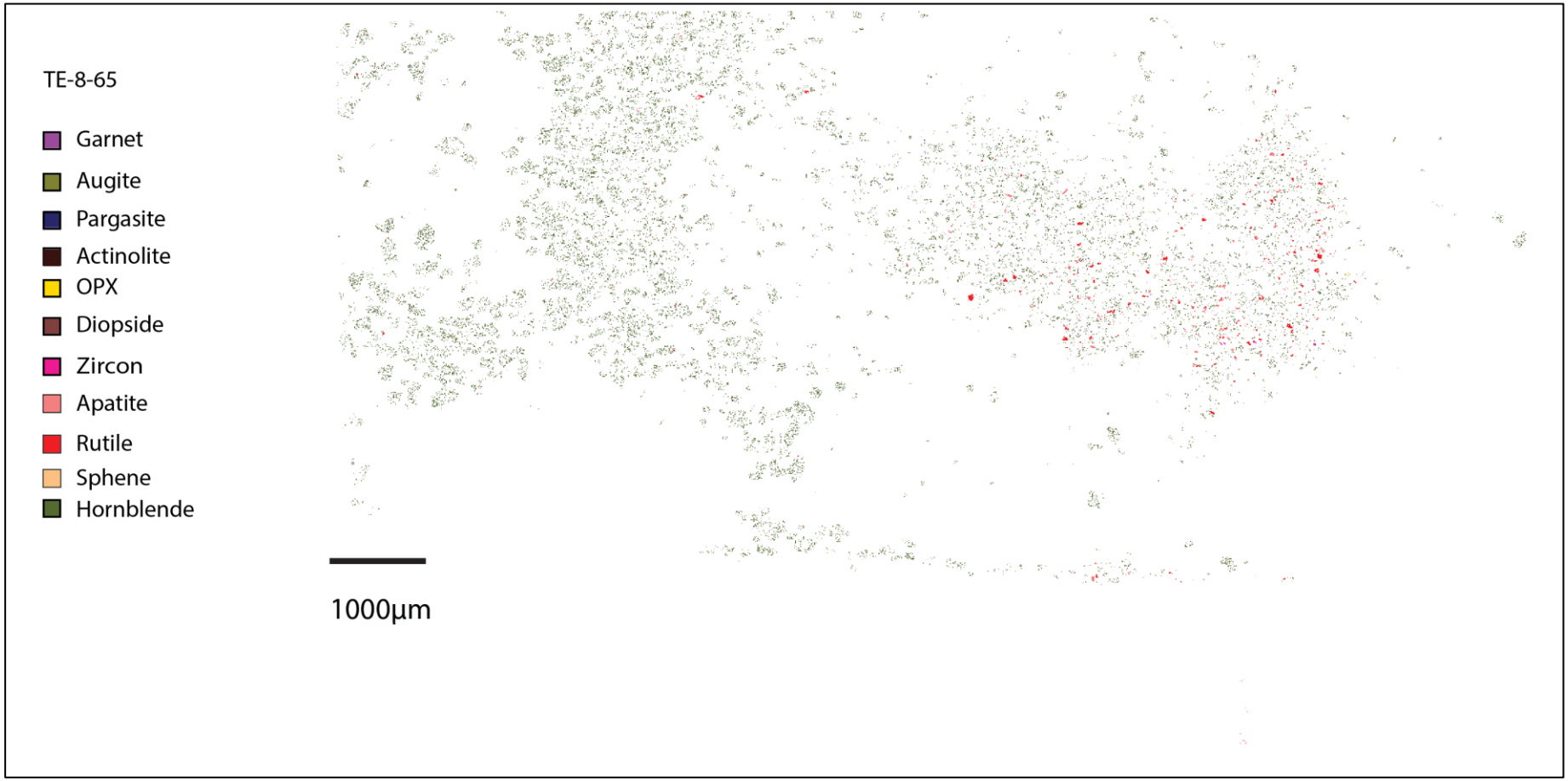
TE-8-65
Garnet
Augite
Pargasite
Actinolite
OPX
Diopside
Zircon
Apatite
Rutile
Sphene
Hornblende
1000µm

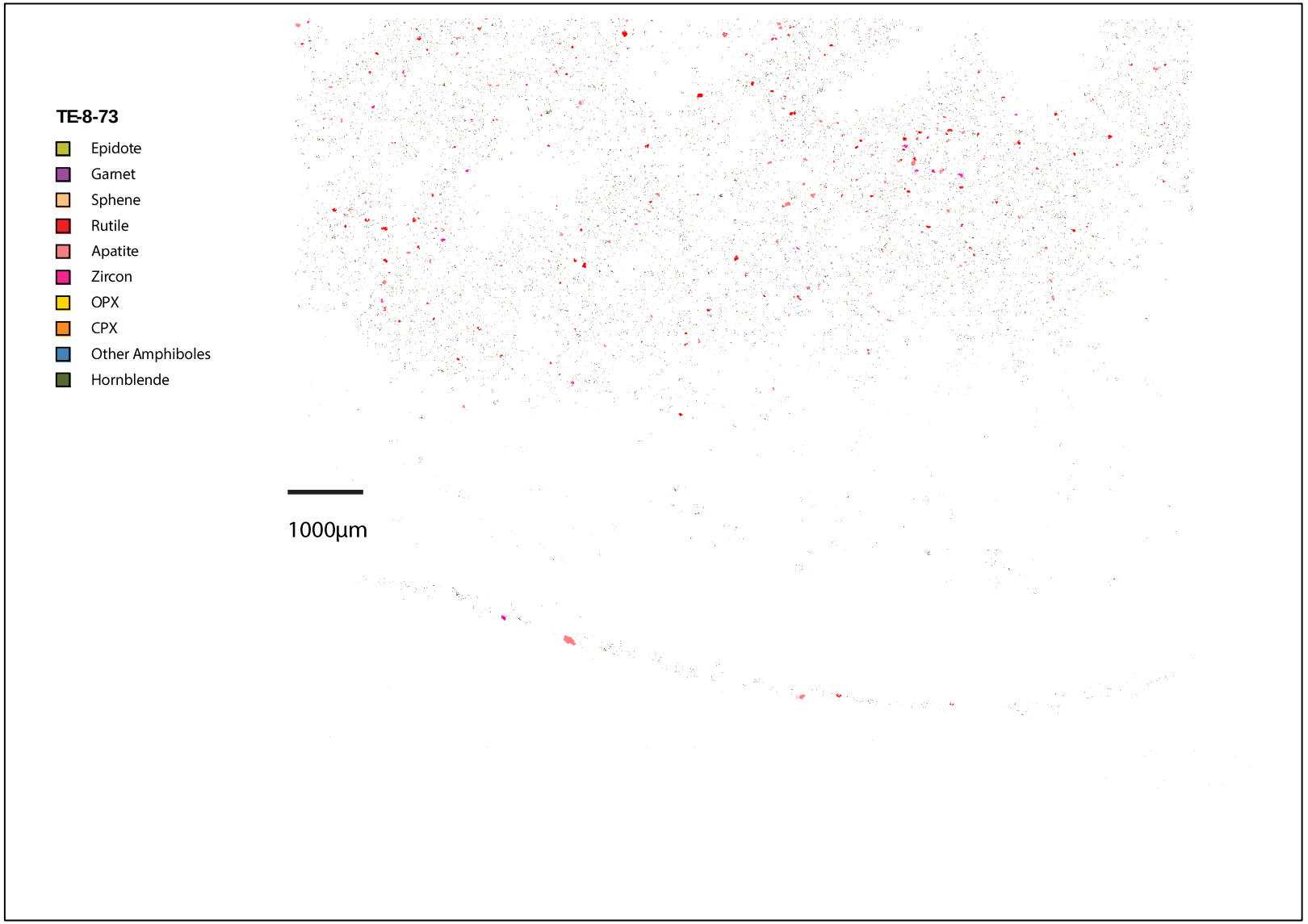
TE-8-73
Epidote
Garnet
Sphene
Rutile
Apatite
Zircon
OPX
CPX
Other Amphiboles
Hornblende
1000µm

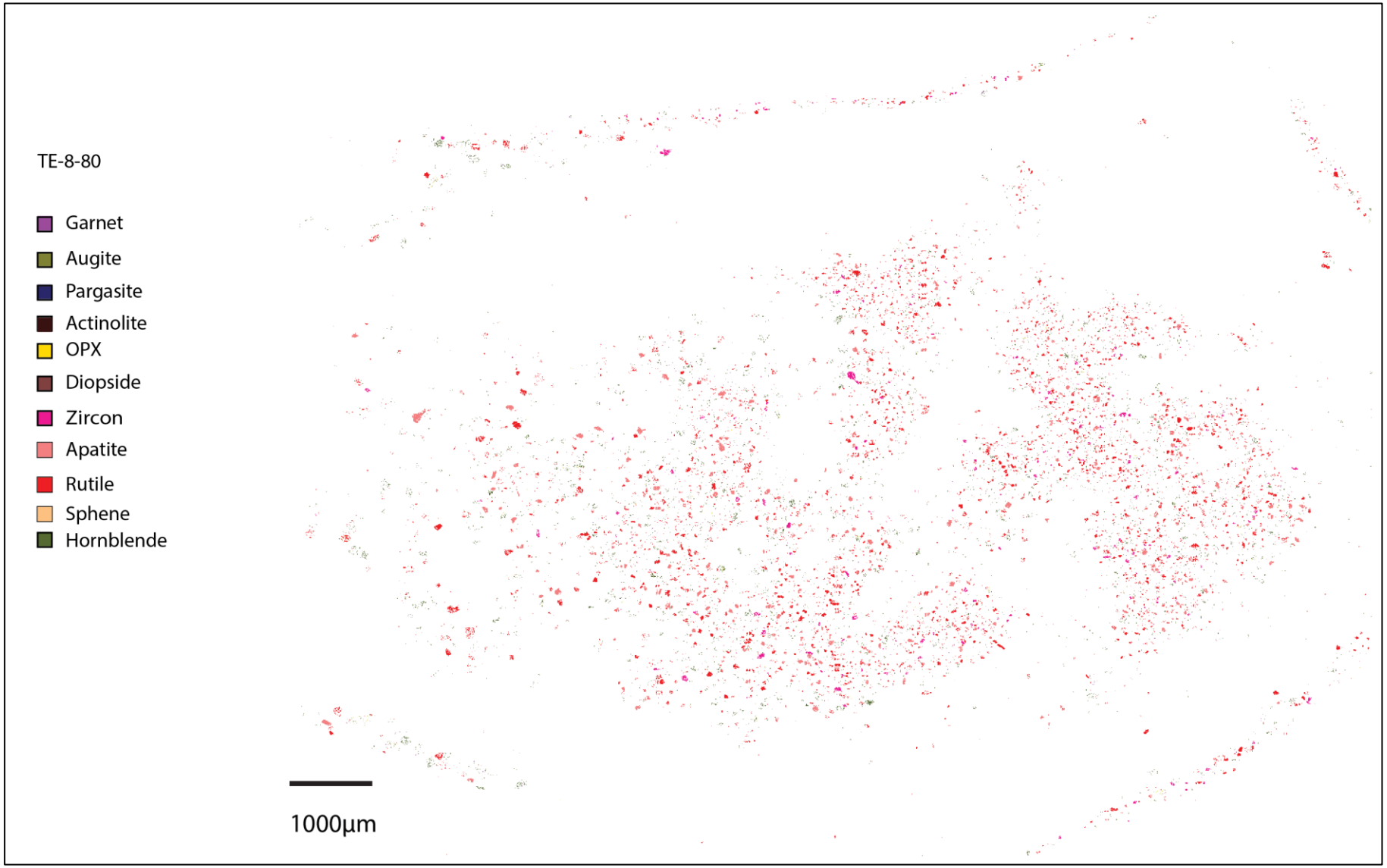
TE-8-80
Garnet
Augite
Pargasite
Actinolite
OPX
Diopside
Zircon
Apatite
Rutile
Sphene
Hornblende
1000µm